

**APRIL 2018**

**M.Sc. Thesis-Civil Engineering**

**KHALID TAWFEEQ AL-SAMMARRAIE**

**UNIVERSITY OF GAZIANTEP  
GRADUATE SCHOOL OF NATURAL & APPLIED  
SCIENCES**

**ULTIMATE LOAD CARRYING CAPACITY OF STEEL FIBER  
REINFORCED SELF-COMPACTING CONCRETE HAUNCHED  
BEAMS WITH STIRRUPS**

**M.Sc. THESIS  
IN  
CIVIL ENGINEERING**

**BY  
KHALID TAWFEEQ AL-SAMMARRAIE**

**APRIL 2018**

**Ultimate Load Carrying Capacity of Steel Fiber Reinforced Self-  
Compacting Concrete Haunched Beams with Stirrups**

**M.Sc. Thesis**

**In**

**Civil Engineering**

**University of Gaziantep**

**Supervisor**

**Assist. Prof. Dr. Mehmet Eren GÜLŞAN**

**By**

**Khalid Tawfeeq AL-SAMMARRAIE**

**April 2018**



© 2018 [Khalid Tawfeeq AL-SAMMARRAIE]

REPUBLIC OF TURKEY  
UNIVERSITY OF GAZİANTEP  
GRADUATE SCHOOL OF NATURAL & APPLIED SCIENCES  
CIVIL ENGINEERING DEPARTMENT

Name of the thesis: Ultimate Load Carrying Capacity of Steel Fiber Reinforced Self-Compacting Concrete Haunched Beams with Stirrups

Name of the student: Khalid Tawfeeq AL-SAMMARRAIE  
Exam date: 16.04.2018

Approval of the Graduate School of Natural and Applied Sciences



Prof. Dr. A. Necmeddin YAZICI

Director

I certify that this thesis satisfies all the requirements as a thesis for the degree of Master of Science.



Prof. Dr. Hanifi ÇANAKCI

Head of Department

This is to certify that we have read this thesis and that in our opinion, it is fully adequate, in scope and quality, as a thesis for the degree of Master of Science.



Assist. Prof. Dr. Mehmet Eren GÜLŞAN

Supervisor


Examining Committee Members:

Signature

Prof. Dr. Abdulkadir ÇEVİK

Assist. Prof. Dr. Derya BAKBAK

Assist. Prof. Dr. Mehmet Eren GÜLŞAN



.....  
.....  
.....



**I hereby declare that all information in this document has been obtained and presented in accordance with academic rules and ethical conduct. I also declare that, as required by these rules and conduct, I have fully cited and referenced all material and results that are not original to this work.**

**Khalid Tawfeeq AL-SAMMARRAIE**

## **ABSTRACT**

### **ULTIMATE LOAD CARRYING CAPACITY OF STEEL FIBER REINFORCED SELF-COMPACTING CONCRETE HAUNCHED BEAMS WITH STIRRUPS**

**AL-SAMMARRAIE, Khalid Tawfeeq**

**M.Sc. in Civil Engineering**

**Supervisor: Assist. Prof. Dr. Mehmet Eren GÜLŞAN**

**April 2018**

**84 pages**

This thesis includes a comprehensive experimental study regarding mechanical behavior of steel fiber reinforced concrete haunched beams. The experimental study were conducted on 12 reinforced concrete beams, 8 of them are RCHBs and 4 are prismatic beams. Different parameters have been adopted by steel fiber ratio, flexural reinforcement and inclination angle. All the beams were classified into three modes depending on the angle of inclination. The beams were divided into two main groups, each contains 6 RC beams, each group has the same ratio as the steel fiber (SF) and main steel reinforcement and differs from the other group while all the RC beams has been used as stirrups. The results have shown that as the steel reinforcement ratio increases, load capacity of the RCHBS with an inclination angle of  $10^\circ$  increases as amount of 40%. Moreover, the effect of increasing the ratio of steel fiber was clear to increase the failure load as compared to the capacity of the beams without steel fiber. Load capacities of these beams are greater than the capacity of prismatic beams with the same parameters. Increasing of steel reinforcement ratio increases the load capacity of the RCHBS with inclination angle of  $15^\circ$  as amount of 26%. However, addition of steel fiber has slightly affected the increase in load failure. It is also noticeable that the increment the angle of inclination decreases the load capacity. The addition of SF has led to an increase in the ductility of the concrete and collapse load, as well as reducing the thickness of cracks compared with specimens that do not contain steel fiber.

**Keywords:** Reinforced Concrete Haunched Beams, Steel fiber, Angle of inclination, Load Capacity, Ductility

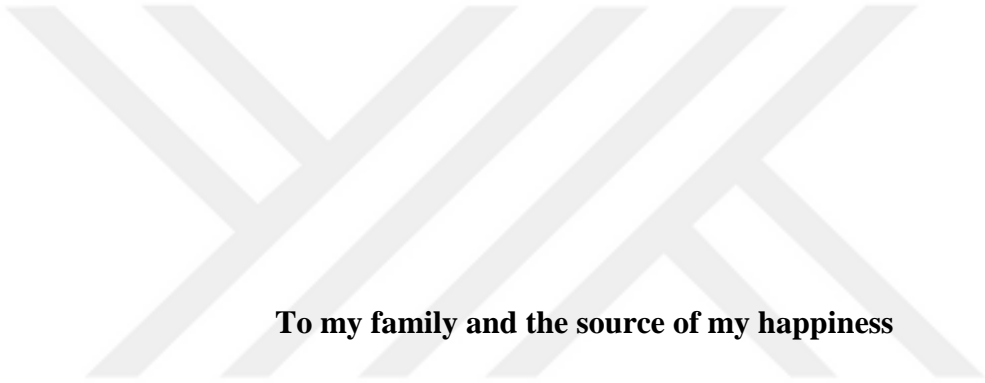
## ÖZET

### ETRİYELİ KENDİLİĞİNDEN YERLEŞEN BETONDAN ÜRETİLMİŞ ÇELİK LİF TAKVİYELİ BETONARME DEĞİŞKEN KESİTLİ KİRİŞLERİN MAKSİMUM YÜK TAŞIMA KAPASİTESİ

**AL-SAMMARRAIE, Khalid Tawfeeq**  
**Yüksek Lisans Tezi, İnşaat Mühendisliği**  
**Tez Danışmanı: Dr. Öğr. Üyesi Mehmet Eren GÜLŞAN**  
**Nisan 2018**  
**84 Sayfa**

Bu tez çelik lif katkılı değişken kesitli betonarme kirişlerin mekanik davranışı ile ilgili kapsamlı bir deneysel çalışmayı kapsamaktadır. Deneysel çalışma 8'i değişken ve 4'ü prizmatik olmak üzere 12 adet kiriş üzerinde gerçekleştirilmiştir. Çalışmada çelik lif oranı, çekme donatısı oranı ve eğim açısı gibi değişik parametreler dikkate alınmıştır. Bütün kirişler eğim açılarına göre 3 ayrı moda sınıflandırılmıştır. Bütün kirişlerde etriye kullanılmış iken; kirişler her biri 6 kirişten oluşan iyi ayrı temel gruba ayrılmıştır. Her gruptaki kirişler aynı çelik lif oranına ve çelik donatı oranına sahiptir. Deneysel sonuçlar çelik donatı oranı artırıldığı zaman  $10^\circ$  eğime sahip değişken kesitli kirişlerin yük taşıma kapasitesinin 40% oranına kadar arttığını göstermiştir. Ayrıca, çelik lif oranını arttırmanın kirişlerin yük taşıma kapasitesinin çelik lif katkısı olmayan kirişlere nazaran artmasında açık bir etkisi vardır. Bu kirişlerin yük taşıma kapasiteleri, aynı özellikteki prizmatik kirişlere göre daha fazladır. Çelik donatı oranı artışı  $15^\circ$  eğim açısına sahip değişken kesitli kirişlerde yük taşıma kapasitesini 26% oranında arttırmaktadır. Ancak çelik lif katkısı bu kirişlerin yük miktarını az bir miktar arttırmaktadır. Şu dikkat çekicidir ki; kirişin eğim açısı arttıkça yük taşıma kapasitesi düşmektedir. Çelik lif katkısı kirişlerin hem sünekliğini, hem de göçme yükünü arttırmanın yanı sıra; çelik lif katkısız kirişlerle kıyaslandığı zaman çatlak genişliğini de azaltmaktadır.

**Anahtar Kelimeler:** Değişken kesitli kirişler, Çelik tel, Eğim açısı, Yük taşıma kapasitesi, Süneklik



**To my family and the source of my happiness**

## ACKNOWLEDGEMENTS

Foremost, I would like to express my sincere gratitude to my supervisor **Assist. Prof. Dr. Mehmet Eren GÜLŞAN** for the continuous support of my M.Sc. Study and research, for his patience, motivation, enthusiasm, and immense knowledge. His guidance helped me in all the time of research and writing of this thesis. I could not have imagined having a better advisor and mentor for my M.Sc. study.

I would also like to express sincere thanks to all lecturers of Mechanical Division of Civil Engineering Department of Gaziantep University, **Dr. Abdulkadir ÇEVİK**, **Dr. Hasan Mohammed ALBEGMPRLI** for their helps and understandings during my thesis works.

My thanks and appreciation to all my colleagues who helped me during the days of the experimental work and who with their efforts was completed the work in his time

I would also like to thank all people who helped me during my experimental works. I might not complete my experimental works without their devoted support.

I would also like to thank the Department of Civil Engineering at the University of Gaziantep for providing them with all necessary facilities to carry out the experimental work in the laboratories of the department

Finally, I would like to extend my thanks and appreciation to my **parents** and family (**my wife and daughters**) for their help and patience throughout the study period, I thank them all from the depths of my heart.

## CONTENT

	<b>Page</b>
<b>ABSTRACT</b> .....	<b>v</b>
<b>ÖZET</b> .....	<b>vi</b>
<b>ACKNOWLEDGEMENT</b> .....	<b>viii</b>
<b>TABLE OF CONTENTS</b> .....	<b>ix</b>
<b>LIST OF FIGURES</b> .....	<b>xi</b>
<b>LIST OF TABLES</b> .....	<b>xv</b>
<b>LIST OF SYMBOLS</b> .....	<b>xvi</b>
<b>CHAPTER ONE</b>	
<b>INTRODUCTION</b> .....	<b>1</b>
1.1 General .....	1
1.2 Steel Fiber Reinforced Concrete (SFRC) .....	2
1.3 Self-Compacting Concrete (SCC) .....	4
1.3.1 Properties of SCC .....	5
1.4 Thesis Aims .....	5
<b>CHAPTER TWO</b>	
<b>LITERATURE REVIEW</b> .....	<b>7</b>
2.1 Introduction .....	7
2.2 Reivew of the Experimental Studies of RCHBs .....	7
2.3 Previous Studies about Steel Fiber Reinforced Concrete (SFRC) .....	11
2.3.1 Overview .....	11
2.3.2 Steel Fiber Reinforced concrete (SFRC) .....	12
<b>CHAPTER THREE</b>	
3.1 Introduction .....	15
3.2 Objectives .....	15
3.3 Materials .....	16
3.3.1 Concrete Mix Design .....	16

3.3.2 Steel reinforcement .....	18
3.4 The Geometries .....	18
3.4.1 Identification .....	19
3.4.2 Group A.....	19
3.4.3 Group B.....	19
3.4.4 Group C .....	20
3.5 Preparing and Casting of Test Specimens.....	24
3.6 Preparing Specimens for test.....	28
3.7 Testing Procedure .....	28
3.7.1 Concrete Samples .....	28
3.7.2 Testing Specimens .....	30
<b>CHAPTER FOUR</b>	
<b>EXPERIMENTAL RESULTS AND DISCUSSION .....</b>	<b>33</b>
4.1 Overview .....	33
4.2 Testing results .....	33
4.2.1 Material properties.....	33
4.2.2 Failure Load.....	33
4.2.3 Relationship between Load and Deflection.....	36
4.2.4 Mode of Failure .....	44
4.2.5 The Shear Critical Section.....	48
4.2.6 Effectictive depth of shear.....	48
4.2.7 Effect Steel Fiber Ratio .....	49
4.2.8 Effect of steel reinforcement ratio .....	53
4.2.9 Effective of angle of inclination .....	57
4.2.10 Flexural behavior of Beams.....	61
4.2.11 Cracks Propagation in the beams.....	61
<b>CHAPTER FIVE</b>	
<b>CONCLUSIONS .....</b>	<b>75</b>
5.1 Overview .....	75
5.2 The four prismatic beams have been adopted and encoded (A) .....	75
5.3 The four haunched beams with the symbol (B) .....	76
5.4 The four haunched beams with the symbol (C) .....	76
5.5 Recommendations for Future Research .....	77
<b>REFERENCES .....</b>	<b>79</b>

## LIST OF FIGURES

	<b>Page</b>
<b>Figure 1.1</b> Reinforced concrete haunched beam .....	2
<b>Figure 1.2</b> Steel fiber hooked end .....	3
<b>Figure 2.1</b> Specimens tested beams by (Debaiky and Elniema 1982) .....	10
<b>Figure 2.2</b> Specimens tested beams by (Stefanou 1983).....	10
<b>Figure 2.3</b> Specimens tested beams by (Tena et al 2008) .....	10
<b>Figure 2.4</b> Specimens tested beams by (Aziz, A.H. 2016) .....	11
<b>Figure 3.1</b> Volumetric gradients for aggregate .....	17
<b>Figure 3.2</b> Used Steel Fiber Specifications. ....	17
<b>Figure 3.3</b> Reinforcement bar on test machine .....	18
<b>Figure 3.4</b> Geometry of beam (B1-P-0 and B2-P-0.5).....	21
<b>Figure 3.5</b> Geometry of beam (B11-P-0 and B12-P-0.5).....	21
<b>Figure 3.6</b> Geometry of beam (B3-H10 <sup>o</sup> -0 and B5-H10 <sup>o</sup> -0.5).....	21
<b>Figure 3.7</b> Geometry of beam (B7-H10 <sup>o</sup> -0 and B9-H10 <sup>o</sup> -0.5).....	22
<b>Figure 3.8</b> Geometry of beam (B4-H15 <sup>o</sup> -0 and B6-H15 <sup>o</sup> -0.5) . ....	22
<b>Figure 3.9</b> Geometry of beam (B8-H15 <sup>o</sup> -0 and B10-H15 <sup>o</sup> -0.5).....	22
<b>Figure 3.10</b> Reinforcement processing works.....	24
<b>Figure 3.11</b> Reinforcement and Formwork preparing.....	24
<b>Figure 3.12</b> Mixing of concrete.....	25
<b>Figure 3.13</b> Slump flow test with steel fiber ratio (0.5%).....	26
<b>Figure 3.14</b> Beams and samples after casting. ....	27
<b>Figure 3.15</b> Curing beams and samples 28 days. ....	27

<b>Figure 3.16</b> Preparing beams for test .....	28
<b>Figure 3.17</b> Compressive strength testing .....	29
<b>Figure 3.18</b> Splitting tensile strength test.....	30
<b>Figure 3.19</b> Testing installation of the beam.....	31
<b>Figure 3.20</b> Loading procedure .....	32
<b>Figure 4.1</b> Flexural failure.....	34
<b>Figure 4.2</b> Shear failure.....	34
<b>Figure 4.3</b> Test result indicators .....	36
<b>Figure 4.4</b> Load-Displacement Relationship B1-P-0 .....	36
<b>Figure 4.5</b> Load-Displacement Relationship B2-P-0.5 .....	37
<b>Figure 4.6</b> Load-Displacement Relationship B11-P-0.....	37
<b>Figure 4.7</b> Load-Displacement Relationship B12-P-0.5 .....	38
<b>Figure 4.8</b> Load-Displacement Relationship B4-H15°-0 .....	38
<b>Figure 4.9</b> Load-Displacement Relationship B6-H15°-0.5 .....	39
<b>Figure 4.10</b> Load-Displacement Relationship B8-H15°-0 .....	39
<b>Figure 4.11</b> Load-Displacement Relationship B10-H15°-0.5 .....	40
<b>Figure 4.12</b> Load-Displacement Relationship B3-H10°-0 .....	40
<b>Figure 4.13</b> Load-Displacement Relationship B5-H10°-0.5 .....	41
<b>Figure 4.14</b> Load-Displacement Relationship B7-H10°-0 .....	41
<b>Figure 4.15</b> Load-Displacement Relationship B9-H10°-0.5 .....	42
<b>Figure 4.16</b> Load-Displacement Relationship Mode A .....	42
<b>Figure 4.17</b> Load-Displacement Relationship Mode B.....	43
<b>Figure 4.18</b> Load-Displacement Relationship Mode C.....	43
<b>Figure 4.19</b> Flexural Failure Mode. ....	47
<b>Figure 4.20</b> Shear Failure Mode.....	48
<b>Figure 4.21</b> Shear Failure shape for the RCHBs.....	49

<b>Figure 4.22</b> Load-Displacement Relationship for two prismatic beams with steel fiber ratio (0&0.5) % .....	50
<b>Figure 4.23</b> Load-Displacement Relationship for two haunched beams with steel fiber ratio (0&0.5) % .....	51
<b>Figure 4.24</b> Load-Displacement Relationship for two haunched beams with steel fiber ratio (0&0.5) % .....	51
<b>Figure 4.25</b> Load-Displacement Relationship for two prismatic beams with steel fiber ratio (0&0.5) % .....	52
<b>Figure 4.26</b> Load-Displacement Relationship for two haunched beams with steel fiber ratio (0&0.5) % .....	52
<b>Figure 4.27</b> Load-Displacement Relationship for two haunched beams with steel fiber ratio (0&0.5) % .....	53
<b>Figure 4.28</b> Load-Displacement Relationship for two prismatic beams with steel reinforcement ratio (B1=0.02 & B11=0.310) .....	54
<b>Figure 4.29</b> Load-Displacement Relationship for two prismatic beams with steel reinforcement ratio (B2=0.02 & B12=0.310) .....	55
<b>Figure 4.30</b> Load-Displacement Relationship for two haunched beams with steel reinforcement ratio (B4=0.02 & B8=0.310) .....	55
<b>Figure 4.31</b> Load-Displacement Relationship for two haunched beams with steel reinforcement ratio (B6=0.02 & B10=0.310) .....	56
<b>Figure 4.32</b> Load-Displacement Relationship for two haunched beams with steel reinforcement ratio (B3=0.02 & B7=0.310) .....	56
<b>Figure 4.33</b> Load-Displacement Relationship for two haunched beams with steel reinforcement ratio (B5=0.02 & B9=0.310) .....	57
<b>Figure 4.34</b> Load-Displacement Relationship for three beams with steel reinforcement ratio 0.02 & steel fiber ratio 0 %.....	58

<b>Figure 4.35</b> Load-Displacement Relationship for three beams with steel reinforcement ratio 0.02 & steel fiber ratio 0 %.....	58
<b>Figure 4.36</b> Load-Displacement Relationship for three beams with steel reinforcement ratio 0.310 & steel fiber ratio 0 %.....	59
<b>Figure 4.37</b> Load-Displacement Relationship for three beams with steel reinforcement ratio 0.310 & steel fiber ratio 0 %.....	59
<b>Figure 4.38</b> Influence of the inclination angle on the shear strength capacity .....	60
<b>Figure 4.39</b> Uncracked compression chord.....	60
<b>Figure 4.40</b> Crack propagation of the beam B1 .....	63
<b>Figure 4.41</b> Crack propagation of the beam B2 .....	64
<b>Figure 4.42</b> Crack propagation of the beam B11 .....	65
<b>Figure 4.43</b> Crack propagation of the beam B12 .....	66
<b>Figure 4.44</b> Crack propagation of the beam B3 .....	67
<b>Figure 4.45</b> Crack propagation of the beam B5 .....	68
<b>Figure 4.46</b> Crack propagation of the beam B7 .....	69
<b>Figure 4.47</b> Crack propagation of the beam B9 .....	70
<b>Figure 4.48</b> Crack propagation of the beam B4 .....	71
<b>Figure 4.49</b> Crack propagation of the beam B6 .....	72
<b>Figure 4.50</b> Crack propagation of the beam B8 .....	73
<b>Figure 4.51</b> Crack propagation of the beam B10 .....	74

## LIST OF TABLES

	<b>Page</b>
<b>Table 3.1</b> Weight of concrete mix components of one cubic meter.....	16
<b>Table 3.2</b> Weight of concrete mix components of one cubic meter with steel fiber.	16
<b>Table 3.3</b> Result of steel bars reinforcement.....	18
<b>Table 3.4</b> Geometries of beams.....	23
<b>Table 4.1</b> Results of experimental tests.....	35

## LIST OF SYMBOLS

$A_f$	Cross-sectional area of steel fibers
$A_s$	Area of steel for flexural zone
$A_s'$	Area of steel in compression zone
$A_{v,min}$	Minimum shear reinforcement in flexural member
$b_w$	Beam width
$d_{cr}$	Effective depth at the critical section
$d_f$	Steel fiber diameter
F	Flexural failure mode
$f_{ct}$	Splitting strength concrete
$f_{cu}$	Cubic Compressive Strength
$f_y$	Reinforcement yield strength
$h_m$	Depth of beam at middle
$h_s$	Depth of beam at the supports
$N_f$	Number of fibers per unit area
$s$	Distance between vertical stirrups
S	Shear failure mode
V	Shear force
$V_f\%$	Steel fiber ratio
$\alpha$	Angle of incilation
$\emptyset$	Diameter of reinforcement bar
$\eta_o$	Orientation factor

## CHAPTER ONE

### INTRODUCTION

#### 1.1 General

The development of the system of buildings construction and the required consideration of the economic aspect or the architecture requirements has become necessary to study the elements of unconventional construction among these elements reinforced concrete haunched beams (RCHBs). The RCHBs are the beams whose cross section thicken or broaden toward its supports. RCHBs have many uses such as bridges and concrete structures with wide spaces as shown in Fig. 1.1. The use of this type of beams is for the provision of the economic side in reducing the amount of concrete used as well as the requirements of architecture, such as easy passage of sewage pipes and air conditioning and electrical installations. This type of beam is the subject of research in this study. This study focuses on two types of haunched beams with different angles and different characteristics such as steel fiber and the main reinforcement steel ratio, and then studying the mechanical behavior and comparing the results with the prismatic beams, which have a constant section. The existing experimental studies concluded that the mechanical behavior of the RCHBs has expressed different behavior compared to prismatic beams, the results of the experimental works pronounced that the depth variance along the beam influence on the mechanism of the shear failure (Debaiky and El-Niema 1982, Stefanou 1983, Tena et al. 2008, Nghiep 2010). The most prominent axes of comparison between the RCHBs compared to the prismatic beams are the effective depth in the critical section, the influence of the inclined reinforcement, the contribution of the inclined compression chord, and influence of the shear span. (Nghiep 2010) has proposed some formulas to estimate shear capacity, but did not mention all cases of inclination. The German code DIN 1045-1 gives the design of RCHBs. other design codes did not mention the shear design of the RCHBs, these structural members are usually divided into strips with average depth to preserve the similar stiffness of the

original structures. This method is acceptable for flexural design but not accurate for shear design.



a. RCHBs in bridge

b. RCHBs in building

[Adapted from FDOT website]

[Adapted from Sceincedirect website]

**Figure 1.1** Reinforced concrete haunched beam

## 1.2 Steel Fiber Reinforced Concrete (SFRC)

Recently, there has been a need to use high performance concrete and improve its specifications for use in high altitude structures and important buildings, because concrete is a brittle and non-ductile material. The cement mix requires some different fibers, especially steel fibers, to convert it into a material with reasonable ductility. Steel Fiber Reinforced Concrete (SFRC) can be defined as Concrete made of cement and aggregates and containing steel fibers of 3 to 8 cm length and diameter from 0,5 to 0.8 mm as shown in Fig. 1.2 are not continuous and distributed randomly in all directions during the concrete mass.



**a.** Shape of steel fiber

[Adapted from FIBSOL website]



**b.** Steel fiber in concrete

[Adapted from thebalance website]

**Figure 1.2** steel fiber hooked end.

The most important features of this type of concrete, increase the resistance of concrete to tensile, cracks increase the ductility and resistance to impacts and friction. And are therefore used mainly in the floor and exposed moving loads such as airports, workshops, roads and stores, it is used for vast areas of land up to 40 \* 40 m without expansion joints or fear of cracking. It is also used in some types of pre-cast concrete such as concrete pipes, tunnels and concrete repairs. The first uses of steel fiber have appeared the patent from 1927 worked out in California by G.C. Martin, regarded the production of SFRC pipes. In 1938, N. Zitkewic patented a way to increase the strength and impact resistance of concrete by adding cut pieces of steel wire (Jamrozy 1985). Steel fibers, patented in 1943 by G. Constancinesco, were already very similar to the ones used at present. The patent, apart from different shapes of fibers, contained information about the kind and dispersion of cracks during loading of SFRC elements and it made mentioned of the great amount of energy which is absorbed by SFRC under impact, Most studies have shown that the addition of steel fiber has a significant effect on the tensile behavior of the composite. In general, the effect of steel fiber is low on the maximum load causing the failure, as well as studies have shown that the addition of steel fiber for concrete increased ductility of concrete as concrete is a brittle material. As for the cracks appear many and have a width and the length of these cracks less than compared to the normal concrete.

### **1.3 Self-Compacting Concrete (SCC)**

In the last decades, the concrete industry has witnessed a significant development in the production of new types of concrete structures for the construction of concrete installations:

These new types of concrete are characterized by the ability to withstand the pressure exerted on it and the high durability with ease of execution (casting and compaction), reduce the period of construction, and reduce dependence on the skill of employment during the execution. Self-Compacting concrete (SCC) is a new type of concrete that meets the properties mentioned above. Self-Compacting concrete is one of the modern types of high performance concrete. SCC is also a product of technological advances in the field of concrete additives. Both viscosity additives and additives (super plasticizers) are the two essential elements for the production of concrete. The Japanese are the pioneers of the manufacture of these concrete, where in the past ten years used in many useful installations and applications. This concrete was then produced in many countries such as Turkey and America.

SCC is a concrete that needs a little of compaction, which was used only in 1980 and in Japan specifically. In Europe, it was used for the first time in Sweden's road networks in the mid-1990s. The European Commission EC funded several civil and governmental projects for self-crushing concrete between 1997 and 2000, in 2002 the European Federation for Specialist Construction Chemicals and Concrete Systems (EFNARC) published the specifications and manual for the use of SCC, and since then has published several reports on SCC. The European Project Group has set up a new document on the specifications and methods of use of SCC, which is known as the European Guidelines for Self Compacting Concrete, which means applications, tests and specifications of this type of concrete.

### **1.3.1 Properties of SCC:**

- Easy casting in places crowded with steel reinforcement and narrow places.
- The ability to casting a large amount of concrete in a short time.
- Less labor is needed.
- There is no segregation.
- Does not need to use vibrators in the site, which leads to easy casting and overcome the noise problem caused by vibrators.
- It has a better shape and appearance and does not need to settle its surface after pouring.
- High fluidity does not need to add water and thus reduce compressive of strength.
- More durability than normal concrete.

### **1.4 Thesis Aims**

This thesis has been conducted to achieve some objectives which can be summarized as follows:

- Experimental study of a specific type of beams (RCHBs) rather than the prismatic beams and study the mechanical behavior of these beams.
- Making comparison between (RCHBs) and the prismatic beams of various mechanical behaviors in terms of failure load and shape of failure.
- Studying the effect of one ratio of steel fiber added to the concrete mix and study the mechanical properties obtained by adding this percentage and suggesting another percentage according to the results obtained from the results.
- Study the influence of the design parameters on the shear strength capacity of the members like inclination angle, inclined reinforcement, material properties and shape mode.
- Obtain the results used in the code equations to prepare for the (RCHBs) because there are no special equations for the RCHBs.

Achieve an economic and architectural aspect of studying such a type of haunched beams if the results show good values compared to the prismatic beams. Encouraging

the study of other new types of RCHBs at different angles and reaching uniform forms with their own equations and recommendations.

### **1.5 Thesis Layout**

**Chapter one:** This chapter contains an introduction about haunched beams, steel fiber, self-compacting concrete, Purpose and objectives of this study.

**Chapter two:** provides the literature review for the experimental investigation of RCHBs

**Chapter three:** This chapter contains all details related to the experimental program like shape all beams, reinforcement details, design of specimens, characteristics of the materials that were used in this research, setup of the test and the procedures of rehabilitation for all beams.

**Chapters four:** This chapter presented and discussed the results of the test.

**Chapter five:** This chapter presents the summary, conclusions and recommendations for future Research.

## **CHAPTER TWO**

### **LITERATURE REVIEW**

#### **2.1 Introduction**

Although there is a few amount of research covering all the cases of the RCHBs, this chapter will discuss the background of the experimental work of RCHBS, as well as the different parameters involved in the design of RCHBs, such as the effect of the angle of inclination, shear and flexural reinforcement, steel fiber ratio. At first: The previous experimental studies available to RCHBs will be discussed, Second, the beams will be addressed with steel fiber because there are no prior studies of RCHBs concrete with the Steel fiber.

#### **2.2 Review of the Experimental Studies of RCHBs**

Debaiky and Eliniema (1982) were among the first to conduct experimental studies on the RCHBs. Their studies included 33 concrete beams to study the shear behavior of the RCHBs, Where they were included on haunched beams as well as on prismatic beams for the purpose of comparison and as shown in Fig. 2.1. The variable parameters whose study included inclination angle, Concrete resistance, shear span, as well as a percentage of reinforcement for both shear and flexural. The most important conclusions were drawn: The nominal shear contribution of the concrete and the longitudinal reinforcement were influenced by the haunch's inclination while the nominal contribution of the stirrups is not. Shear strength is not increased by increasing the depth of the beam toward the support, at the same time, the reverse is not true that the decrease depth of the beams towards the beam did not decrease shear capacity (Debaiky and Elniema 1982).

Stefanou (1983), an experimental study was conducted on the non-prismatic concrete beams to study the shear behavior and to compare the results with the prismatic beams adopted. The study included several beams with variable parameters such as: inclination angle, main longitudinal reinforcement, depth of beams at the support,

with shear reinforcement (stirrups) and without stirrups as shown in Fig. 2.2. In general, the research relied on finding the ultimate shear strength on non-prism beams based on the discussion of the performance of the building codes such as the American code (ACI), the British code and the Russian code. In his conclusion, the author pointed out that stirrups did not increase the value of maximum load, and the collapse load for the sloping beams were all of the same arrangement of proportion. In general, the author did not produce clear, specific results that were analyzed to the point of persuasion. (Stefanou 1983).

Macleod and Houmsi in 1994, they were conducted a study to estimate the shear strength on six RCHBS without stirrups, the angle of inclination of this RCHBs ranged between (5-10) degrees, a novel form of testing that allows shear failure in the negative moment region of a haunch was used. The authors concluded that the RCHBs increase the ductility and the researchers concluded that the RCHBs increase the susceptibility shear strength as the angle of inclination increases, the improvement increases (Macleod and Houmsi in 1994).

Tena et al. in 2008. A special study was based on the development of shear failure under the effect of static loading of RCHBs the study included a total of ten beams divided into two groups, each group has 5 beams (four of which are haunched and one prismatic) one of the two groups without shear reinforcement (stirrups) and the other group with stirrups. The stirrups were designed to meet the minimum requirements of the prismatic beams and according to Mexico's Federal District Code (MFDC). The depth of the beams was increased at the support, and the conducted beams have different slopes in bottom surface and the angle of inclination of the RCHBs ranged from 3 to 12 degrees as shown in Fig. 2.3. The experimental results observed that RCHBs indeed have more deformation capacity compared to the prismatic beams; however, ultimate shear strengths developed with compared to the prismatic beams then causing a failure mechanism that is less fragile than the typical sudden shear failure observed in prismatic beams. Tena et al published another article for reinforced concrete haunched beams. The authors have tested another ten beams with same geometries at the previous work under cyclic loading. The haunched beams develop higher deformation and energy dissipation capacities and smoother crack patterns compared to the prismatic beams (Hans and Tena 2013).

(Chenwei et al 2015). A study on shear failure mechanism was presented. The study included ten beams distributed over four groups with different parameters such as (thickness of concrete cover, existence stirrups, position of haunched portions, and arrangement of main steel reinforcement), the results experimental work demonstrated that the thicker concrete cover in the middle affected the crack propagation but no effect is obvious on the shear capacity. Various diagonal crack angles and produced in variation contribution by shear reinforcement (stirrups) in haunched beams with stirrups. The bending place of the main bars reinforcement as well as the different in the shear capacity due to variation contributions of the arch action.

(Aziz et al 2016). An experimental study was conducted to determine the shear behavior of the tapered beams (RCHBs) using self-compacted concrete. The work included six beams, one of which was Prismatic beam and the remaining five were tapered (non-prismatic shape). The dimensions of the RCHBs were kept constant for all tested beams, The variable parameters was adopted, shape of the tested beams, amount of stirrups and strengthening by CFRP strips as shown in Fig. 2.4. Test results show that the increase in shear capacity for haunched beam without web reinforcement as compared with the prismatic beam about (12%). The load capacity increased for RCHBS with half- minimum, and minimum web reinforcement, were (20%) and (33%) respectively as compared with RCHBs without web reinforcement, comparing with prismatic beam.

Albegmprli in 2017. The prospector presented a comprehensive study to highlight the behavior of different types of RCHBs. The experimental work consists of 20 RCHBs and 4 prismatic RC beams. The parameters that considered are inclination angle, beam type, flexural reinforcement and failure mode. The inclination angle and the inclined reinforcement are the most influential parameters on the behavior of RCHBs. The flexure behavior of RCHBs did not show a significant difference compared to prismatic beams. In addition, twenty-four experimentally tested beams and sixty-five existing experimentally tested beams in literature modeled via deterministic nonlinear finite element method. The comparison showed a good agreement between the results and thus the models can be effectively used for further studies of RCHB with high accuracy.

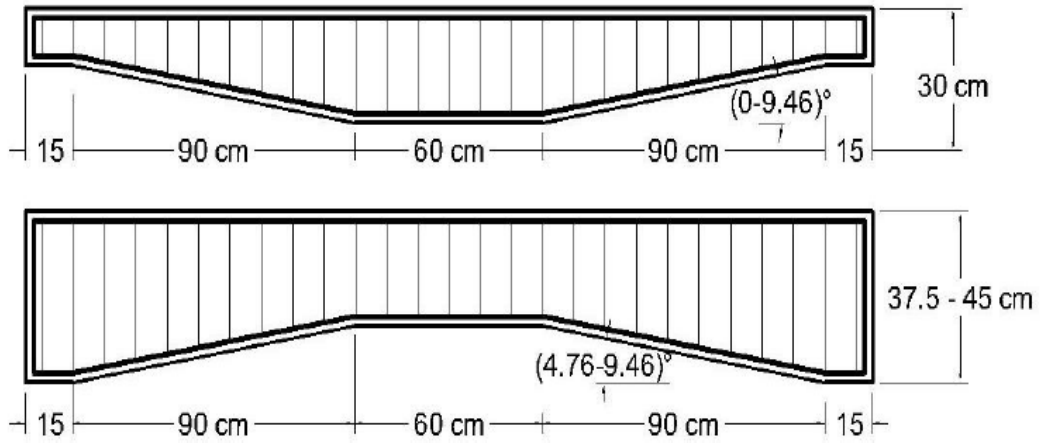


**Figure 2.1** Specimens tested beams by (Debaiky and Elniema 1982)

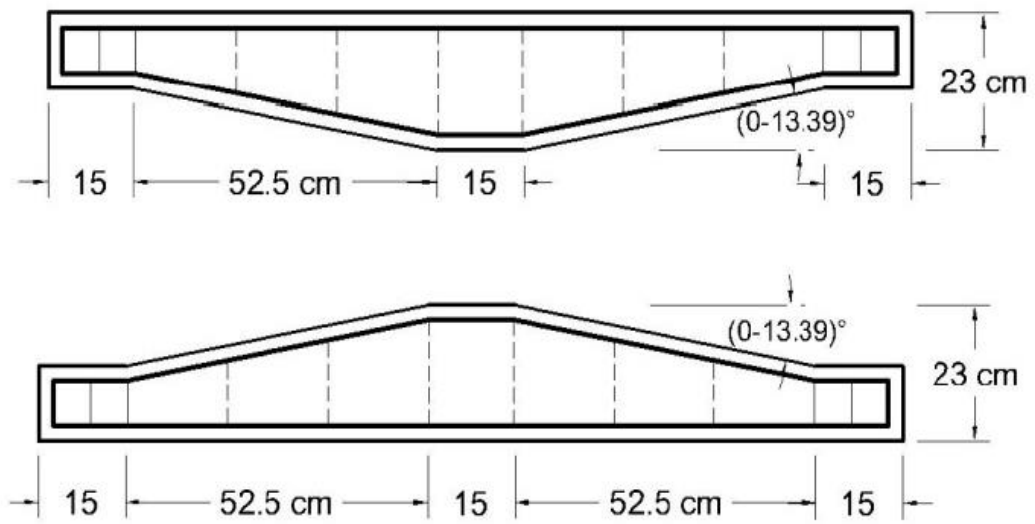


**Figure 2.2** Specimens tested beams by (Stefanou 1983)

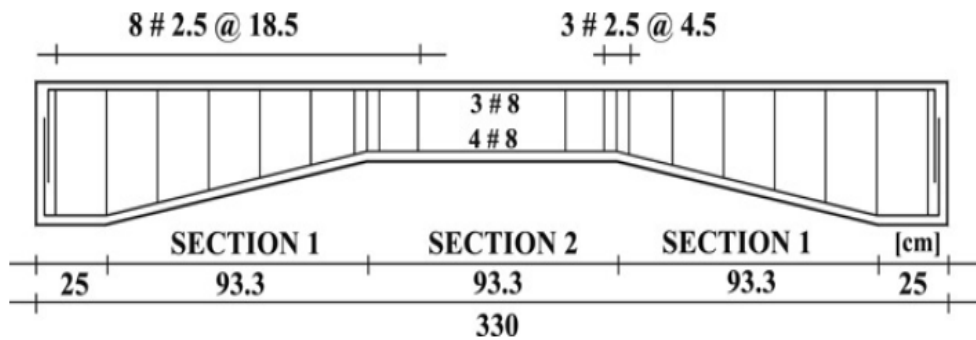


**Figure 2.3** Specimens tested beams by (Tena et al 2008)

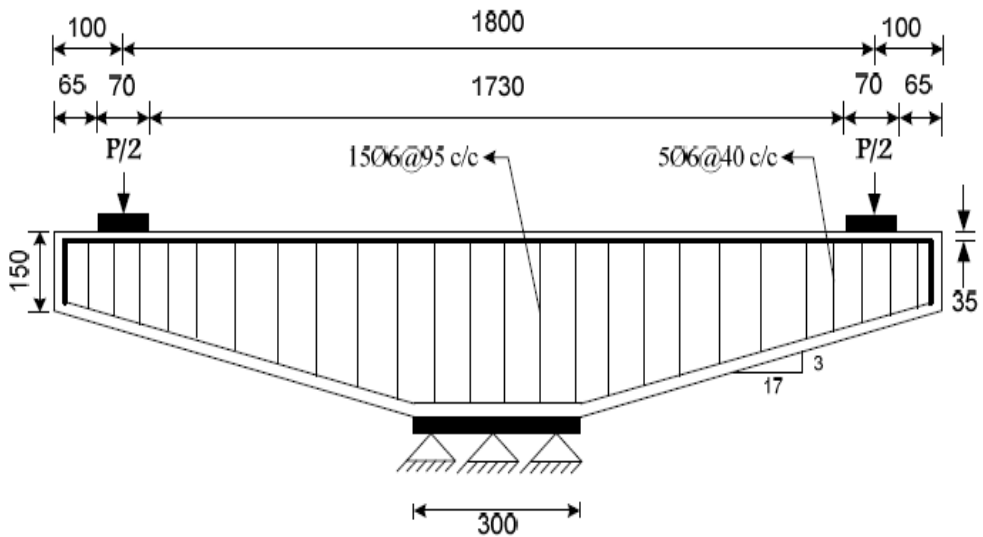
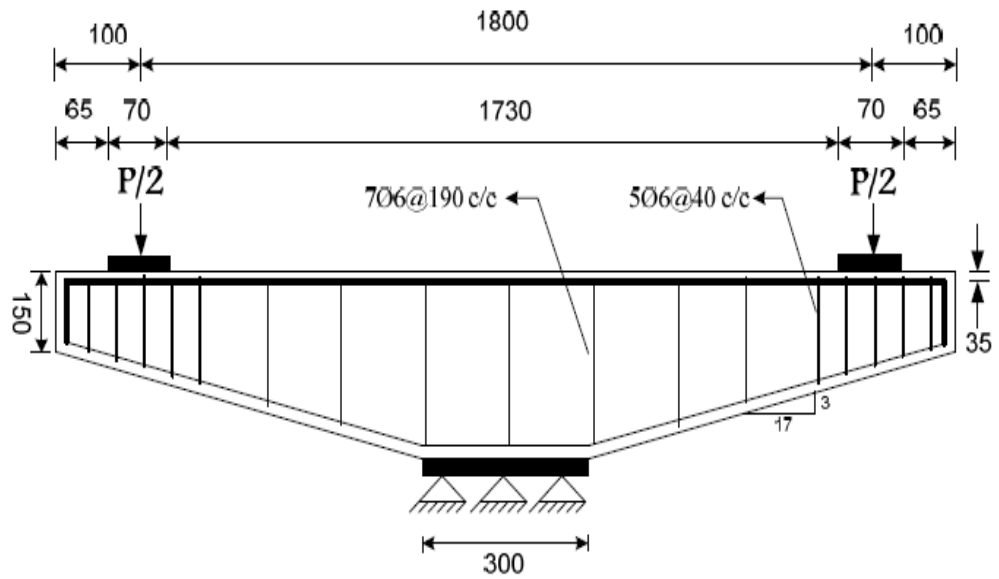


**Figure 2.4** Specimens tested beams by (Aziz, A.H. 2016)

### 2.3 Previous Studies about Steel Fiber Reinforced Concrete (SFRC)

**2.3.1 Overview:** Concrete is one of the most widely used materials in the structural applications of civil engineering. It is known that concrete is a brittle material; this property is not desirable constructively. So it became necessary to add some materials to the concrete mixture to make the concrete more ductility. Experience shows that concrete is weak in tension due to its brittle nature; that causes a sudden structural collapse without warning signs (ACI 544.1R-1996). One of the most important materials used is the steel fiber, which makes the concrete more ductility.

Romualdi and Batson (1963) initiated interest in steel fiber reinforced concrete (SFRC) in the late 1950's, where the behavior of tension poor concrete is improved by combination of steel fibers into the plain concrete mixture. The resulting interest has led to the main advantage is that the concrete continues to carry decreasing load after the maximum load is reached. Although the maximum load carrying capacity is not significantly changed by adding steel fibers to concrete. The post cracking resistance is primarily provided by pulling out of fibers from the cracked surface and this shape of failure results in an improved performance of the structure/component by giving the concrete some stiffness. According to ACI 318-08 permits use of (SFRC) (60 kg/m<sup>3</sup> or more of steel fibers giving a post cracking flexure prism strength greater than or equal to 90% of the cracking strength) as minimum shear reinforcement in flexural member.

$$(A_{v,min} = 0.0625 \sqrt{f'_c} b_w s / f_y \geq 0.35 b_w s / f_y) \quad (2.1)$$

### 2.3 Steel Fiber Reinforced Concrete (SFRC)

Graig et. al. (1987) study title the increased ductility of reinforced concrete sections subjected to clear bending with and without flexural reinforcement, and with and without SFRC. 4 beams with dimensions (178 x 380 mm ) were considered, 2 beams without steel fibers (SF) and the other two with SF ( for each group, one singly reinforced while the other beam is doubly reinforced ). The fiber volume fraction was 1.75% by volume and had aspect ratio of 100, the beams were tested under 4 point loads with a simply supported length of 2750 mm. The theoretical moment-rotation relationship was computed for each section using a computer program developed for this study. It was found that the use of SFRC increased the ductility of the section and improved the maximum moment capacity of the beam. The section ductility improved with the addition of fiber.

Soroushian and Lee (1990) presented theoretical expression for the quantity of fibers per unit cross-sectional area. Orientation of steel fibers in concrete and the amount of fibers per unit area are influenced by the limit to the random orientation of fibers and that steel fibers tend to stabilization. An important task of steel fibers in concrete is to detention and deflects micro cracks increase in concrete under external load effect.

The equation generally given in the study (Soroushian and Lee, 1990) to estimate the number of fibers per unit cross sectional area of concrete is of the form;

$$N_f = \eta_o \frac{V_f}{A_f} \quad (2.2)$$

where:

$N_f$  = Number of fibers per unit area

$V_f$  = Volume fraction of steel fiber in concrete

$A_f$  = Cross-sectional area of steel fibers =  $\pi \frac{d_f^2}{4}$

$d_f$  = Fiber diameter

$\eta_o$  = Orientation factor (0.41 -0.82)

When uniformly dispersed in an indeterminate large amount of concrete, SF are expected to be randomly guided with equal prospect in various directions in space.

Steel fibers may increase the maximum tensile strength of concrete because much capacity is absorbed in remove the bond and pulling out of fibers from the texture before occur complete separation and collapse of concrete occurs (Hwan Oh, 1992).

Steel Fibers also increase the shear-friction strength of concrete. Steel fibers have been used as shear reinforcement (stirrups) to resist shear, restriction crack propagation, and preserving post-micro crack safety of the surrounding concrete mix (ACI544-IR-82).

It is known that the workability of the concrete is reduced by the addition of the steel fiber. Therefore, practical percentage of steel fibers in normal concrete between from 0.5 to a maximum of 3 percent by volumetric ratio (Bayasi and Soroushian, 1992).

Workability of steel fiber concrete can be increased by using additional cementitious materials such as fly ash, silica fume, slag, , etc (ACI-544.1R, 1996). Steel fiber concrete mixes with good workability can be made by using additional cementitious materials up to 15% by cement weight (Balaguru and Dipsia, 1993 and ACI-544.1R, 1996).

Mitchell et. al. (1996) studied the effect of SFRC on the behavior of reinforced concrete subjected to clear tension. 12 tension specimens by cross section 95x172 mm and 1500 mm long were tested. 6 specimens were prepared with normal-strength concrete with and without SFRC, and another 6 specimens were prepared with high-strength concrete, with and without, SFRC. The SFRC used was hooked end with

length of 30 mm and diameter of 0.5 mm. The ratio of SFRC used was 1%. A single No. 15 bar was used in each specimen with a 1.23% reinforcement ratio. A Transducer (LVDT) was adjusted on two sides of the specimens. By using a crack width comparator the cracks were measured after each load stage. It was found that the SFRC increased the ductility tensile and tension strength for normal and high strength concrete. After cracking and noticeably deformation, reinforced concrete exhibit some degree of tension stiffening. After reach the reinforcement bars to yielding, only the specimens with steel fiber observed stiffening. SFRC reduced crack widths in each high strength and normal concrete, normal concrete appeared bigger crack widths than high strength concrete specimens. SFRC prevented bond-splitting cracks from propagating in each high strength and normal concrete.

Cohen M. (2012) the experimental study concerned to the behavior self-compacting concrete beams with steel fiber, the study included 12 concrete beams under four points load; the aim of the study is to verify the use of steel fiber instead of the stirrups bars used to resist shear forces. The results showed the combined use of SCC and SFRC can increase the shear resistance of reinforced concrete beams, improve crack control and can increase flexural ductility. This study presents a rational model, which can exactly predict the shear resistance of SFRC.

## CHAPTER THREE

### EXPERIMENTAL PROGRAM

#### 3.1 Introduction

In this part of experimental work, 12 RC beams were included. To study several the mechanical behavior of beams, it was adopted variables parameters such as reinforcement ratio, angle of inclination and steel fiber ratio. The RC beams was divided into two main groups every group 6 beams. There is a difference between two groups reinforcements ratios the first group whose value 0.020 (3Ø12 Bottom, 2Ø8 Top) and for second group 0.0310 (2Ø18 Bottom, 3Ø8 Top) used. Every group includes two prismatic beams, two haunched beams (H10°) and two haunched beams (H15°).

In general, half beams are contain steel fiber ratio 0.5 % (as volumetric) and another half have 0 % steel fiber ratio.

#### 3.2 Objectives

The purpose of the experimental work:

1. To get information for mechanical properties of haunched beams comparison with prismatic beam.
2. Study the effectiveness the steel fiber ratio.
3. Study the influence inclination of angle for RCHBs to mechanical properties.
4. Investigation of influence for steel reinforcement ratio and observed the shape of failure.

### 3.3 Materials

#### 3.3.1 Concrete Mixture Design

The type of concrete self-compact (SCC) was used and the amount of materials for this mix design shown in Table. (3.1), specification of mix design set by (EFNARC) requirements.

**Table 3.1** Weight of concrete mix components of one cubic meter

Material	Gravel	Sand	Cement	Fly Ash	Water	Super plasticizer
Weight Kg/m <sup>3</sup>	730	900	300	250	170	5

**Table 3.2** Weight of concrete mix components of one cubic meter with steel fiber

Material	Gravel	Sand	Cement	Fly Ash	Water	Super plasticizer	Steel fiber
Weight Kg/m <sup>3</sup>	730	900	300	250	170	5.5	39.250

Properties of materials for concrete mix design

1. The aggregate crush stone (gravel) and sand are brought from the same origin, the gavel was 12mm maximum aggregate size and the sand passed through 4mm (sieve no.) and volumetric gradients of aggregate as shown in Fig. 3.1
2. Fly Ash (type F).
3. Type of cement Portland class (32.5 R).
4. Sika ViscoCrete- SF 18 is used (superplasticizer), this type suitable for Self-Compact Concrete (SCC).
5. Steel fiber type 3D 45/35 B in this study a 0.5% ratio of steel fiber was used for 6 beams to compare with another beams without steel fiber. This type production conforms to ASTM A820 and his specification as shown in Fig. 3.2.

- To all beams, two concrete mixtures were adopted with a single compressive strength.

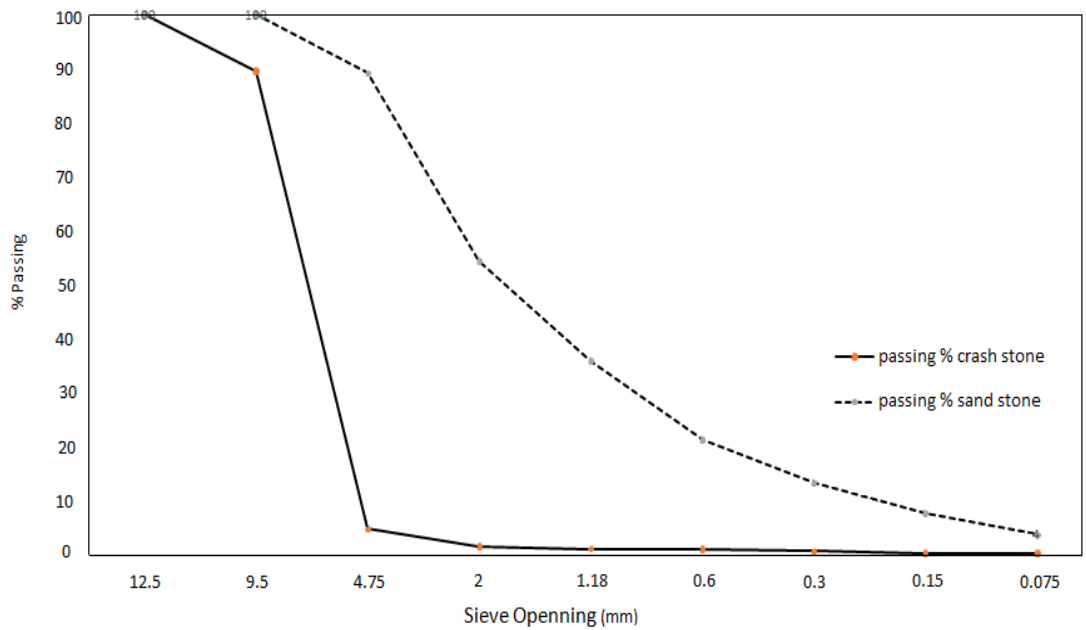


**Figure 3.1** Volumetric gradients for aggregate


### PERFORMANCE


**Material properties**


**Tensile strength:**  $R_{m, nom}$ : 1.225 N/mm<sup>2</sup>  
Tolerances:  $\pm 7,5\%$  Avg


**Young's Modulus:**  $\pm 210.000$  N/mm<sup>2</sup>

**Geometry**

**Fibre family**      **3D**      

**Length (l)**      35 mm      










**Diameter (d)**      0,75 mm      

**Aspect ratio (l/d)**      45      

**Fibre network**

8,7 km per m<sup>3</sup> (for 30 kg/m<sup>3</sup>)  
7.814 fibres/kg

**Dramix® range**

	5D	4D	3D
Tensile strength			
Wire ductility			
Anchorage strength			

**Figure 3.2** Used Steel Fiber Specifications [Adapted from srfiber website]

### 3.3.2 Steel reinforcement

Three variable diameters bars of steel reinforcement were used. The diameters bars of steel were included (18, 12 and 8) mm for longitudinal reinforcement and  $\text{Ø}6$  mm for stirrups was used. The results of the test of reinforcement bars as shown in the Table (3.2).

**Table 3.3** Result of steel bars reinforcement



Diameter mm	18	12	8
Yield Strength MPa	456	485	550
Ultimate strength MPa	560	595	640

**Figure 3.3** Reinforcement bar on test machine

### 3.4 The Geometries

The experimental work contains 12 beams divided to three groups by the shape of the beam (inclination of angle).

The beams were distributed to three groups A, B and C, classification of modes as follows.

- Mode A refers to the prismatic beam (P)
- Mode B refers to RCHBs ( $H10^\circ$ ) inclination of angle the depth of the beam increase toward the mid-span.
- Mode C refers to RCHBs ( $H15^\circ$ ) inclination of angle the depth of the beam increase toward the mid-span.

Every beam has length 1200 mm, length of beam was supported 1050 mm and width 120 mm. Fixing The depth of the beams at the mid-span; 210 mm for all beams.

The depths are selected due to the effective depth  $a/d > 2.5$ , the details for every beam will be explained in Table 3.3.

### 3.4.1 Identification

The identification of the beams depends of three symbols [Character (B) + Number-Character (Mode)-Steel fiber ratio] like B1-P-0.5:

- The first character (B) with Number refers to the number of the beam like B1, B2.... etc., the total quantity of beam is 12 were encoded from B1 to B12.
- The second character refers to the type of beam like ( P,H10°&H15°) the character P refers to the prismatic beam type; H10° refers to RCHBs inclination of angle (10) degree, and the character H15° refers to RCHBs inclination of angle (15) degree.
- The third number refers to the percentage steel fiber ratio like (0,0.5)
- From numbers (B1 to B6) the beams were reinforced by 3 bars 12 mm (diameter) in flexural and 2 bars 8 mm in compression zone.
- From numbers (B7 to B12) the beams were reinforced by 2 bars 18 mm (diameter) in flexural and 3 bars 8 mm in compression zone, all the beams were reinforced shear stirrups bar 6 mm (diameter) each 90 mm.

### 3.4.2 Group A

In this group, all the beams made are prismatic encoded (P).

- This group includes 4 beams divided to (B1 and B2) reinforced by 3 bars 12 mm (diameter) in flexural and 2 bars 8 mm in the compression zone as shown in Fig. 3.2 and steel reinforcement ratio (0, 0.5) respectively.
- The beams (B11 and B1) reinforced by reinforced by 2 bars 18 mm (diameter) in flexural and 3 bars 8 mm in compression zone as shown in Fig. 3.3 and steel reinforcement ratio (0, 0.5) respectively.

### 3.4.3 Group B

In this group all the beam made are RCHBs encoded (H10°) In this group the upper face of the beam was inclined where the mid-span has constant height 210 mm and decreased toward the support.

- The inclination of angle ( $\alpha$ ) equals (9.74)°

- This group includes 4 beams divided to (B3 and B5) reinforced by 3 bars 12 mm (diameter) in flexural and 2 bars 8 mm in the compression zone as shown in Fig. 3.4 and steel reinforcement ratio (0,0.5) Respectively.
- The beams (B7 and B9) reinforced by 2 bars 18 mm (diameter) in flexural and 3 bars 8 mm in the compression zone as shown in Fig. 3.5 and steel reinforcement ratio (0,0.5) Respectively.

### 3.4.5 Group C

In this group all the beam made are RCHBs encoded (H15°) In this group the upper face of the beam was inclined where the mid-span has constant height 210 mm and decreased toward the support.

- The inclination of angle ( $\alpha$ ) equals (14.45)°
- This group includes 4 beams divided to (B4 and B6) reinforced by 3 bars 12 mm (diameter) in flexural and 2 bars 8 mm in compression zone as shown in Fig. 3.6 and steel reinforcement ratio (0,0.5) Respectively.
- The beams (B8 and B10) reinforced by 2 bars 18 mm (diameter) in flexural and 3 bars 8 mm in compression zone as shown in Fig. 3.7 and steel reinforcement ratio (0,0.5) Respectively.

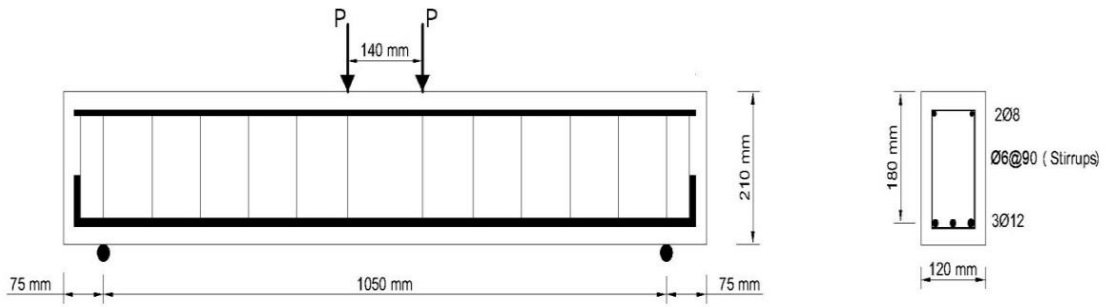


**Figure 3.4** Geometry of beam (B1-P-0 and B2-P-0.5)

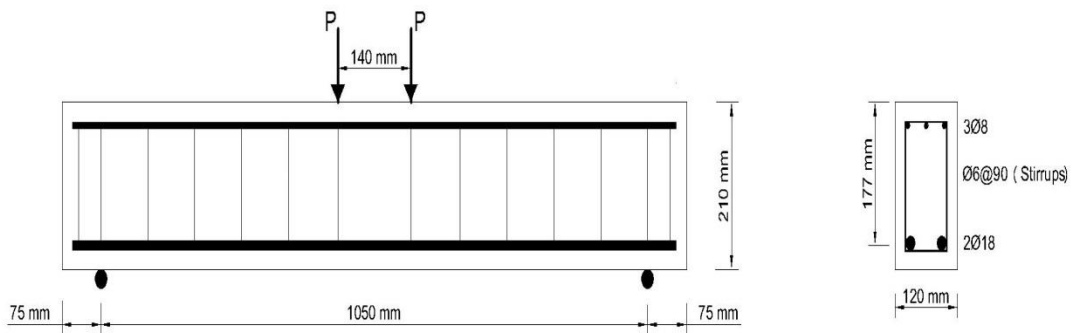


**Figure 3.5** Geometry of beam (B11-P-0 and B12-P-0.5)

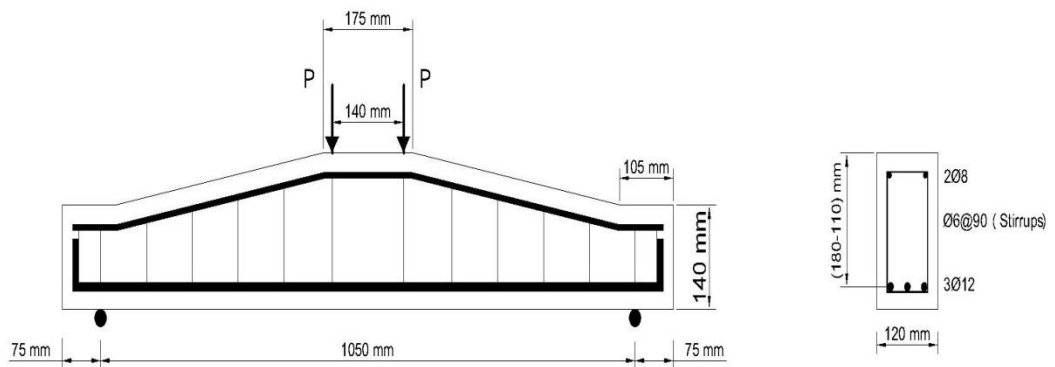


**Figure 3.6** Geometry of beam (B3-H10<sup>0</sup>-0 and B5-H10<sup>0</sup>-0.5)

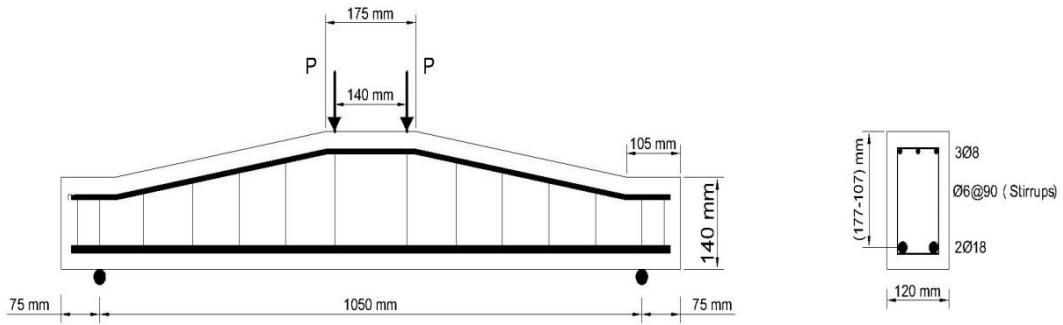


**Figure 3.7** Geometry of beam (B7-H10°-0 and B9-H10°-0.5)

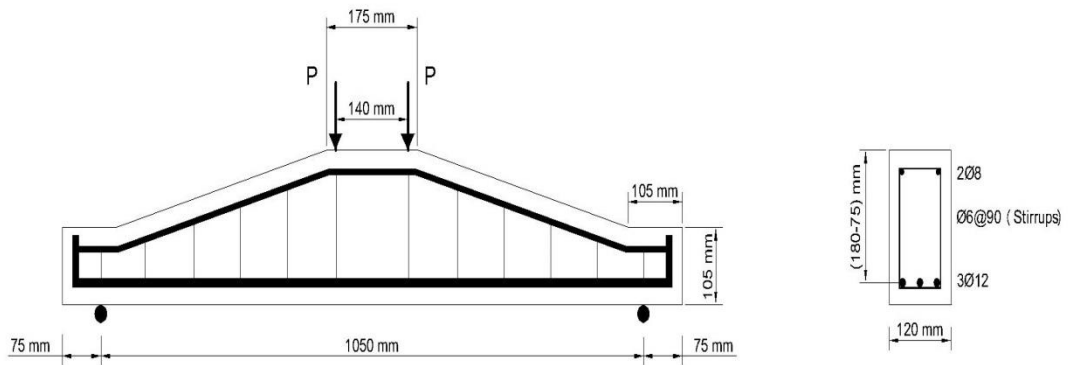


**Figure 3.8** Geometry of beam (B4-H15°-0 and B6-H15°-0.5)

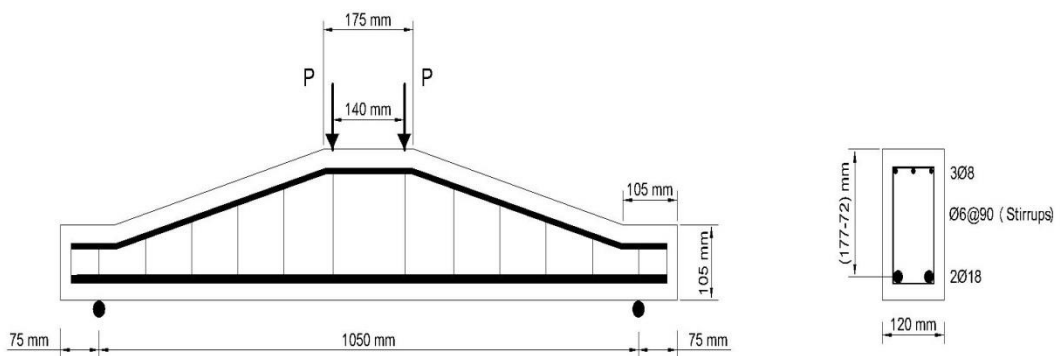


**Figure 3.9** Geometry of beam (B8-H15°-0 and B10-H15°-0.5)

**Table 3.4** Geometries of beams.

Beam code	Mod e	$\alpha^\circ$	$h_m^*$ (mm)	$h_s^*$ (mm)	Vf %	Reinforced details			
						$A_s$ (mm <sup>2</sup> )	N0. Steel	$A_{s'}$ (mm <sup>2</sup> )	N0. Steel
B1-P-0	A	0	210	210	0	340	3Ø12	100	2Ø8
B2-P-0.5	A	0	210	210	0.5	340	3Ø12	100	2Ø8
B11-P-0	A	0	210	210	0	509	2Ø18	150	3Ø8
B12-P-0.5	A	0	210	210	0.5	509	2Ø18	150	3Ø8
B3-H10 <sup>0</sup> -0	B	9.74	210	140	0	340	3Ø12	100	2Ø8
B5-H10 <sup>0</sup> -0.5	B	9.74	210	140	0.5	340	3Ø12	100	2Ø8
B7-H10 <sup>0</sup> -0	B	9.74	210	140	0	509	2Ø18	150	3Ø8
B9-H10 <sup>0</sup> -0.5	B	9.74	210	140	0.5	509	2Ø18	150	3Ø8
B4-H15 <sup>0</sup> -0	C	14.45	210	105	0	340	3Ø12	100	2Ø8
B6-H15 <sup>0</sup> -0.5	C	14.45	210	105	0.5	340	3Ø12	100	2Ø8
B8-H15 <sup>0</sup> -0	C	14.45	210	105	0	509	2Ø18	150	3Ø8
B10-H15 <sup>0</sup> -0.5	C	14.45	210	105	0.5	509	2Ø18	150	3Ø8

$\alpha^\circ$ : Inclination of angle       $h_m$ : depth at middle       $h_s$ : depth at the supports

Vf % : Steel fiber percentage amount       $A_s$ : Area of steel for flexural zone

$A_{s'}$  : Area of steel in compression zone

### 3.5 Preparing and Casting of Test Specimens

Formwork for all beams have been processed from (plywood) and mold of angle was prepared from steel and Reinforcement steel was made in accordance with the mold, all activities have been conducted at the university Lab. Processing of the reinforcement works and laying the steel reinforcement in the formwork as shown in Fig.3.8 & Fig.3.9.



**Figure 3.10** Reinforcement processing works



**Figure 3.11** Reinforcement and Formwork preparing.

The concrete was mixed with one mix for each of the two beam with cylinders and cubes specimens about 170 liters shown in Fig.3.12, It was a self-Compacting Concrete tested by examining slump flow test T50, rating the apparent stability of the

slump flow according “Testing-SCC” (De Schutter 2001). The result of T50 was (715 mm by 2.7 seconds) as shown in Fig.3.13. Every two beams were prepared by one mixer with 1 cube (150\*150\*150)mm,3 cubes (100\*100\*100) mm and 3 cylinders (100\*200) mm, they were made as sampled cube to find compressive strength while as cylinders to find splitting strength as shown in Fig.3.14. The beams and samples were extracted after 24 hours of casting and placed in the water basin for 28 days as shown in Fig.3.15. After the curing period (28 days), the beams and samples were ready for testing as shown in Fig.3.16.



**a. Mixing**



**b. Concrete dump**

**Figure 3.12** Mixing of concrete



a. Slump flow test and T50 apparatus

b. Slump flow test

**Figure 3.13** Slump flow test with steel fiber ratio (0.5%)



a. Removing formwork after casting



b. Samples for each one mix (2 beams)

**Figure 3.14** Beams and samples after casting



**Figure 3.15** Curing beams and samples 28 day

### 3.6 Preparing Specimens for test

All beams and samples have been cured in water tank for 28 days where they are prepared for the test of each group that completes its curing and thus sequentially. After drying each beam, it is cleaned well and then was painted with a white concrete paint, and then a grid is drawn on the beam face with a distance of (5\*5cm) as shown in Fig.3.16. The cracking load was fixed by a red color and when the failure load is reached, it is encoded in green color the purpose of the painting process and the work of the grid is to clarify the cracking paths and load values of each crack. At the same time, each set of samples of the cubes and cylinders of each beam is prepared to be tested for compressive strength values and splitting strength test.



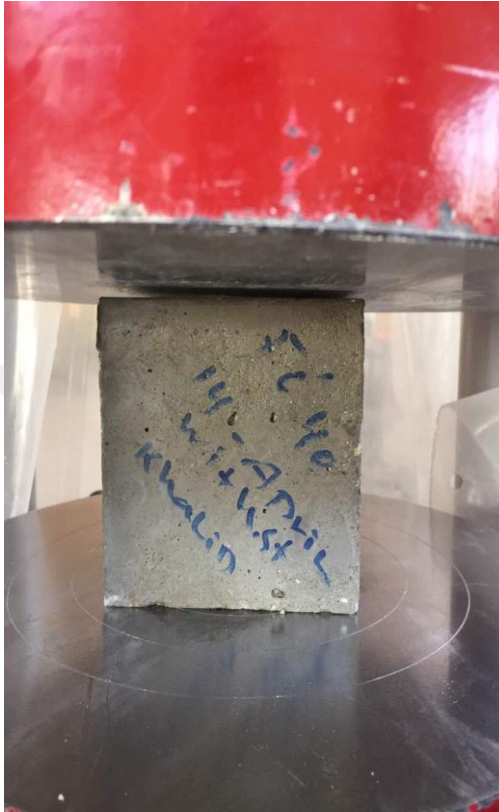
**Figure 3.16** Preparing beams for test

### 3.7 Testing Procedure

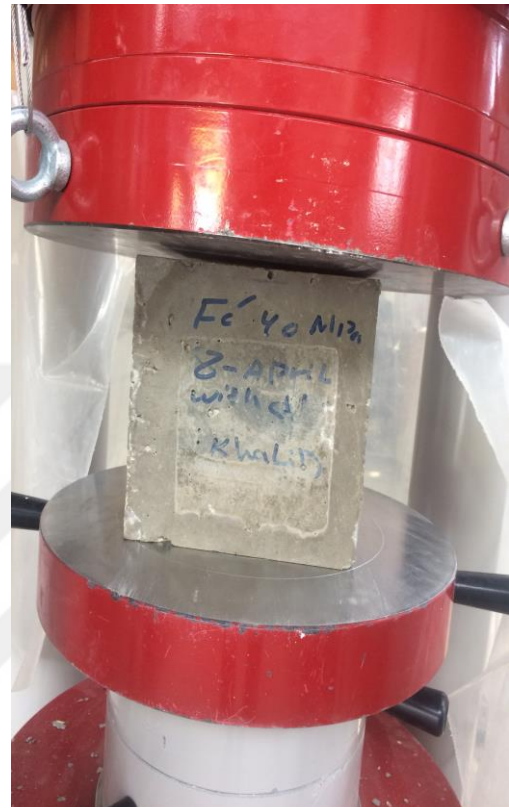
#### 3.7.1 Concrete Samples

Each concrete mixture contains one beam, three (100\*100\*100) mm cubes and three (100\*200) mm cylinders and one (150\*150\*150) mm cube have been taken to test the concrete properties. The cubes (100\*100\*100) mm and (150\*150\*150) mm are used to find compressive strength of concrete mixture as shown in Fig.3.17, While testing the cylinders is used to find splitting tensile strength as shown in Fig.3.18 . The concrete samples were tested using Load and displacement controlled hydraulic compression testing machine 3000 kN capacity. The compressive strength was

founded according to BS1881-116 specification with a rate of loading 4 kN/s using (100 \*100\*100) mm and (150\*150\*150) mmm cubes, the splitting tensile strength was founded by testing small cylinder (100 \*200) mm according to ASTM C496 and EN 12390-6 specifications.



a. Small cube



b. Big cube

**Figure 3.17** Compressive strength testing



a. Installation of sample



b. Sample after crush

**Figure 3.18** Splitting tensile strength test

### 3.7.2 Testing Specimens

All of the beams were tested by a displacement controlled servo-hydraulic flexural testing machine of 500 kN maximum capacity. Load was applied to samples and it is controlled using an advanced hydraulic system. All of the beams were tested under three bending points using displacement control. The displacement was applied using two rods at mid-span the distance between the rods is 14 cm. The distance between the two point's supports was 1050 mm; one of the supports was fixed and another support is free to rotate.

Gradually displacement was increased by 0.2 mm / min and the load value is stabilized at each increase in the displacement rate, displacement and crack propagation. The increase continues to load as well as the displacement beam that fails, and then fixed. The beam installation on the test machine is shown in Fig.3.19 and Fig.3.20 shows the loading procedure.

The following tools were used in sampling and fixing results:

- A computer device for controlling and reading load and displacement.
- Three LVDT transducers for measuring the deflection connected to the computer.
- Camera for high-resolution images showing the evolution of cracks for each stage with load.
- A high-magnification camera for monitoring the cracks.

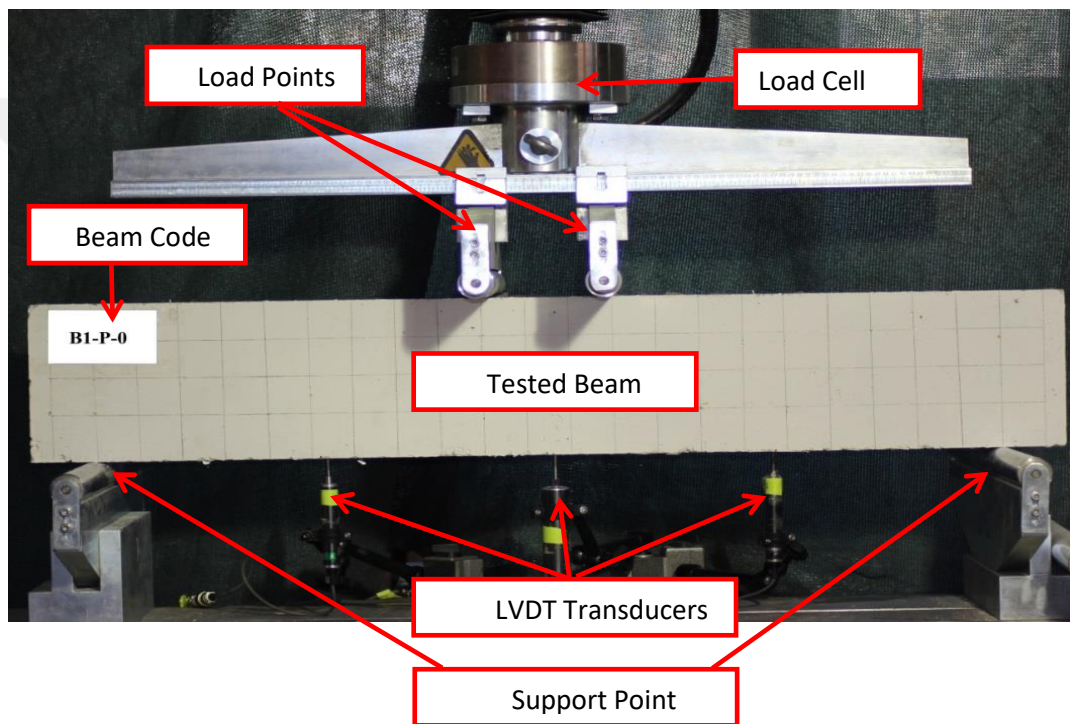


**Figure 3.19** Testing installation of the beam

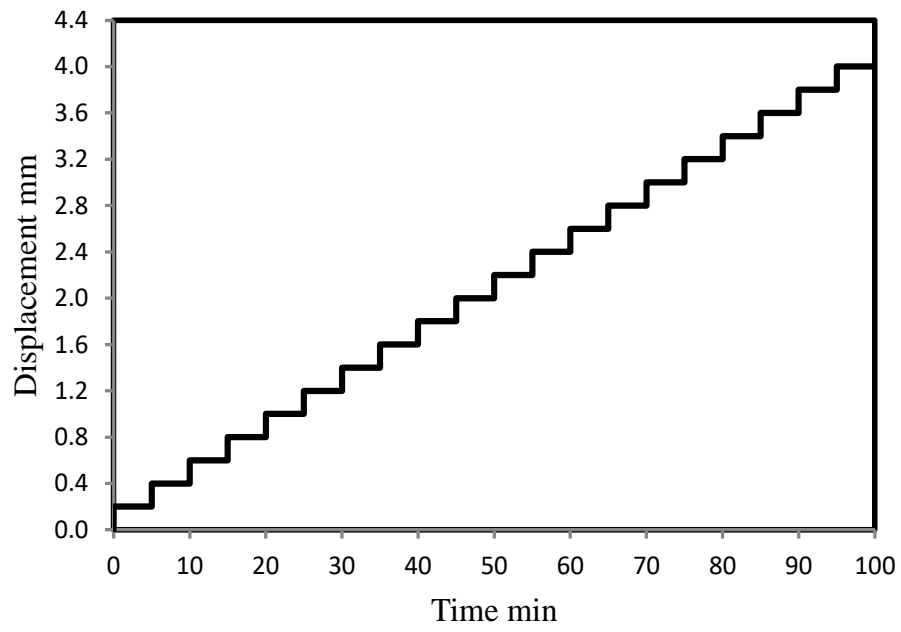


**Figure 3.20** Loading procedure

## **CHAPTER FOUR**

### **EXPERIMENTAL RESULTS AND DISCUSSION**

#### **4.1 Overview**

All of the 12 beams with cubes and cylinders samples were tested. All results and readings were documented and details will be documented later such as compressive strength, splitting strength, shape of failure, primary and maximum cracks. Moreover, maximum load causing failure in this chapter, the results of the tests and the comparison and the extent of the influence of the variables parameters that were introduced in this study will be based on the results and readings. The effect of the variable parameters will be shown in the shape of failure for each beam and its effect on the maximum load value represented by the following:

1. Effect reinforcement steel ratio.
2. Effect angle of inclination.
3. Effect steel fiber ratio.

In addition, the relationship between load and displacement of each beam will be determined, as well as the extent of the effect of the same relationship on one group of beams and the extent of the influence of different parameters on the relationship of load with displacement. In addition, will clarify the cracks on the sample with the load causing these cracks.

#### **4.2 Testing results**

##### **4.2.1 Material properties**

Table 4.1 contains the results of tests for each beam such as compressive strength, splitting strength test for concrete and others, as indicated.

**4.2.2 Failure Load** Figure 3.19 shows the installation mechanism and the process of testing all beams. This method is based on the principle of application load, with

continuous displacement leading to the failure of the beam (collapse). Generally, all the samples were reinforced against the shear stresses (stirrups). Most of the specimens were 8 beams where failure occurred in the form of flexure. The load continues to remain with the displacement until a large cracking in the middle of the beam from the bottom with cracks in the middle of the top between the two points load and after the drop of the value of the force indicating the failure of the beam and as shown in Fig. 4.1

While 4 beams have failed in the form of a diagonal shear crack, suddenly occur on one side of the beam, and continue to apply. The load begins to force the value of descent indicating the failure of the sample is shown in Fig.4.2.

In Table 4.1, the process will include the shape of failure for each beam with the maximum load causing failure with the primary and maximum cracks that occurred for each beam with the load value causing the crack and in detail.

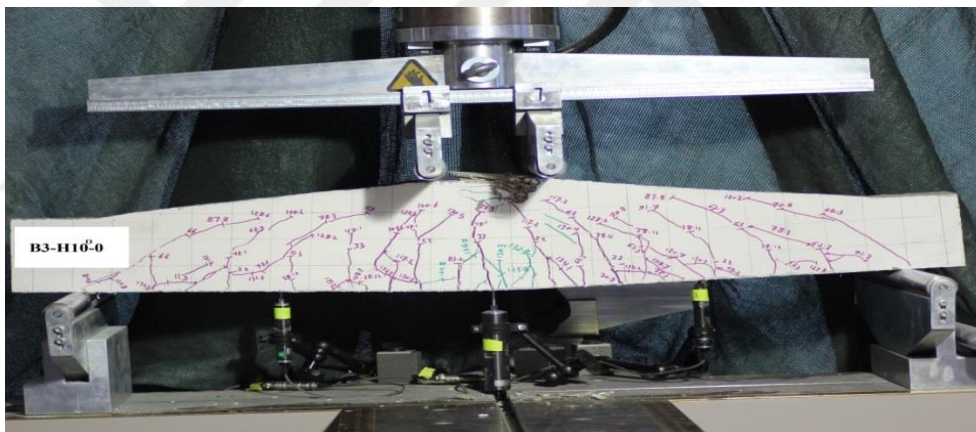


**Figure 4.1** Flexural failure

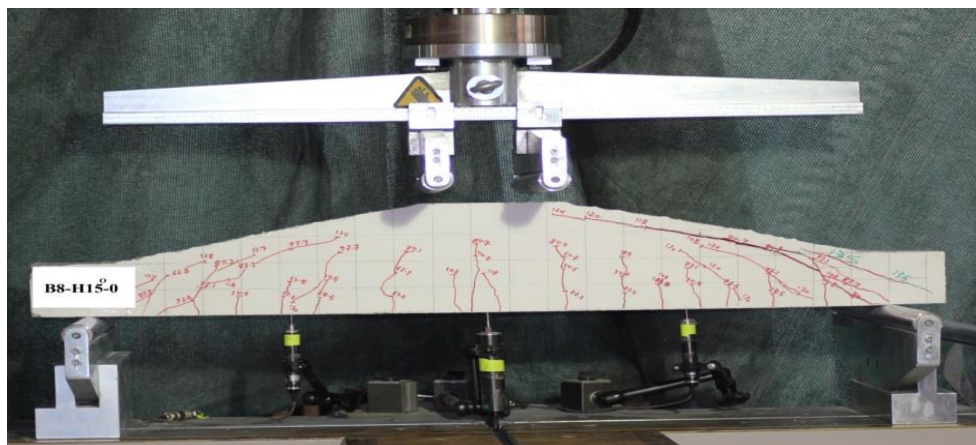


**Figure 4.2** Shear failure

**Table 4.1** Results of experimental tests

<b>Beam No.</b>	<b><math>f_{cu}</math> Mpa</b>	<b><math>f_{ct}</math> Mpa</b>	<b>Load at First crack kN</b>	<b>First crack width (mm)</b>	<b>Diagonal crack load kN</b>	<b><math>d_{cr}</math> mm</b>	<b>Max. Load 2P (kN)</b>	<b>Max. crack width (mm)</b>	<b>Fail. Mode</b>
<b>B1</b>	46	3.67	27	0.4	----	----	130	1.80	F
<b>B2</b>	43	3.91	28	0.32	----	----	134	1.60	F
<b>B11</b>	41	3.43	31	0.37	----	----	166	1.30	F
<b>B12</b>	43	4.13	27	0.31	----	----	175	1.15	F
<b>B3</b>	45	3.97	22	0.32	----	----	134	1.15	F
<b>B5</b>	50	4.18	30	0.28	----	----	138	1.10	F
<b>B7</b>	49	3.1	23	0.31	110	155	181	1.5	S
<b>B9</b>	44	4	24	0.25	----	----	194	1	F
<b>B4</b>	43	4.12	17	0.30	127	160	127	2	S
<b>B6</b>	50	4.18	20	0.33	----	----	138	1.7	F
<b>B8</b>	49	3.1	22	0.4	135	140	136	1.75	S
<b>B10</b>	44	4	17	0.34	174	120	174	1.4	S

 **$f_{cu}$** : Cubic Compressive Strength **$f_{ct}$** : Splitting strength**S**: Shear failure Mode**F**: Flexural failure mode **$d_{cr}$** : Critical effective depth

### 4.2.3 Relationship between Load and Deflection

The relationship between the load and displacement was determined for each beam as shown from the figures 4.4 - 4.15. The value of the displacement was taken through the three sensors LVDT transducers where TML-CPD transducers are used to read the displacement and NI cDAQ-9184 data, LVDT were distributed in the middle and the right and the other in the left, as shown in the figure 4.3. The readings are taken automatically to the computer taking into account the value of the load causing the displacement. The relationship between load and displacement of similar beams will be drawn in the angle of inclination, such as the A,B and C mode. As shown in the figures (4.16- 4.18),The effect of the angle of inclination, the effect of the steel reinforcement ratio and the steel fiber ratio of the beams will be shown by drawing the relationship between load and displacement and will be shown successively.

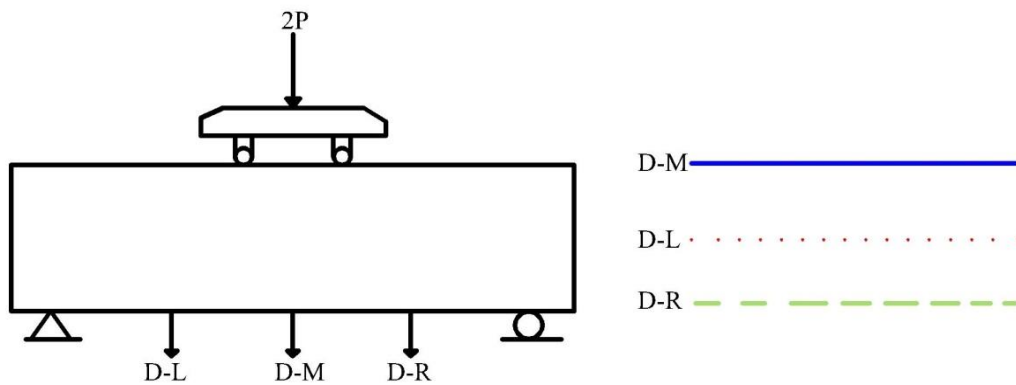


**Figure 4.3** Test result indicators

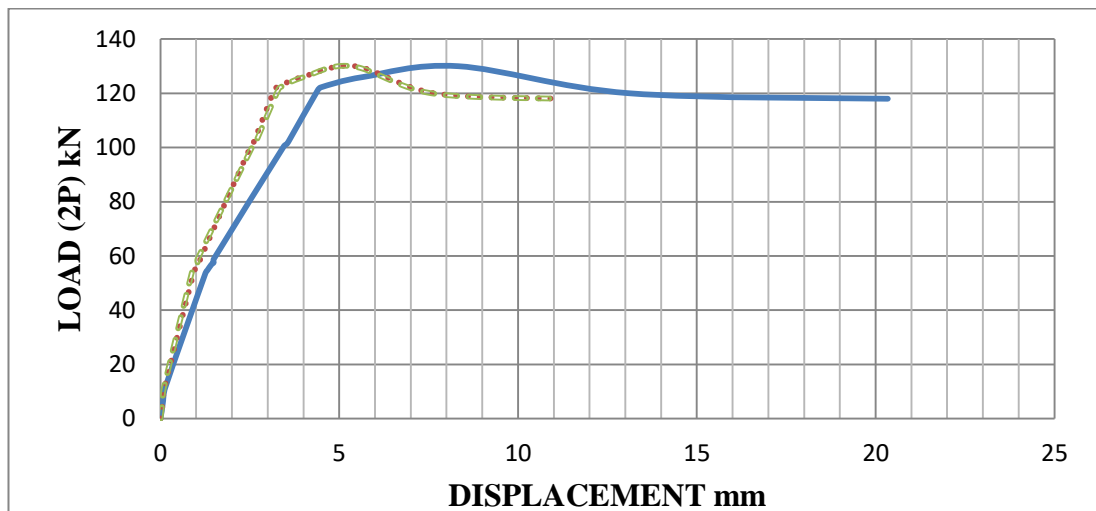


**Figure 4.4** Load-Displacement Relationship ( B1-P-0)

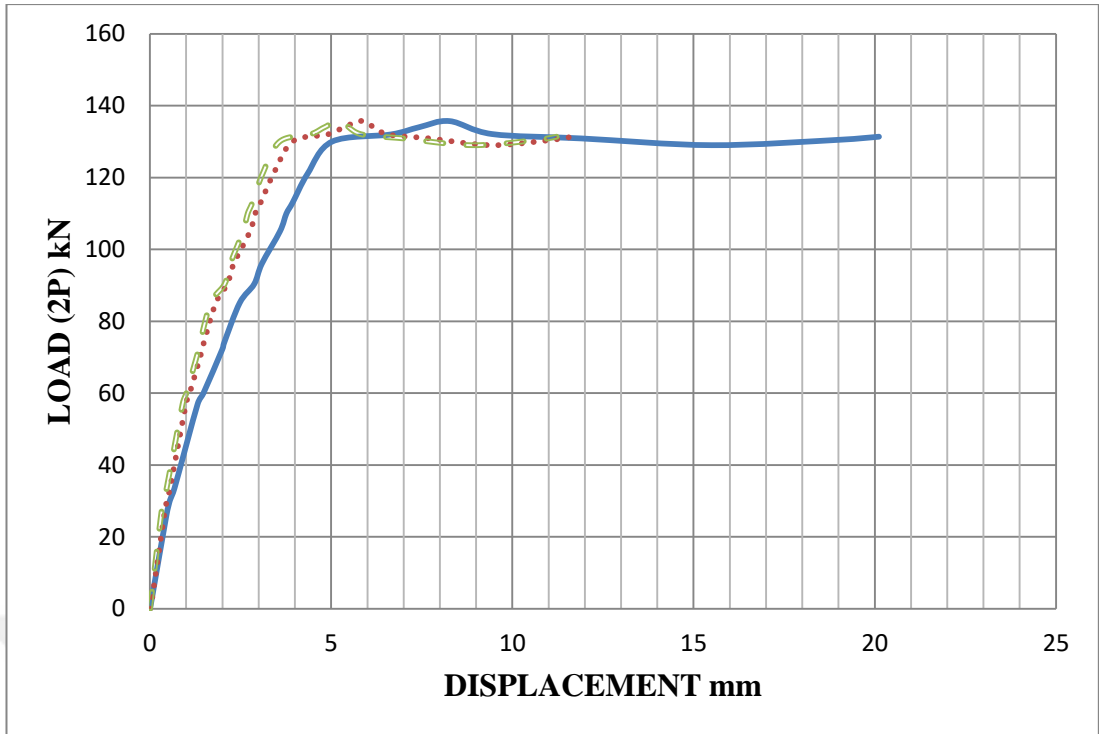


**Figure 4.5** Load-Displacement Relationship (B2-P-0.5)

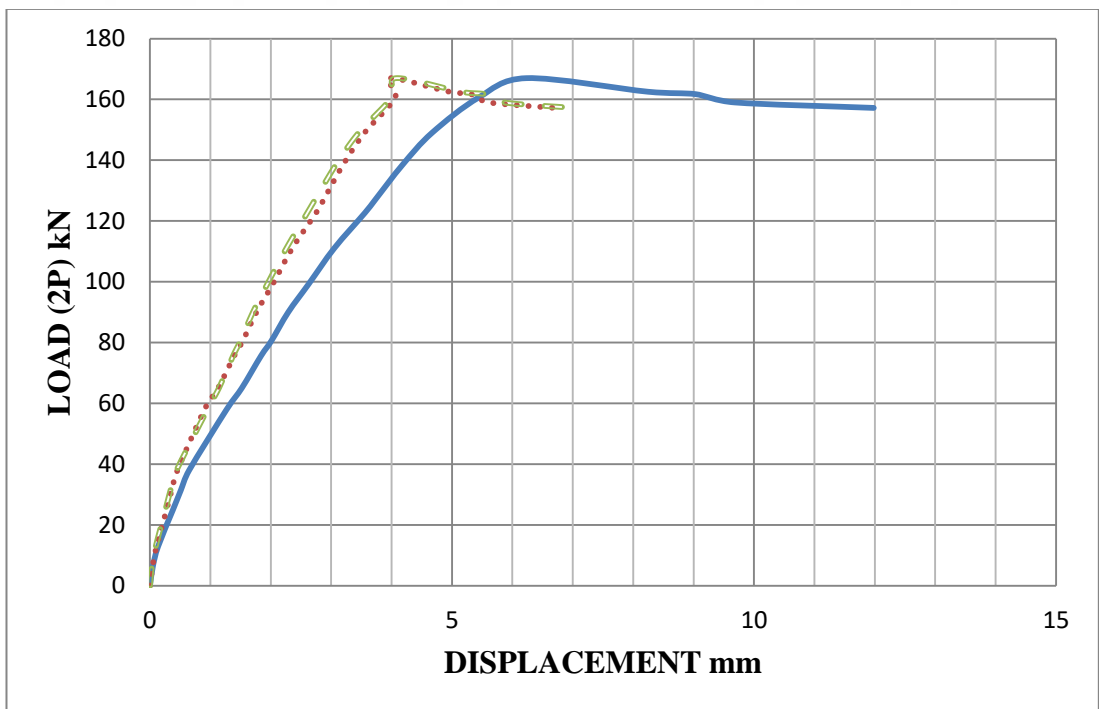


**Figure 4.6** Load-Displacement Relationship (B11-P-0)

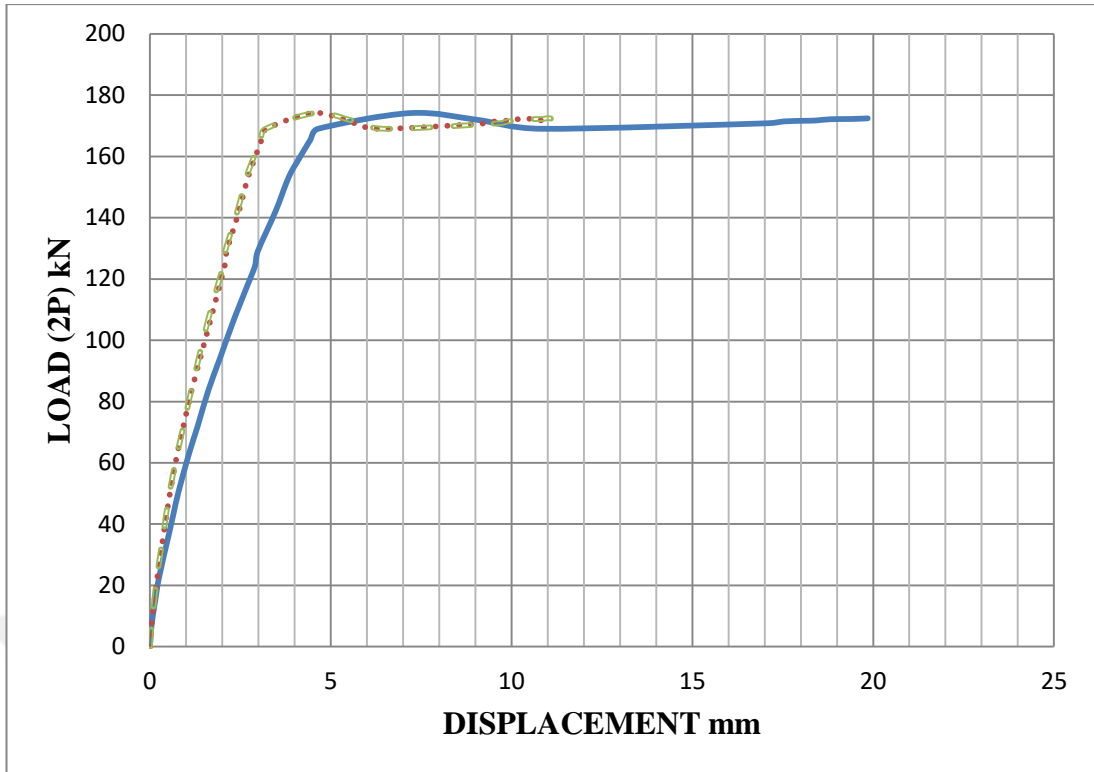


**Figure 4.7** Load-Displacement Relationship (B12-P-0.5)

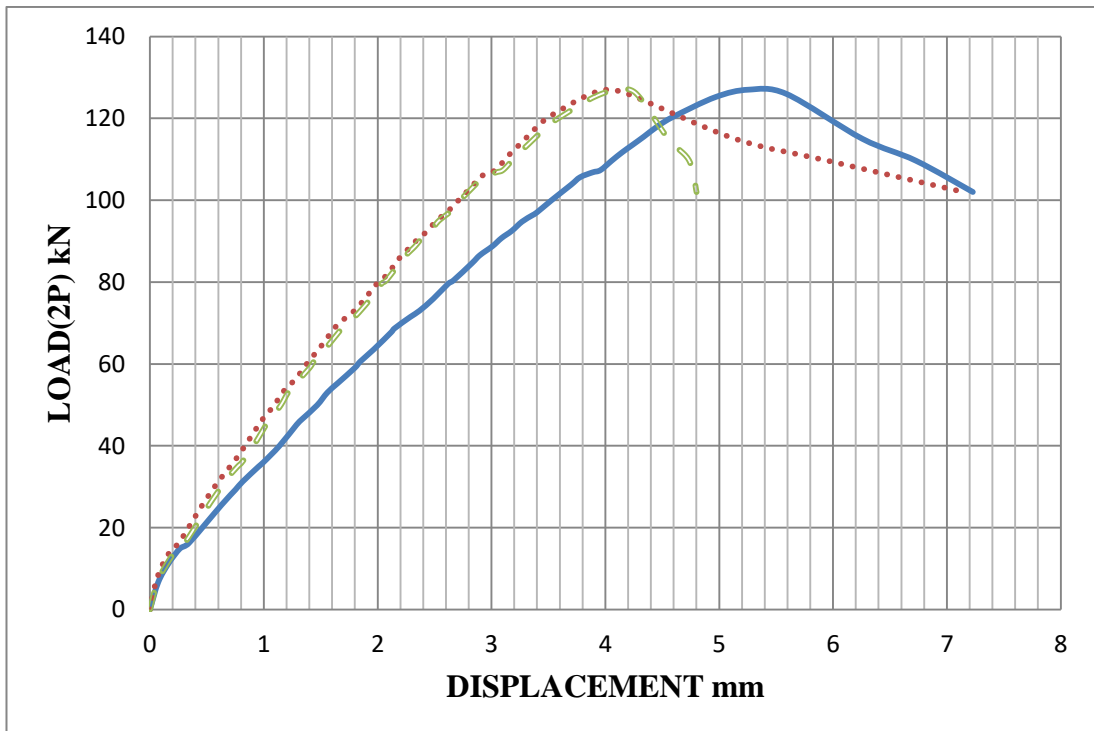


**Figure 4.8** Load-Displacement Relationship (B4-H15°-0)

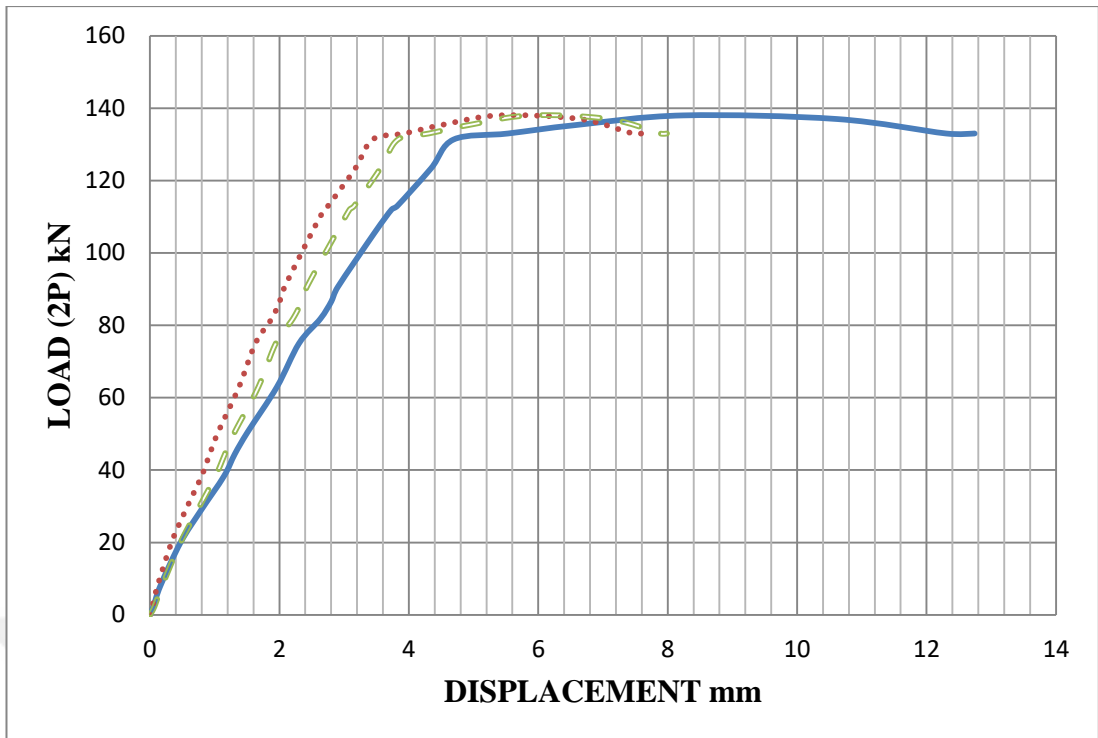


**Figure 4.9** Load-Displacement Relationship (B6-H15°-0.5)

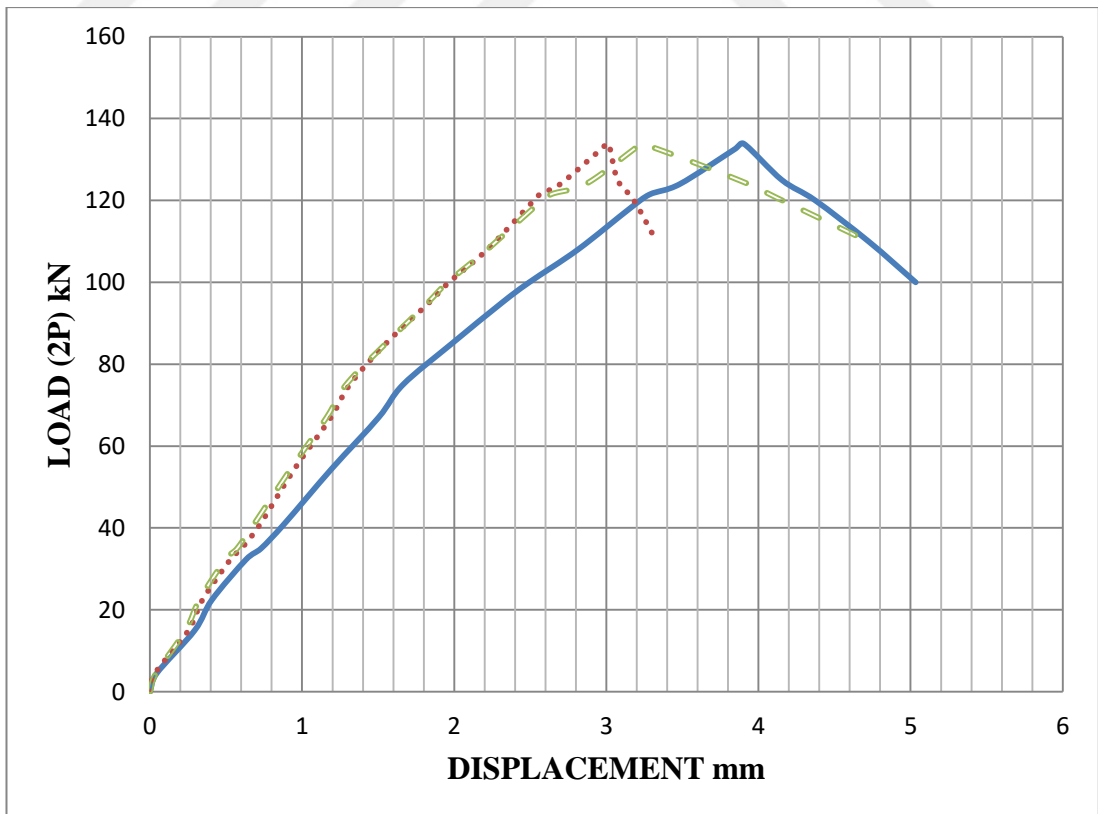


**Figure 4.10** Load-Displacement Relationship (B8-H15°-0)

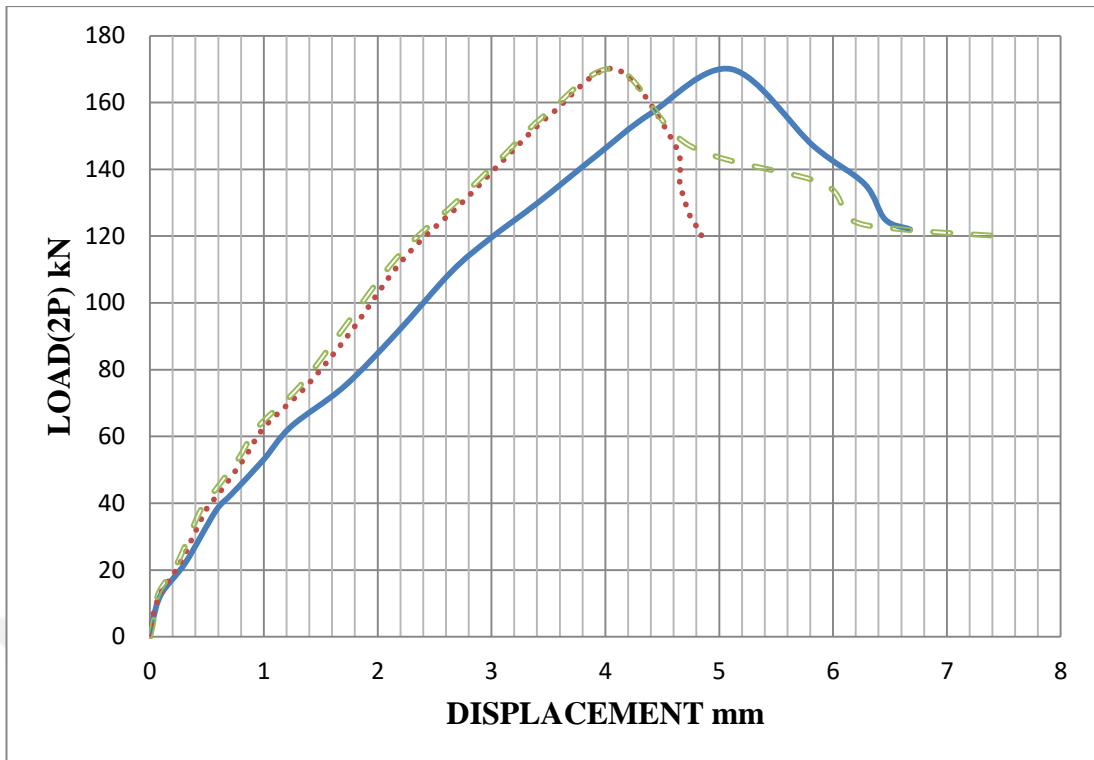


**Figure 4.11** Load-Displacement Relationship (B10-H15°-0.5)

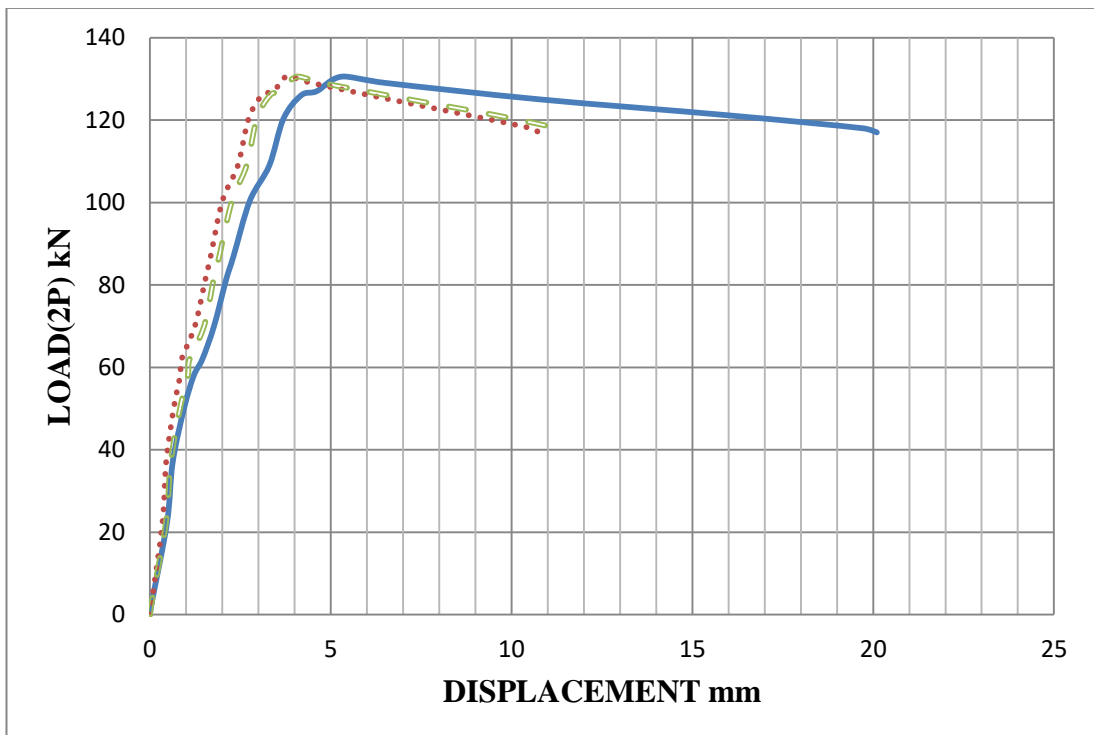


**Figure 4.12** Load-Displacement Relationship (B3-H10°-0)

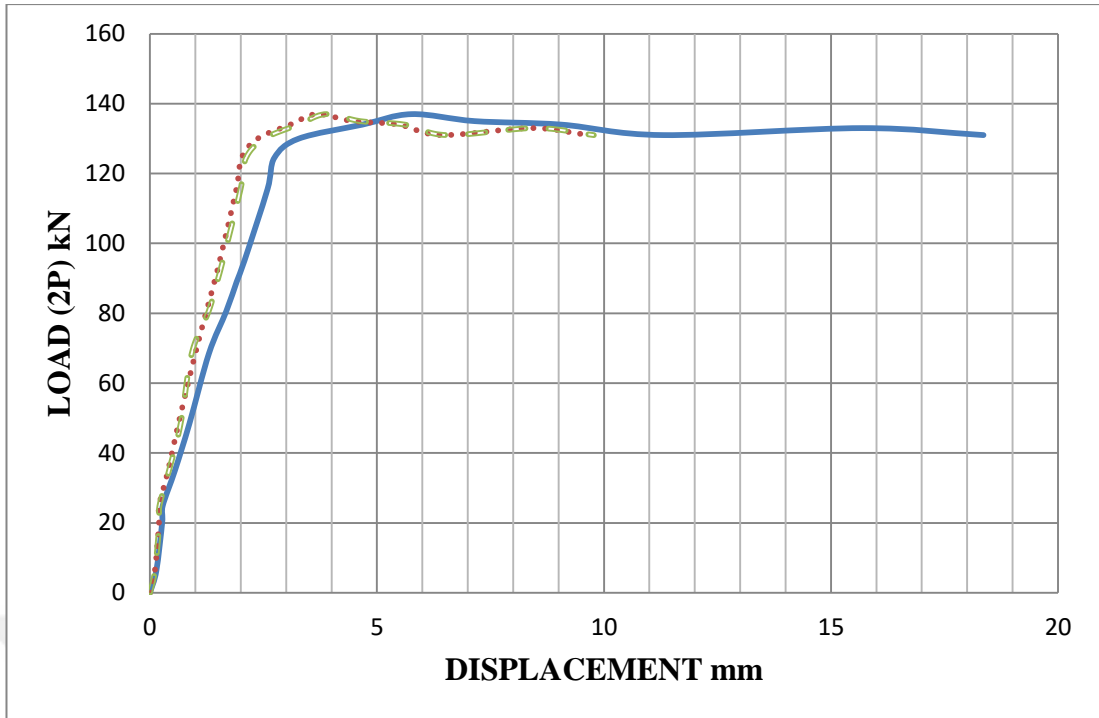


**Figure 4.13** Load-Displacement Relationship (B5-H10<sup>0</sup>-0.5)

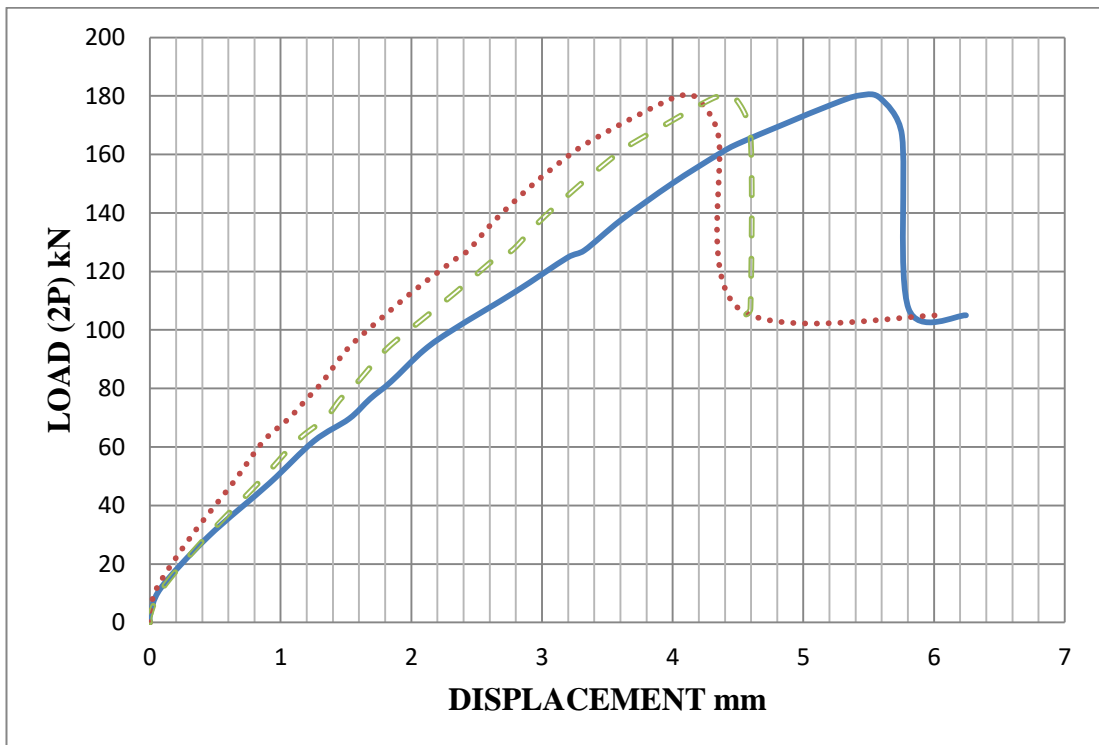


**Figure 4.14** Load-Displacement Relationship (B7-H10<sup>0</sup>-0)

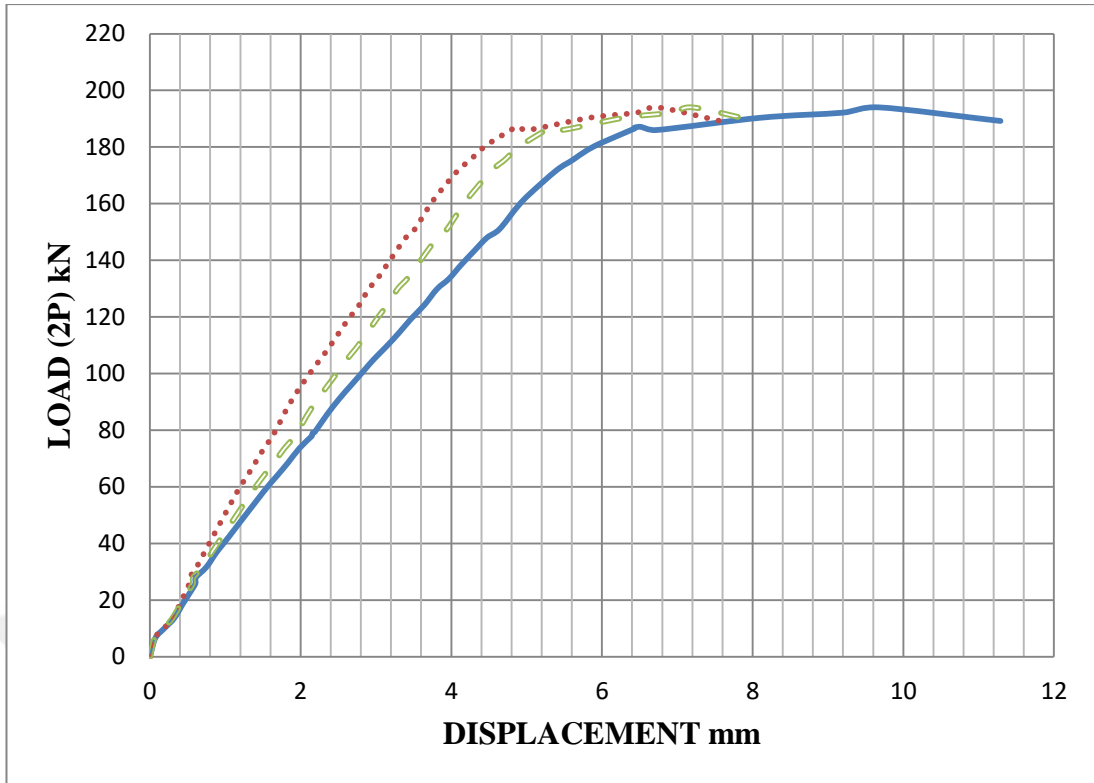


**Figure 4.15** Load-Displacement Relationship (B9-H10<sup>0</sup>-0.5)

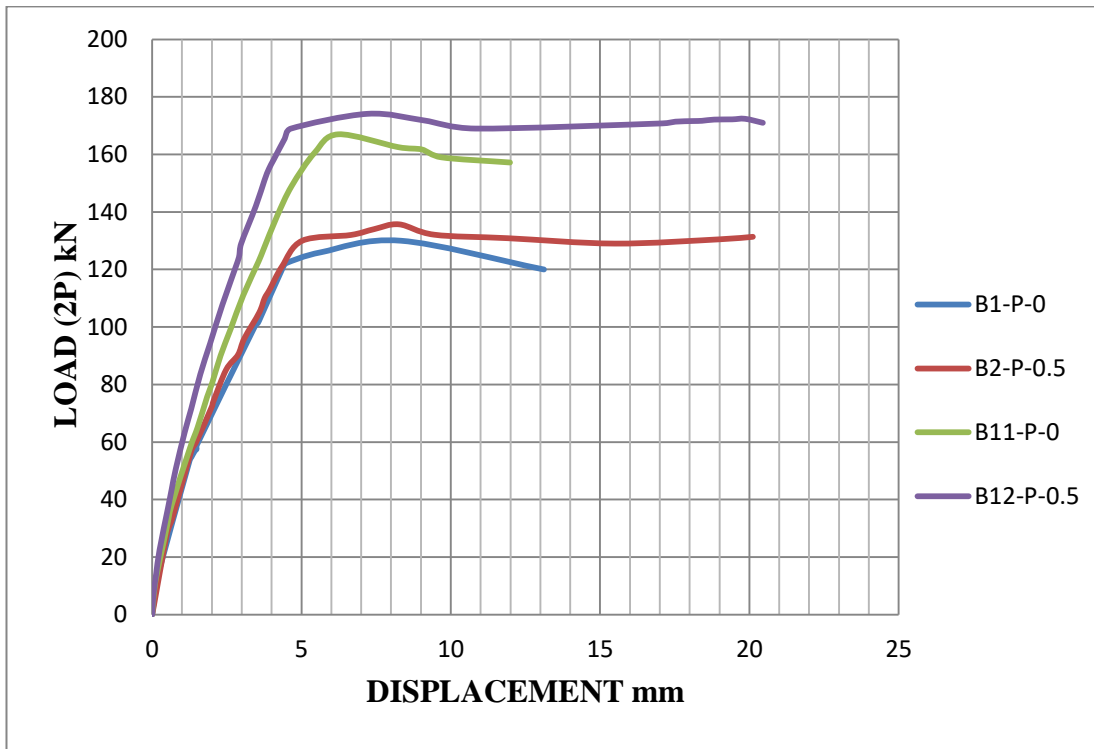


**Figure 4.16** Load-Displacement Relationship Mode A

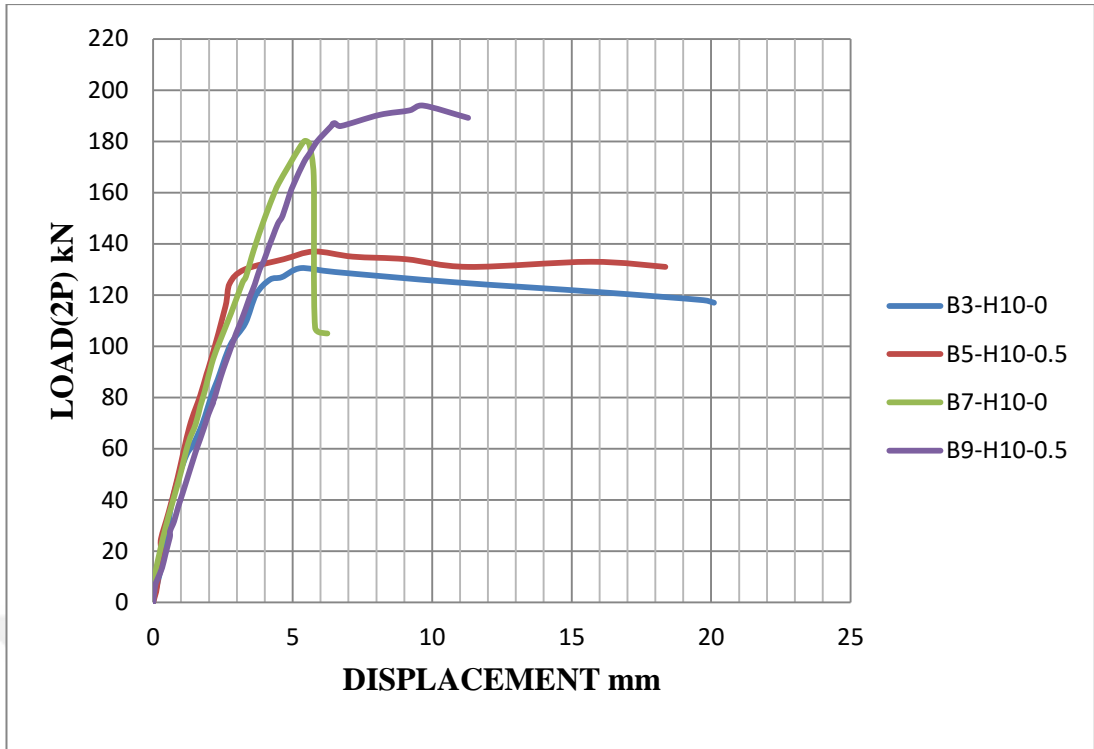


Figure 4.17 Load-Displacement Relationship Mode B

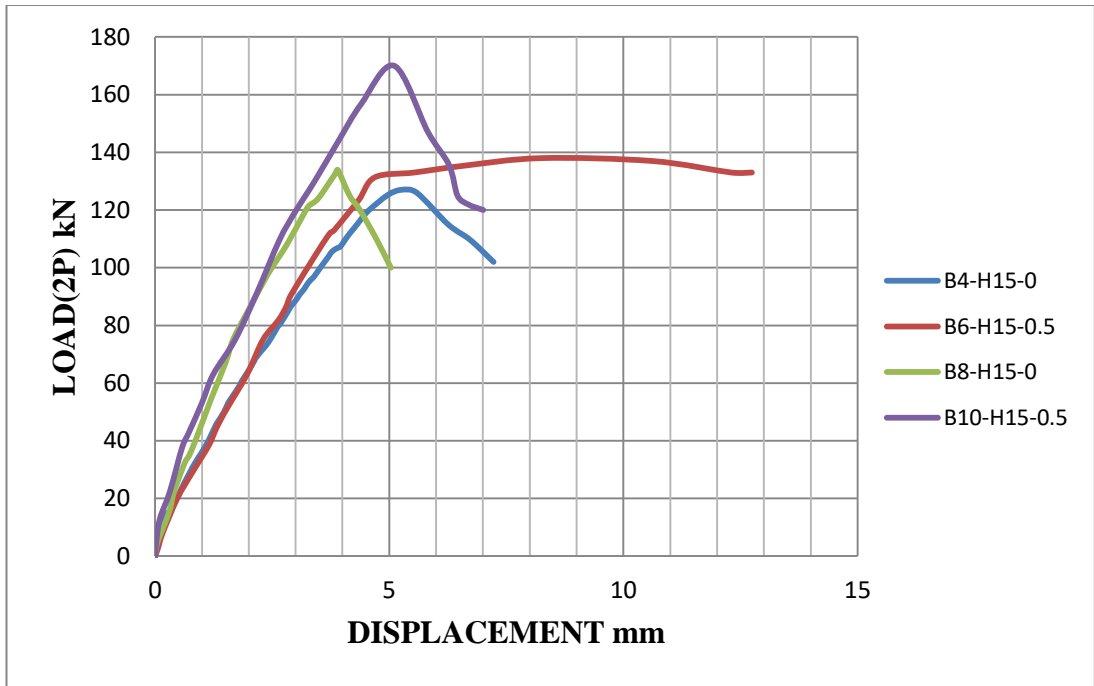
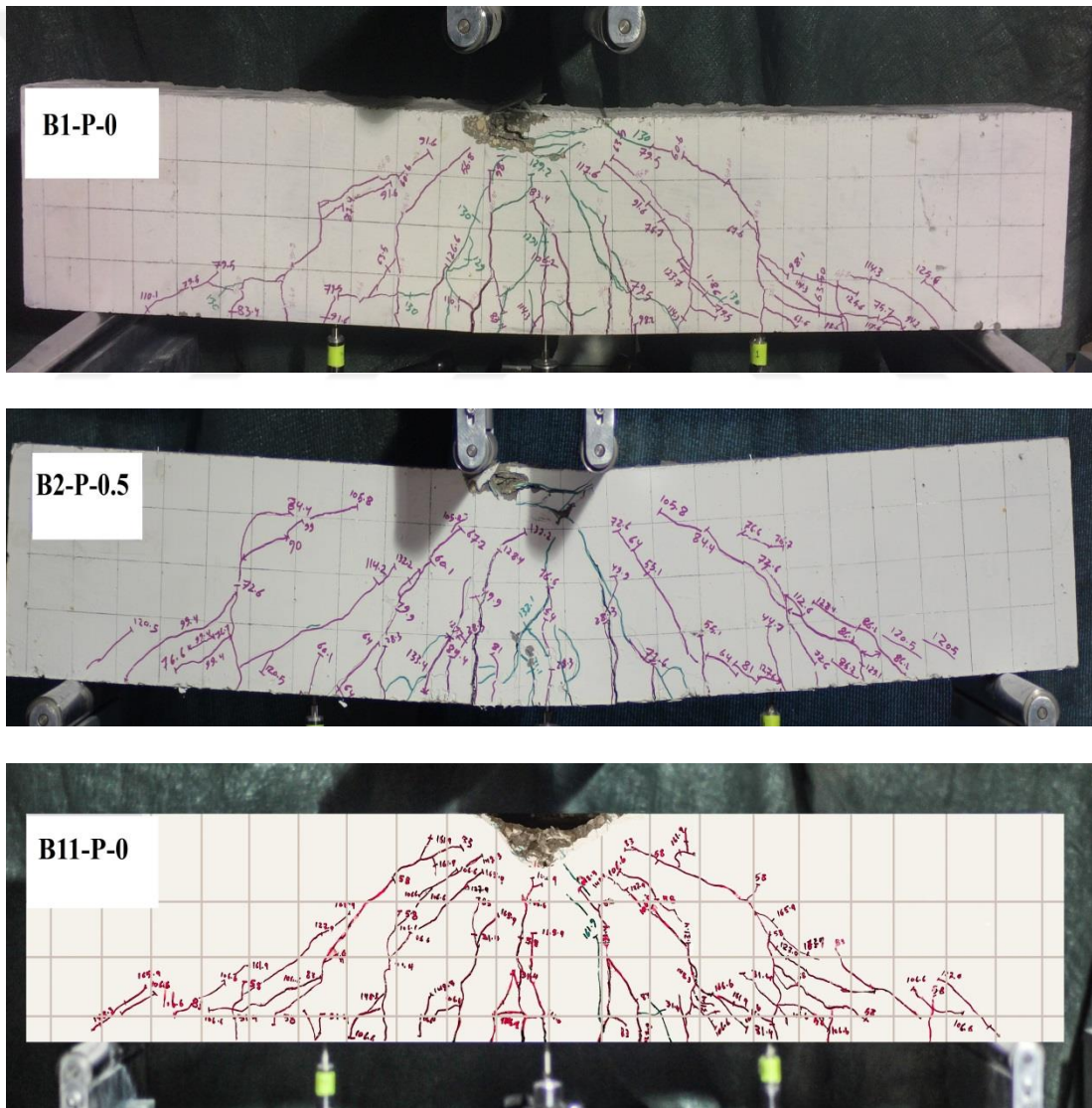


Figure 4.18 Load-Displacement Relationship Mode C

#### 4.2.4 Mode of Failure

Generally, the mode of failure of the beams depends on a way to form cracks and the cracks that cause the element to collapse. During the loading process, several patterns of crack formed in the RCHBs before the failure. The crack propagation and modes of failure have been widely investigated by experimental and theoretical studies for the prismatic beams. Whereas, it had not been a study which presents this topic in detail for RCHBs. The 12 beams designed to study the shear and flexure behavior of RCHBs, They have been reinforced with stirrups, 4 beams out of 12 got her a failure of the Shear type where the diagonal failure took place in all 4 beams. The other eight beams have failed to flexure. The crack propagation of the RCHBs has differed depending on the beam shape, inclination angle, steel fiber ratio and steel reinforcement ratio. In general, all of the beams were collapsed in shear where the diagonal tension cracks appeared suddenly, whereas the other beams are failing in flexure or concrete crushing. The flexural cracks appear along the beam in early load levels, the first crack emerges close to the mid-span or below of the loading points. Generally, the cracks begin perpendicular to the longitudinal main reinforcements. The paths of the cracks inclined toward the loading point at higher load and turned as flexural-shear cracks. At a certain load level before failure, the inclined cracks in the web of beam is moderate and continue to resist shear forces due to the residual tensile strength and aggregate interlock, At the subsequent loading, crack considerably increases until collapse. The important observation from the flexural and flexural shear cracks were existed symmetrically on both sides of the beam until the beam fails in shear. When the diagonal tension crack appears, all of the cracks stop growing and some of cracks go to close. The beams continue to bear a certain limit of loads less than the ultimate load because the displacement control procedure was used in the testing, especially in Modes A and C. The beams shown different behavior after the beams arrived to the failure period, the cracks prorogation and mechanical behavior for each beam and mode will be discussed in detail. The types of failure for each beam are mentioned in Table 4.1. An addition to the flexural and shear cracks, horizontal cracks formed parallel to the longitudinal reinforcements which cause to splitting the concrete cover which surrounding the reinforcement bars.

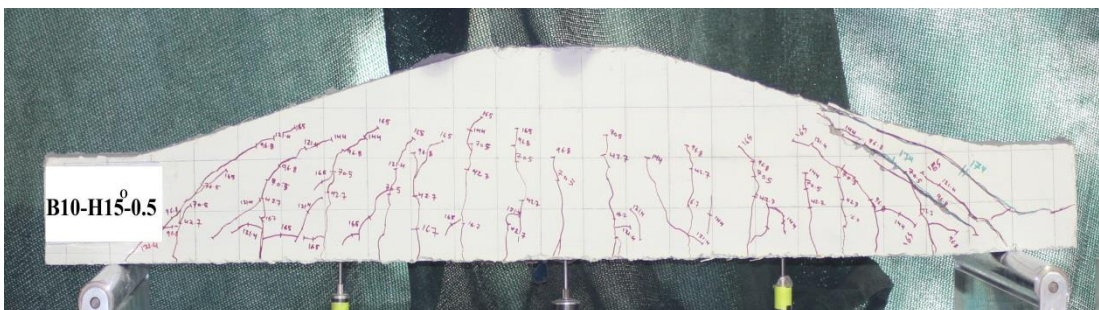
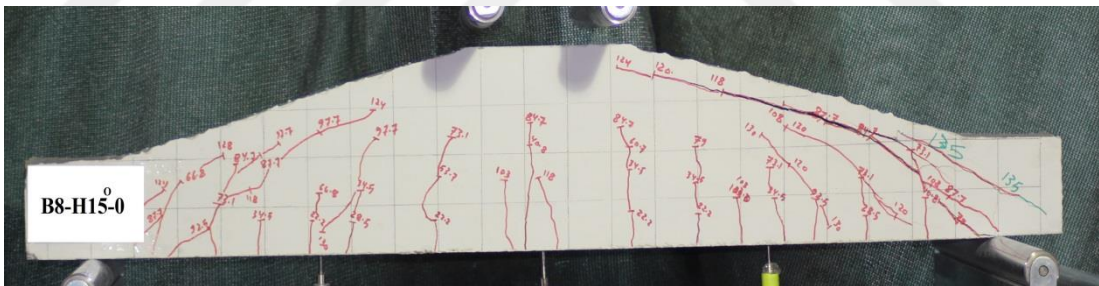
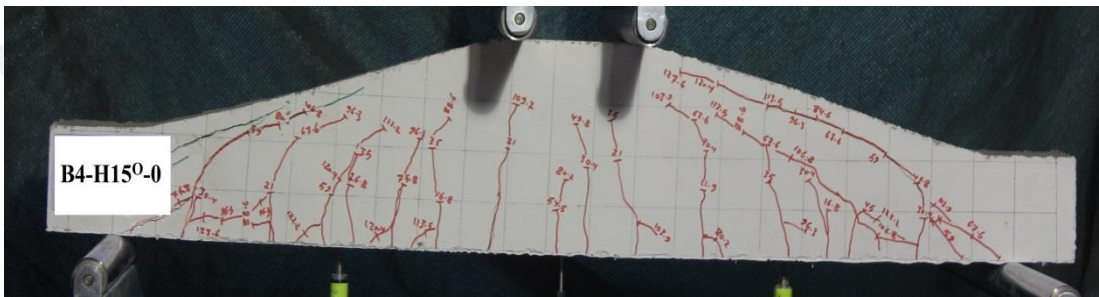
Fig. 4.19 shows the failure of the beams, where all of the beams failed in flexural and concrete compression crush. The main failure crack in Mode A&C was at mid-span, The horizontal splitting cracks appeared in Modes B especially in beams that do not contain steel fiber, while it was almost non-existent in Mode A&C. Mostly, the concrete crushes in compression immediately when the reinforcement bars was yield. Figure 4.20 presents the path and position of the diagonal tension cracks for the beams that collapsed in shear. The shear crack angle varies between the beams. The inclination of the shear crack was observed near to  $45^\circ$ , the shear crack angle did not show a fixed format of failure.







**Figure 4.19** Flexural Failure Mode



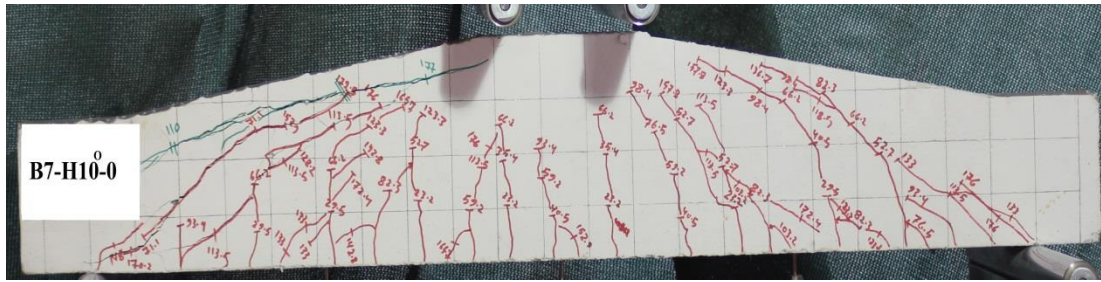


**Figure 4.20** Shear Failure Mode

#### **4.2.5 The Shear Critical section**

The shear critical section is the position of the major diagonal shear crack. The critical section for the beams formed in different districts. For the prismatic beams (Mode A) the major cracks were in the middle of the shear span. Whereas, the critical section observed near of the support for the beams have a smaller depth of support for Modes B and C and the crack approached to the support with increasing the inclination angle and the major crack constitute  $45^\circ$  with the main flexural reinforcement bars, the inclination angle for major cracks varies between the beams.

#### **4.2.6 Effective depth of shear**

The effective depth of the beam represents the depth of the beam at the position of the major diagonal shear crack. The effective depth for prismatic beams is constant (Mode A) wherever they are, whereas the haunched beams have variable depth and most of the practical design code did not distinct the effective depth of haunched beams. The experimental test realized different modes as shown in Figure 4.21.

The effective depth of the critical section for Mode B greater than Mode C, and inclination angle of the major crack observed asymptotic to  $45^\circ$  with the flexural reinforcement. Whereas, beginning of cracks are differed from beam to another.

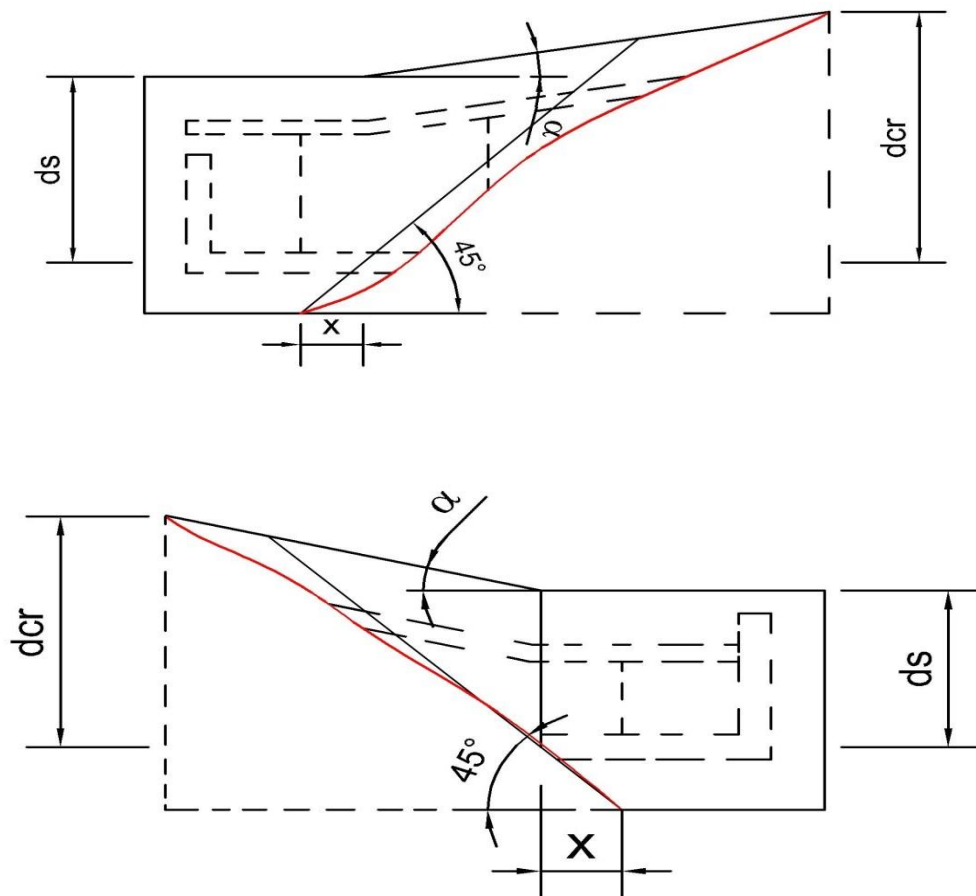


**Figure 4.21** Shear Failure shape for the RCHBs

#### 4.2.7 Effect Steel Fiber Ratio

In this study, only one steel fiber ratio of 0.5% was adopted as a volume ratio and the results for beams that do not contain steel fiber were compared. The effects on the mechanical properties of the samples, such as the collapse load, ductility and shape of the beam failure are not expected to be significant because they were based on the one of steel fiber ratio. In general, the steel fiber is connected with the splitting tensile strength of the concrete and by a percentage ratio. The higher percentage of the steel fiber is the stronger tensile strength of the concrete. In this study, the Figures (4.19-4.24) are shown there is an increase in the collapse load of the beam with beams containing steel fiber ranging from simple to medium. Thus, if the percentage of steel fiber is increased to more than 0.5%, the maximum collapse load of the beam will certainly increase. It was also observed that the beams that were added a steel fiber have the same angle of inclination and the same ratio of steel

reinforcement was observed an increase in the deformation ability of the beam. This behavior is considered to be good and desirable to provide safety to the structure if exposed to loads that may lead to its collapse. That mean, the steel fiber prevents or reduces the chance of a sudden collapse of the structural member, as it is observed increases the steel fiber of the ductility of the beams.

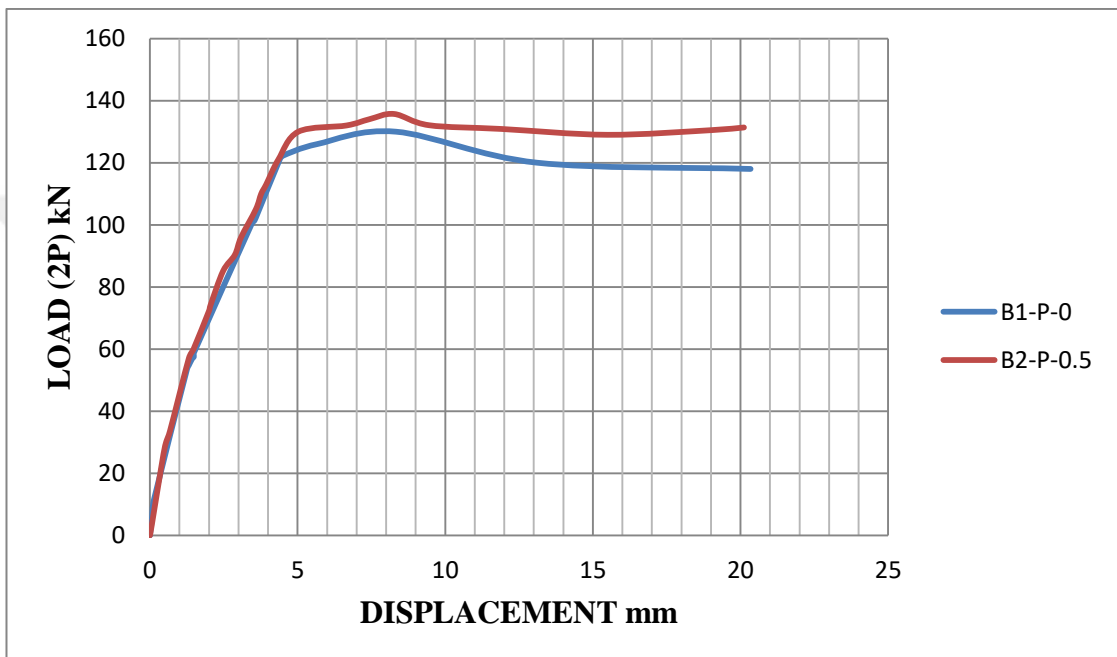


**Figure 4.22** Load-Displacement Relationship for two prismatic beams with steel fiber ratio (0&0.5) %.

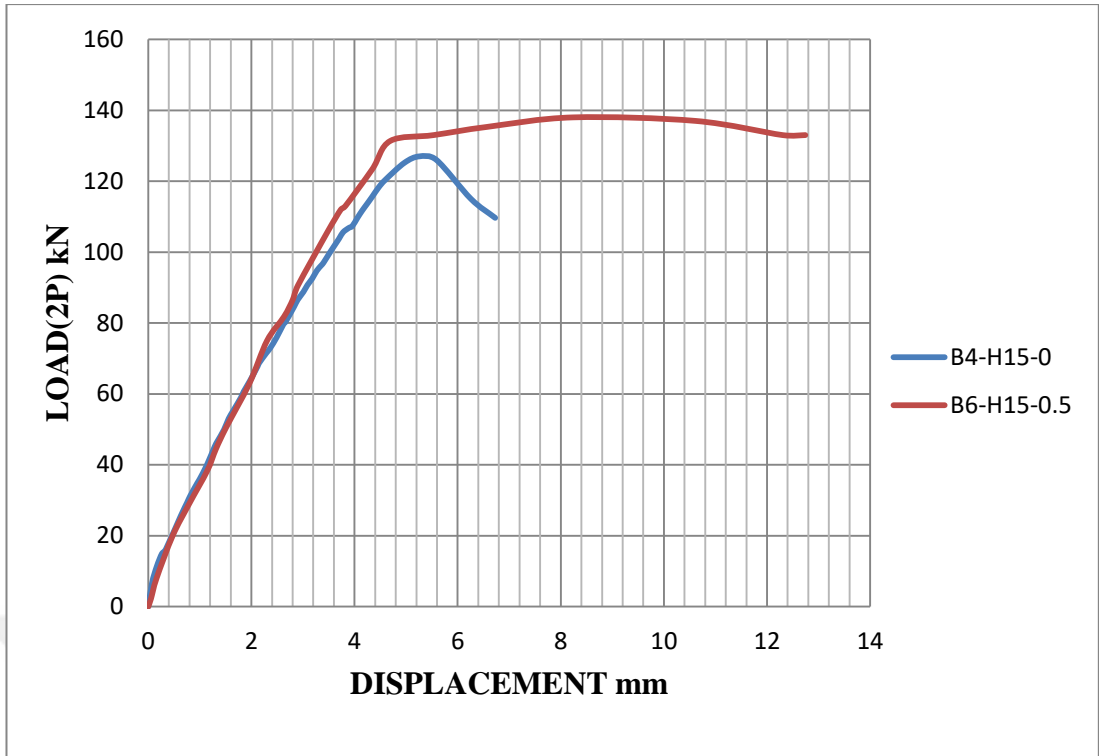


**Figure 4.23** Load-Displacement Relationship for two haunched beams with steel fiber ratio (0&0.5)% .

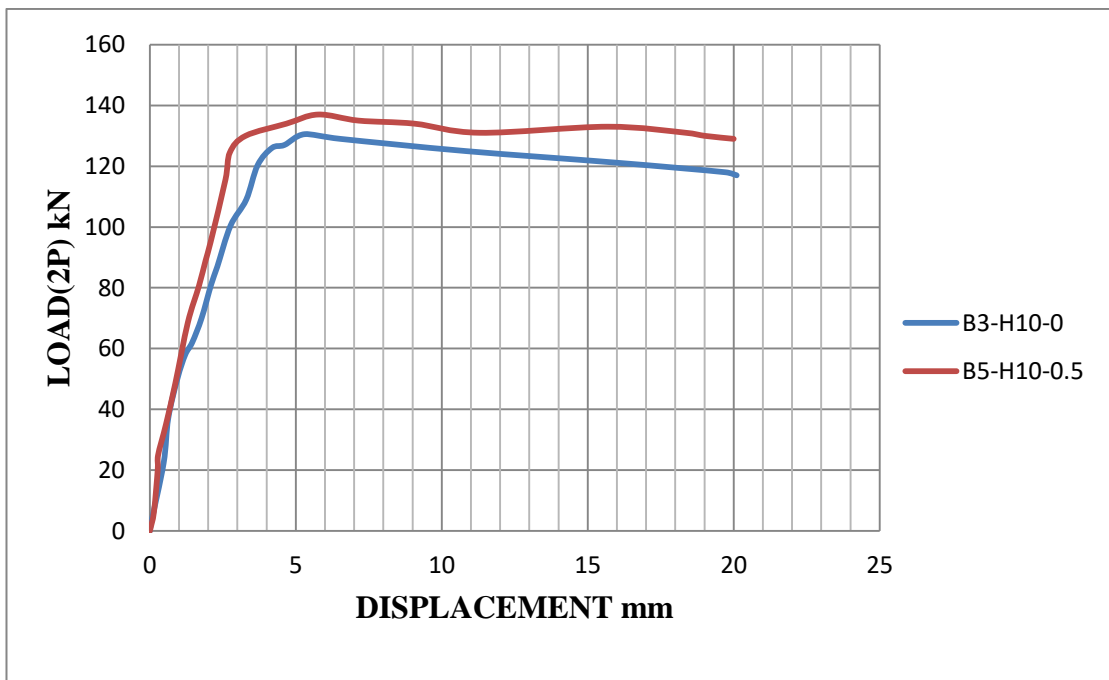


**Figure 4.24** Load-Displacement Relationship for two haunched beams with steel fiber ratio (0&0.5)%

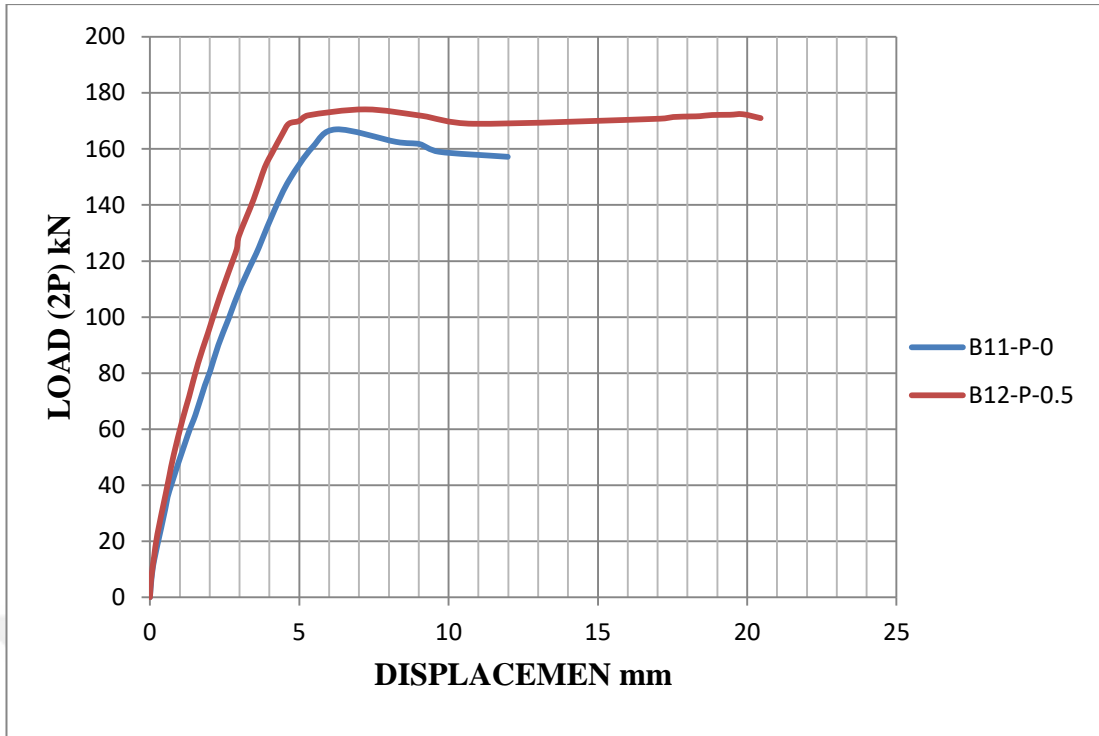


**Figure 4.25** Load-Displacement Relationship for two prismatic beams with steel fiber ratio (0&0.5)%

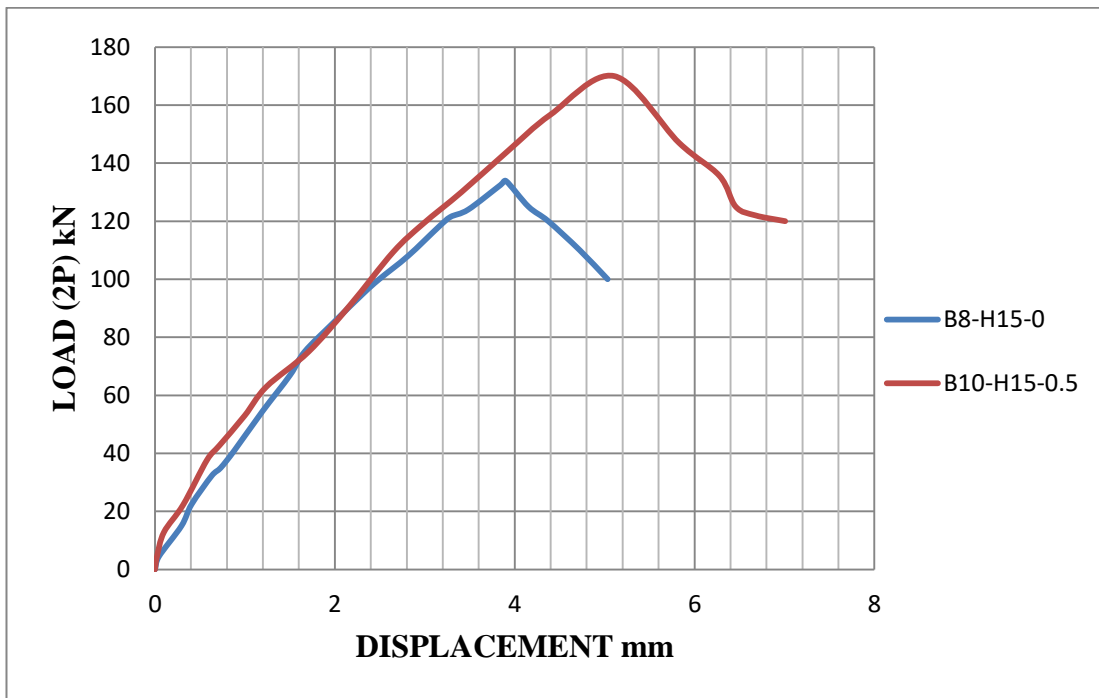


**Figure 4.26** Load-Displacement Relationship for two haunched beams with steel fiber ratio (0&0.5)%

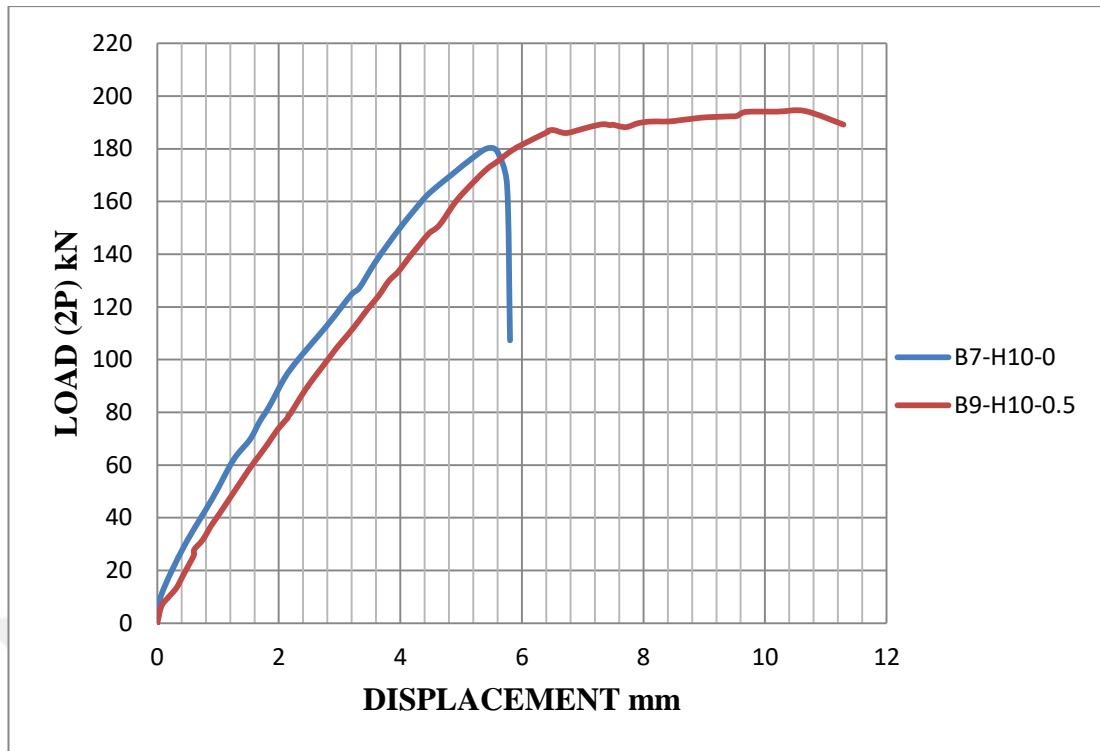


**Figure 4.27** Load-Displacement Relationship for two haunched beams with steel fiber ratio (0&0.5)%

#### 4.2.8 Effect of steel reinforcement ratio

In this study, two ratios of steel reinforcement were adopted for 12 beams. The beams were divided into two equal groups. Each group had a one steel reinforcement ratio. The beams from B1 to B6 had a steel ratio of 0.02. The samples from B7 to B12 had a steel ratio 0.310. The comparison was done on beams that have the same parameters from the angle of inclination and the same steel fiber ratio of and differ only in the ratio of steel reinforcement and as shown in the figures (4.25- 4.30). It was noticed that the collapse load of the beams is remarkable. Especially, in the beams which contained a percentage of steel fiber more than beams that did not contain a percentage of steel fiber and the foregoing, this gives an indication that the addition of a certain percentage of steel fiber with an increase percentage of steel reinforcement the collapse load value rises. The increment in the steel reinforcement ratio did not affect the ductility in the thresholds and as shown in the drawing. On the contrary, the ductility in the ratio of the lower steel reinforcement is the highest and this confirms that it is not preferable to have the over reinforcement section because it will reach the concrete to failure before reaching yield of steel reinforcement.

Thus, the structure is unsafe. It was observed that the increase in the steel reinforcement ratio changed the shape of the failure in the beams and its effect was evident in the haunched beam with angle  $10^\circ$ . Since the beam B7 was the shape of failure in which the shear and compared to B3, which was the shape of the failure of flexure, and which has the same parameters of angle of inclination and steel fiber ratio. As well as the beam B10 with angle  $15^\circ$  also was the shape of failure shear compared to the counterpart beam B6, which was the shape of failure in flexure. In addition, in the haunched beam  $15^\circ$ , steel reinforcement ratio was increased. Without the addition of steel fiber, the shape of failure was changed from flexure to shape and haunched  $10^\circ$  by adding steel fiber ratio, which changed the form of flexure to shear while there was no effect on the shape failure of the other beams.

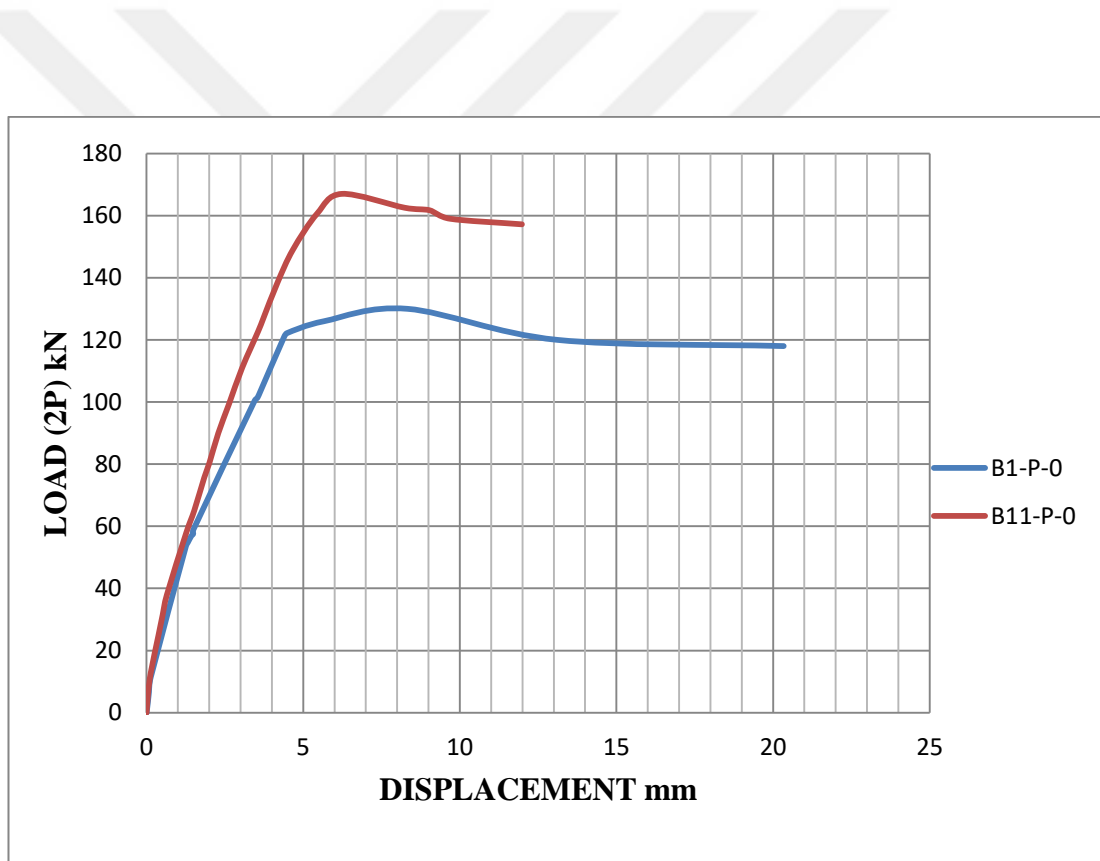


**Figure 4.28** Load-Displacement Relationship for two prismatic beams with steel reinforcement ratio ( $B1=0.02$  &  $B11=0.310$ ).

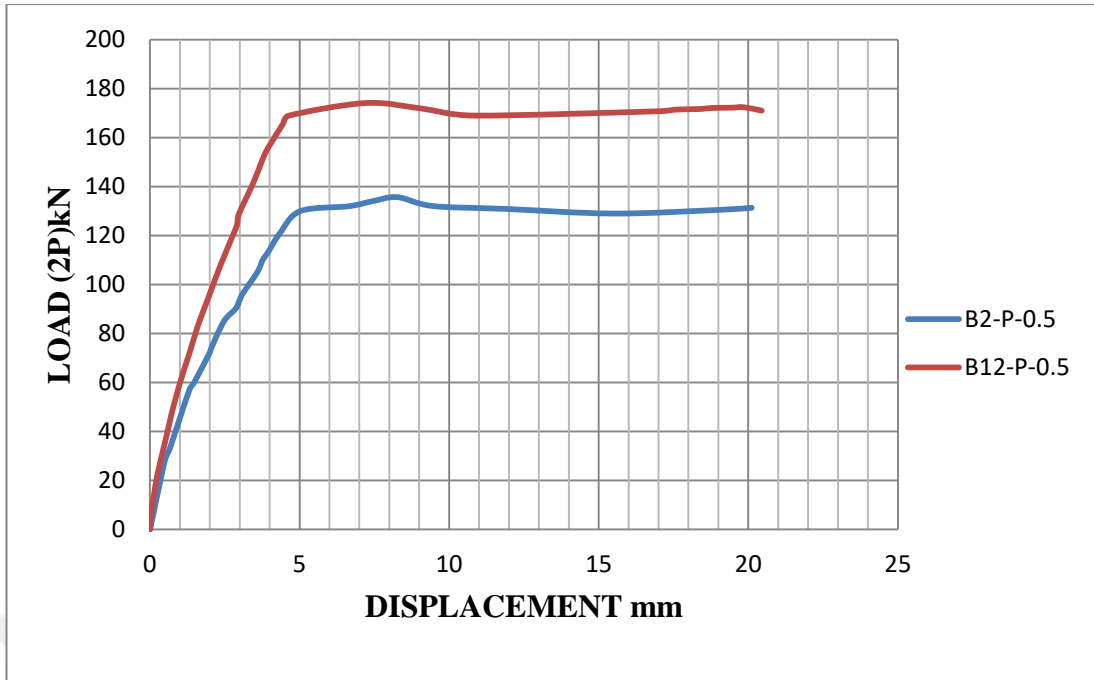


**Figure 4.29** Load-Displacement Relationship for two prismatic beams with steel reinforcement ratio ( $B2=0.02$  &  $B12=0.310$ ).

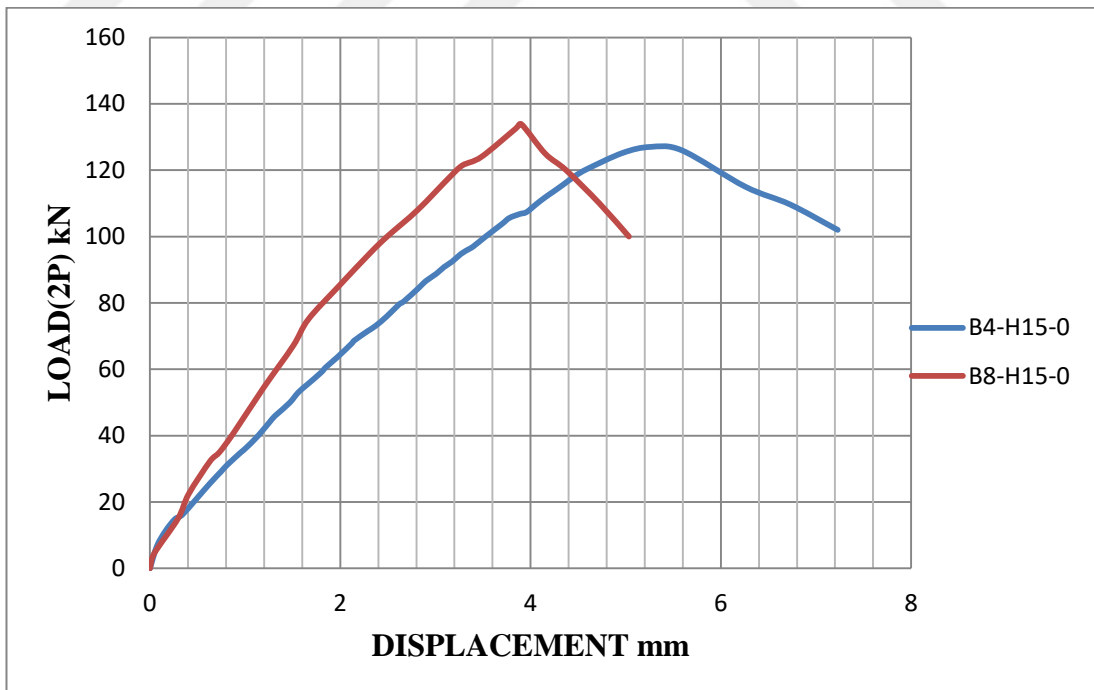


**Figure 4.30** Load-Displacement Relationship for two haunched beams with steel reinforcement ratio ( $B4=0.02$  &  $B8=0.310$ ).

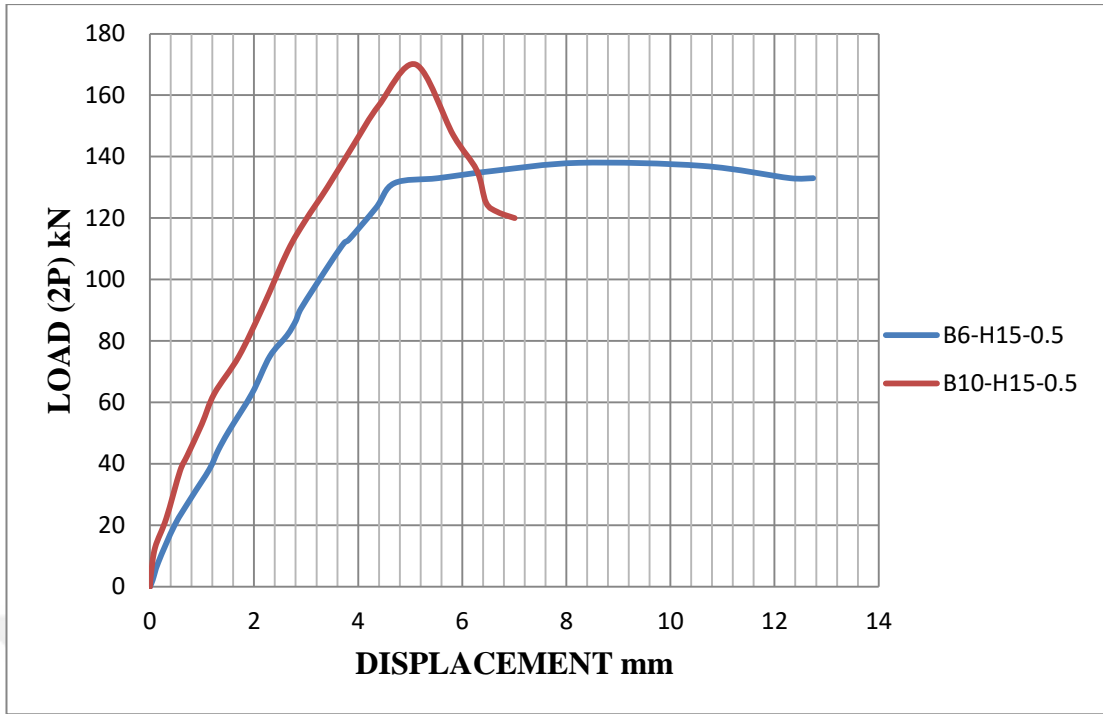


**Figure 4.31** Load-Displacement Relationship for two haunched beams with steel reinforcement ratio ( $B6=0.02$  &  $B10=0.310$ ).

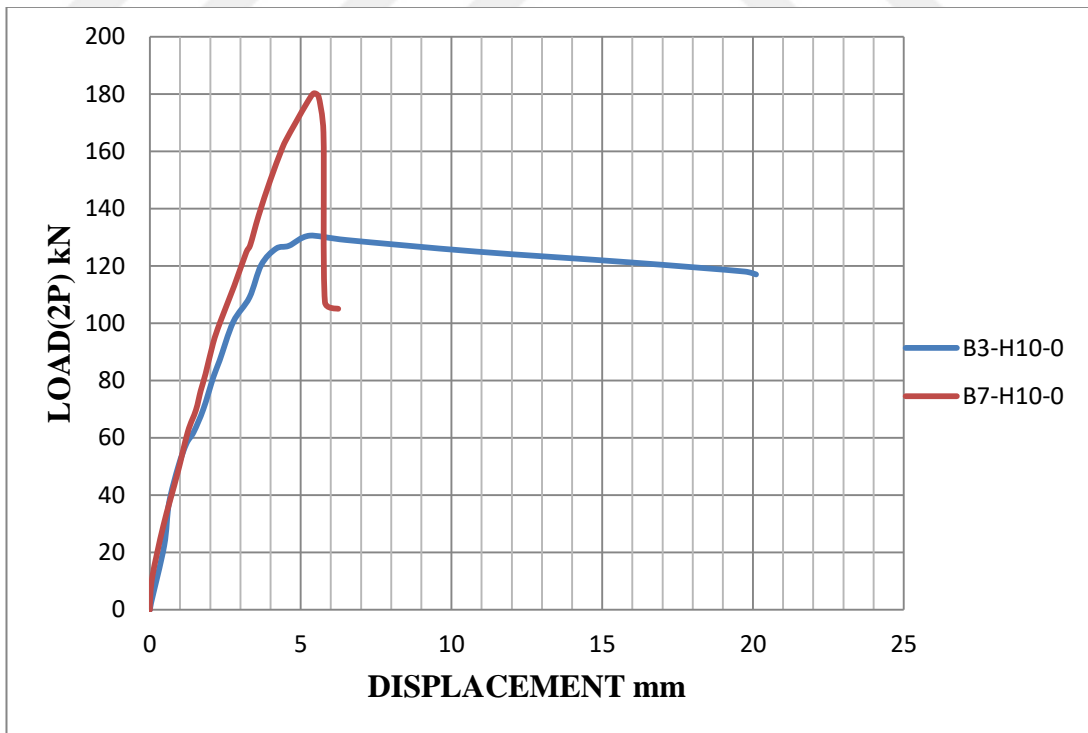


**Figure 4.32** Load-Displacement Relationship for two haunched beams with steel reinforcement ratio ( $B3=0.02$  &  $B7=0.310$ ).

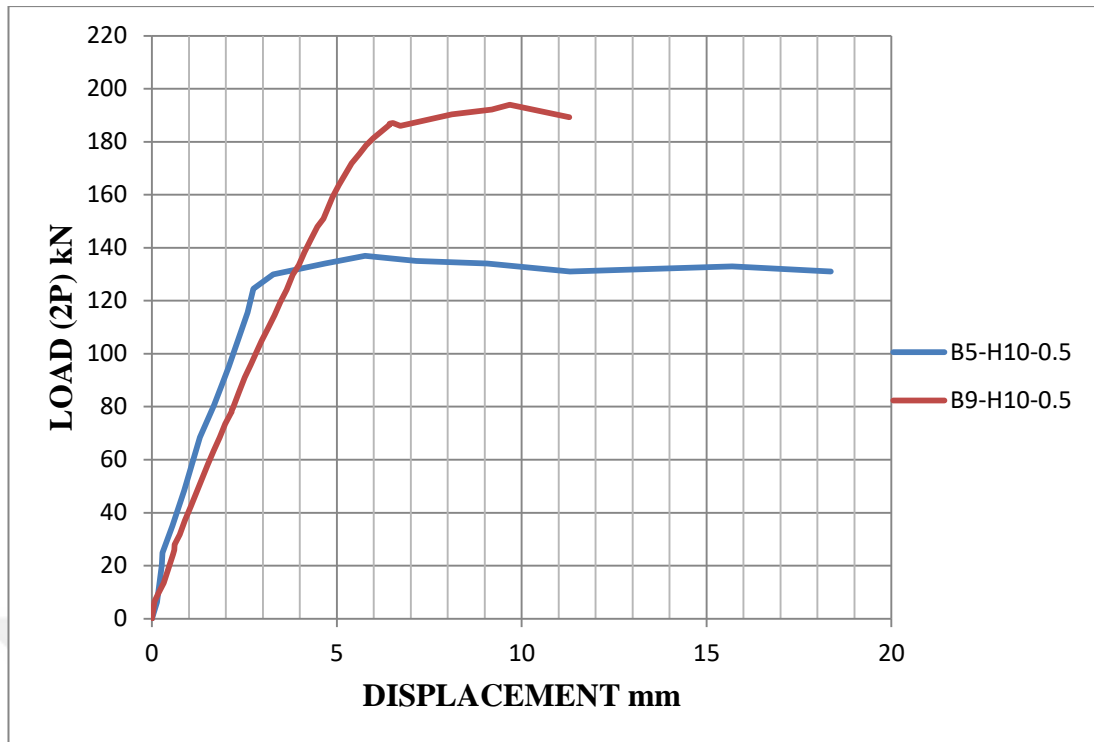


**Figure 4.33** Load-Displacement Relationship for two haunched beams with steel reinforcement ratio ( $B5=0.02$  &  $B9=0.310$ ).

#### 4.2.9 Effect of angle of inclination

The relationship was drawn between load and displacement of the beams was determined, and three different values were adopted for the beams in this research ( $0^\circ$ ,  $10^\circ$  &  $15^\circ$ ). The comparison was done for each of the three beams that differ in the angle of inclination and have the same steel reinforcement ratio and the same ratio of the steel fiber as shown in Figures (4.31-4.34). It was noted that the value of the collapse load of the beams increased only and was noticeable in the haunched beams angled angle  $10^\circ$ , especially in shapes (4.33 & 4.34). The other beams did not have a significant effect to change the angle of inclination on the collapse load of the remaining beams.

As for the shape of the failure, the shape of the failure in three haunched beams with angle  $15^\circ$  is a shear out of four beams and this means that the angles with ( $15^\circ$ ) are a few resistant of shear a few. Regarding the haunched beams with angle  $10^\circ$  sample was the failure of the shear and the reason for this the steel reinforcement ratio was increased, leading to an increase in the resistance of the flexure. However, after the

addition of Steel fiber, the shape of the failure was changed from shear to flexure. The remaining beams failed flexure.

The study showed that the ability of shear resistance decreased by increasing the angle of inclination, Figure 4.38 The relationship between the angle of inclination of the RCHBs and shear capacity (V). It is noted that the shear capacity increased by increasing the ratio of the main steel reinforcement and adding the ratio of the steel fiber as in the haunched beam B10. In Fig. 4.39 shows the increment arch of the compression chord with the angle of inclination, the compression chord prevents crack formation in the upper zone at the same time.

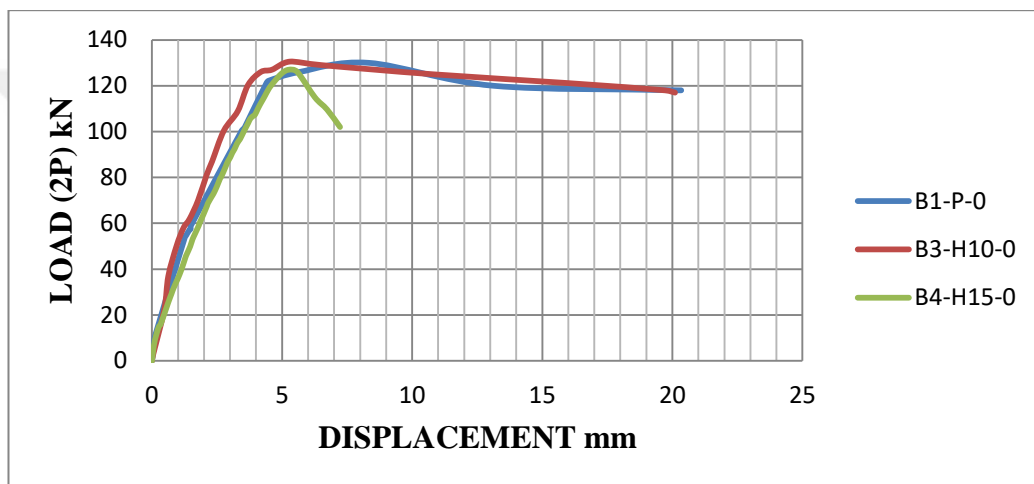


**Figure 4.34** Load-Displacement Relationship for three beams with steel reinforcement ratio 0.02 & steel fiber ratio 0 %.

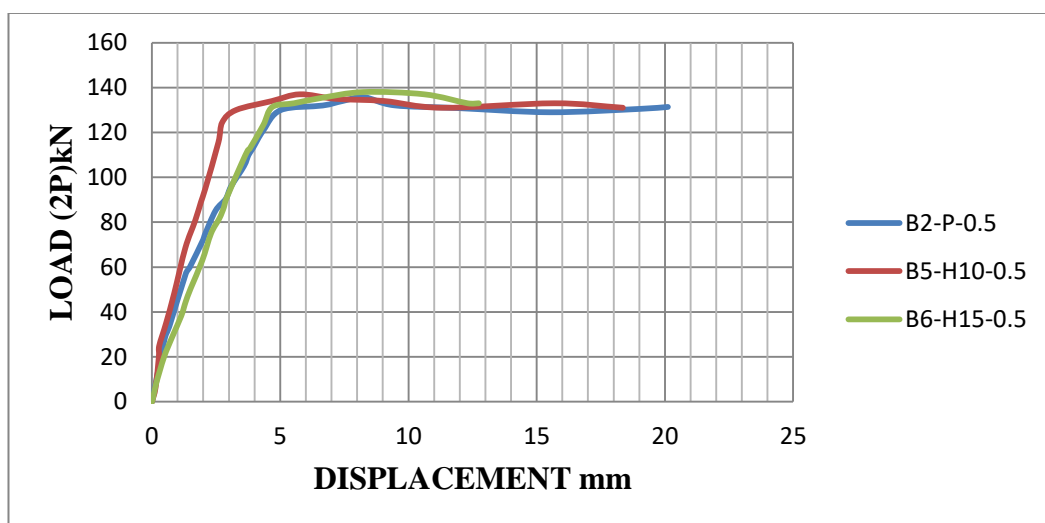


**Figure 4.35** Load-Displacement Relationship for three beams with steel reinforcement ratio 0.02 & steel fiber ratio 0.5 %.

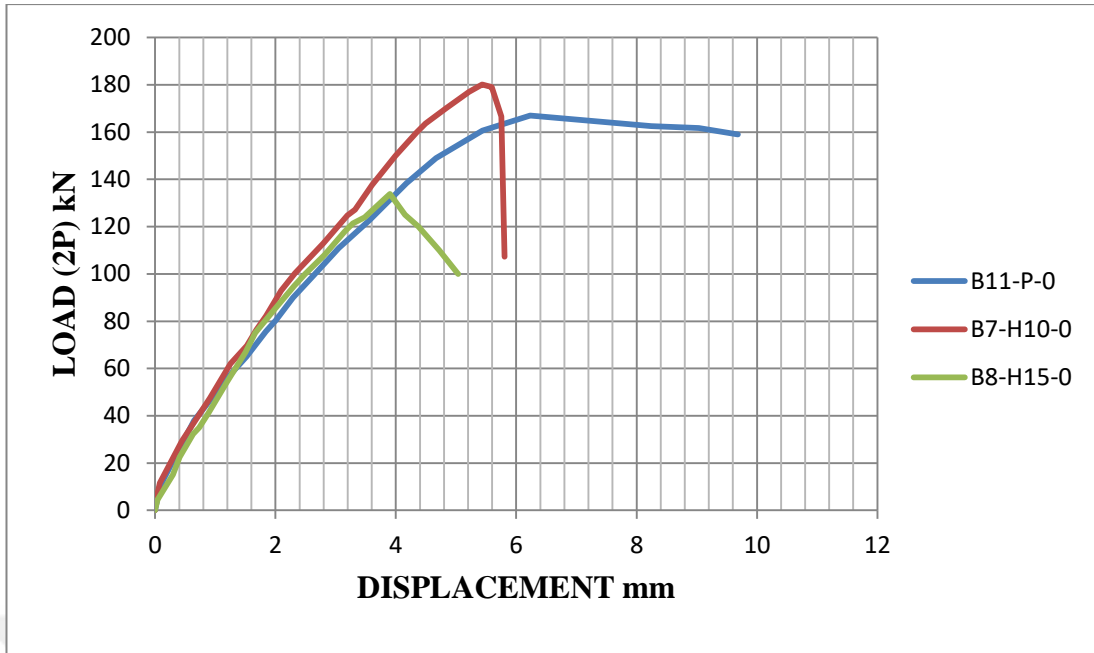


**Figure 4.36** Load-Displacement Relationship for three beams with steel reinforcement ratio 0.310 & steel fiber ratio 0 %.

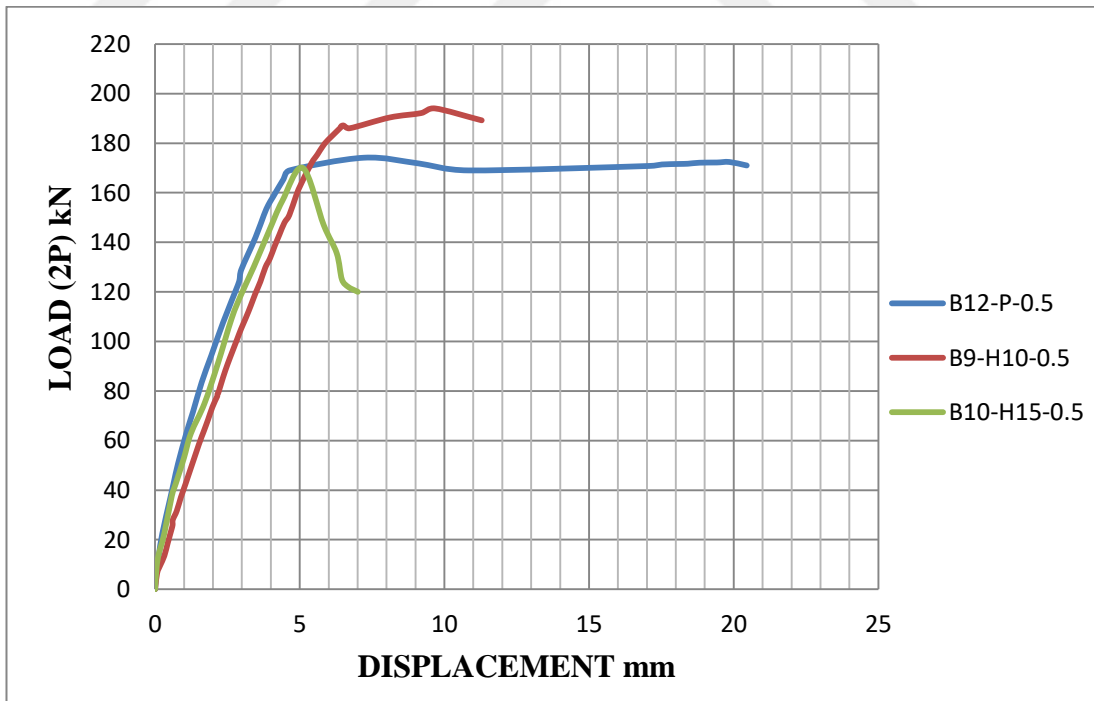


**Figure 4.37** Load-Displacement Relationship for three beams with steel reinforcement ratio 0.310 & steel fiber ratio 0.5 %.

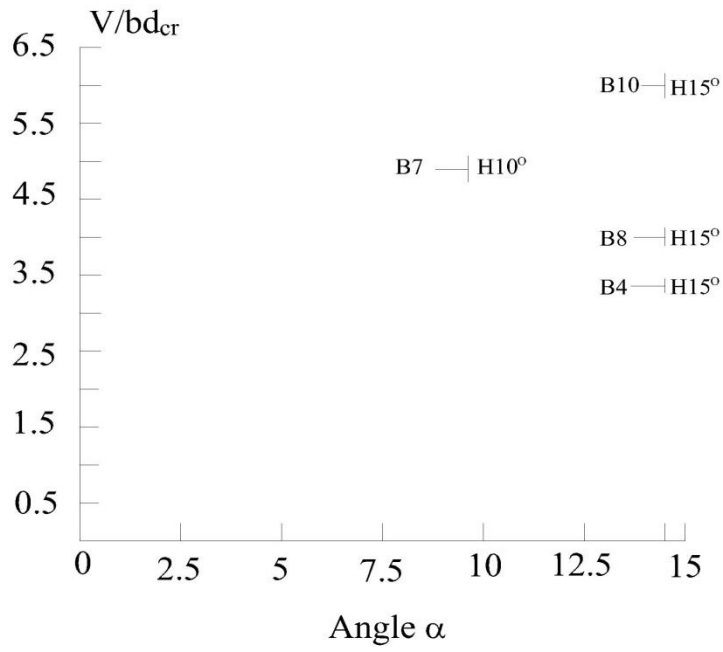


**Figure 4.38** Influence of the inclination angle on the shear strength capacity

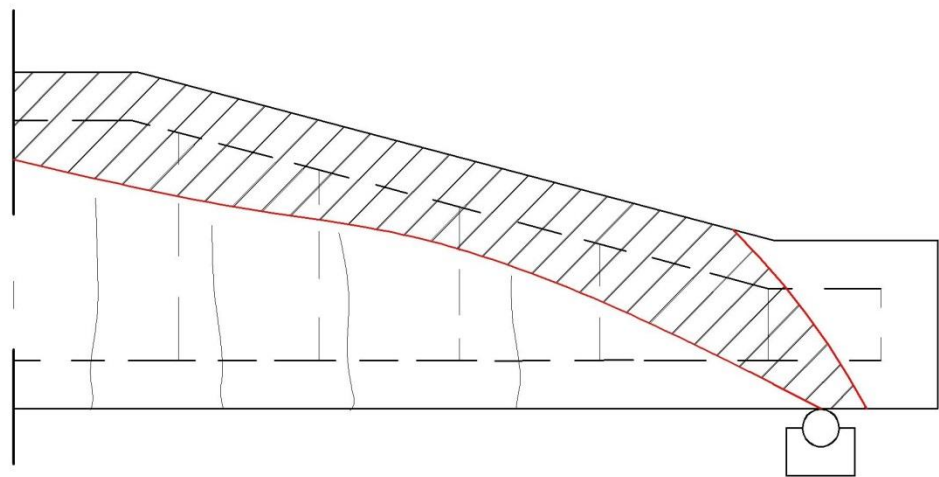


**Figure 4.39** Uncracked compression chord

#### **4.2.10 Flexural behavior of Beams**

In this study, all 12 beams reinforced by shear stirrups ( $\varnothing 6$  mm each 90 mm). The beam (B1, B2, B11&B12) was prismatic and the other beams (B3, B5, B6&B9) were RCHBs which were failed in flexure. All the beams failed in flexure and concrete crushing. Fig. 4.19 shows the crack patterns of the beams that reinforced by shear stirrups.

The main observed points for these beams (flexural failed) are as follows:

- The main flexure crack and the yield point appear in the middle of the beam in Mode A and close to the bend point in Modes (B&C).
- The load became constant for the beams under the yield load while the deflection increased. After the applied load exceeds yield load by nearly 5-10 %, concrete crushing observed between the loading points.
- The results did not show any significant effect regarding the load of failure for prismatic beams and the RCHBs. The beams B2,B5&B6, failed at 134, 137 and 137 kN respectively, due to yield of reinforcement. The yield load of beam B9 found to be 41 % greater than the prismatic beam due to the increase in the proportion of reinforcing steel and the addition of iron fiber due to the increase in the proportion of steel reinforcement steel and the addition of steel fiber. The beams B1,B11,B12 and B3 failed in flexure-concrete crushing, with failure loads of 130,166,172 and 134 kN, respectively.
- In Modes A&C, horizontal splitting cracks appeared along the longitudinal flexural reinforcement.
- In Mode C beams, the concrete cover on the bending point of the reinforcement was split due to the concentration of the negative component of the stress in reinforcement bars at this point.

#### **4.2.11 Cracks Propagation in the beams**

Reinforced concrete members have a complex crack pattern depending on the geometry of the member and the reinforcement arrangement. The cracks in RCHBs exhibit different behavior as compared to the prismatic beam. In general, the cracks initiate perpendicular to the flexure reinforcement and evolve differently in higher

load. The crack propagation in the beams reinforced by shear stirrups is similar to each other for prismatic beams and RCHBs.

In beams of Modes A,B&C the first flexural crack was initiated at mid-span, then another flexural crack formed along the beam. The cracks at mid-span continued perpendicular to the flexural reinforcement until to fail. The other cracks in the shear span began perpendicular and inclined toward the loading points at sequence loading. Figures (4.37 to 4.48) present the cracks propagation of the experimental tested beams at different levels of loading to all beams.



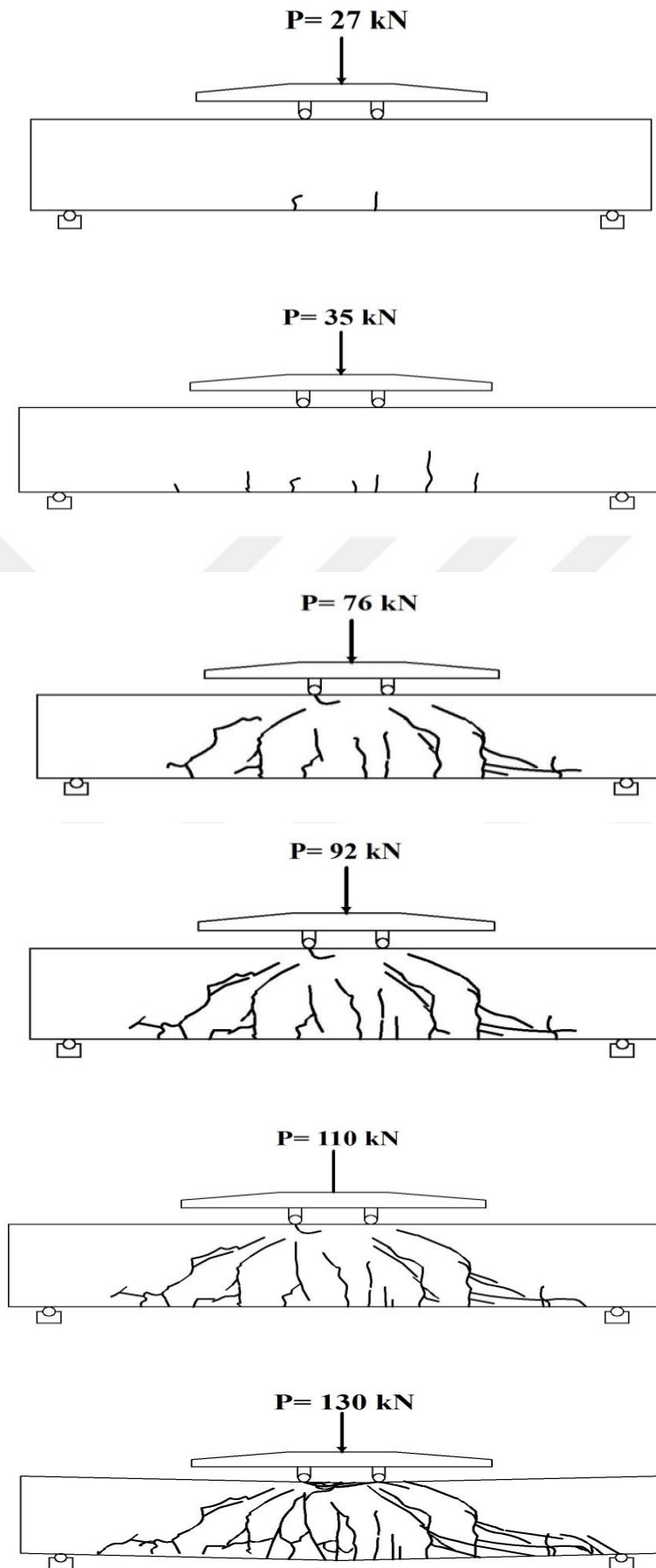


**Figure 4.40** Crack propagation of the beam B1

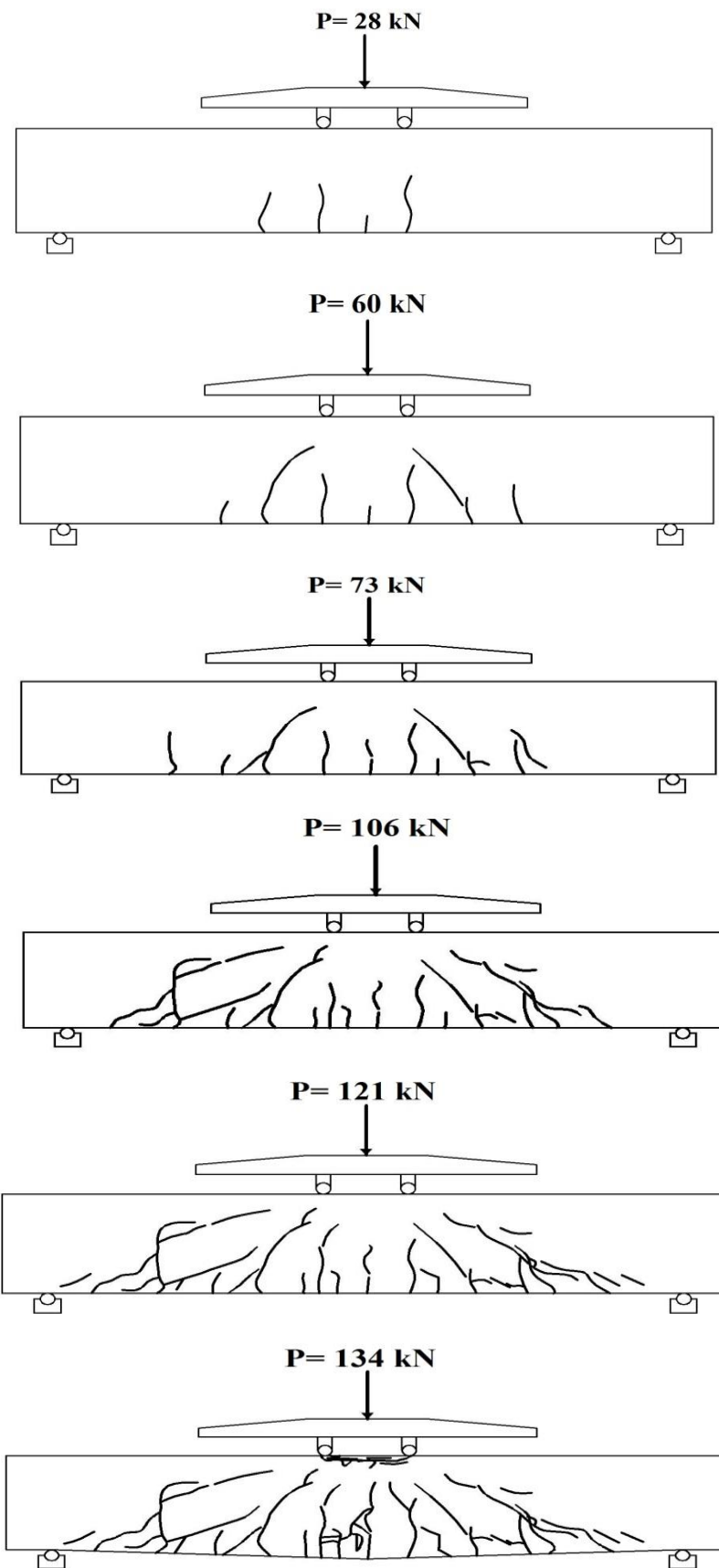


**Figure 4.41** Crack propagation of the beam B2

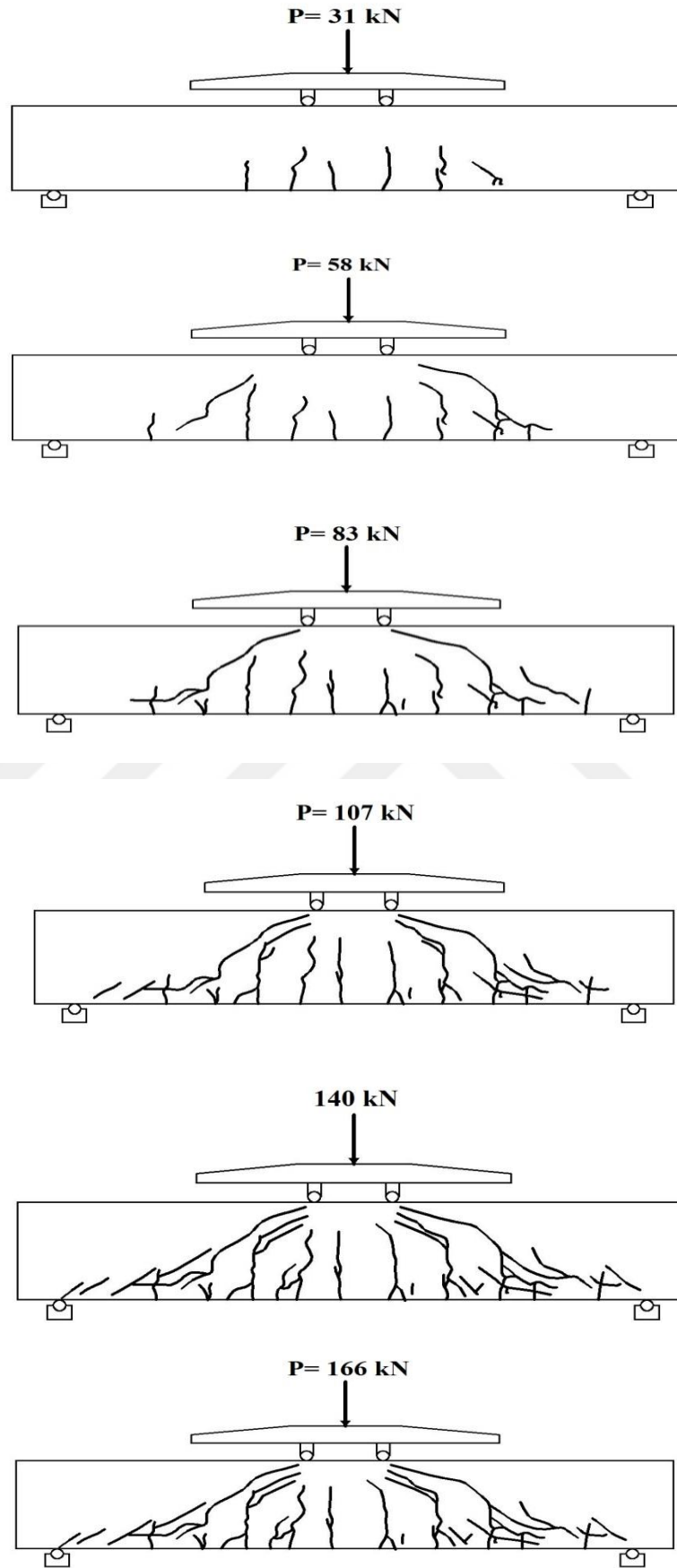


**Figure 4.42** Crack propagation of the beam B11

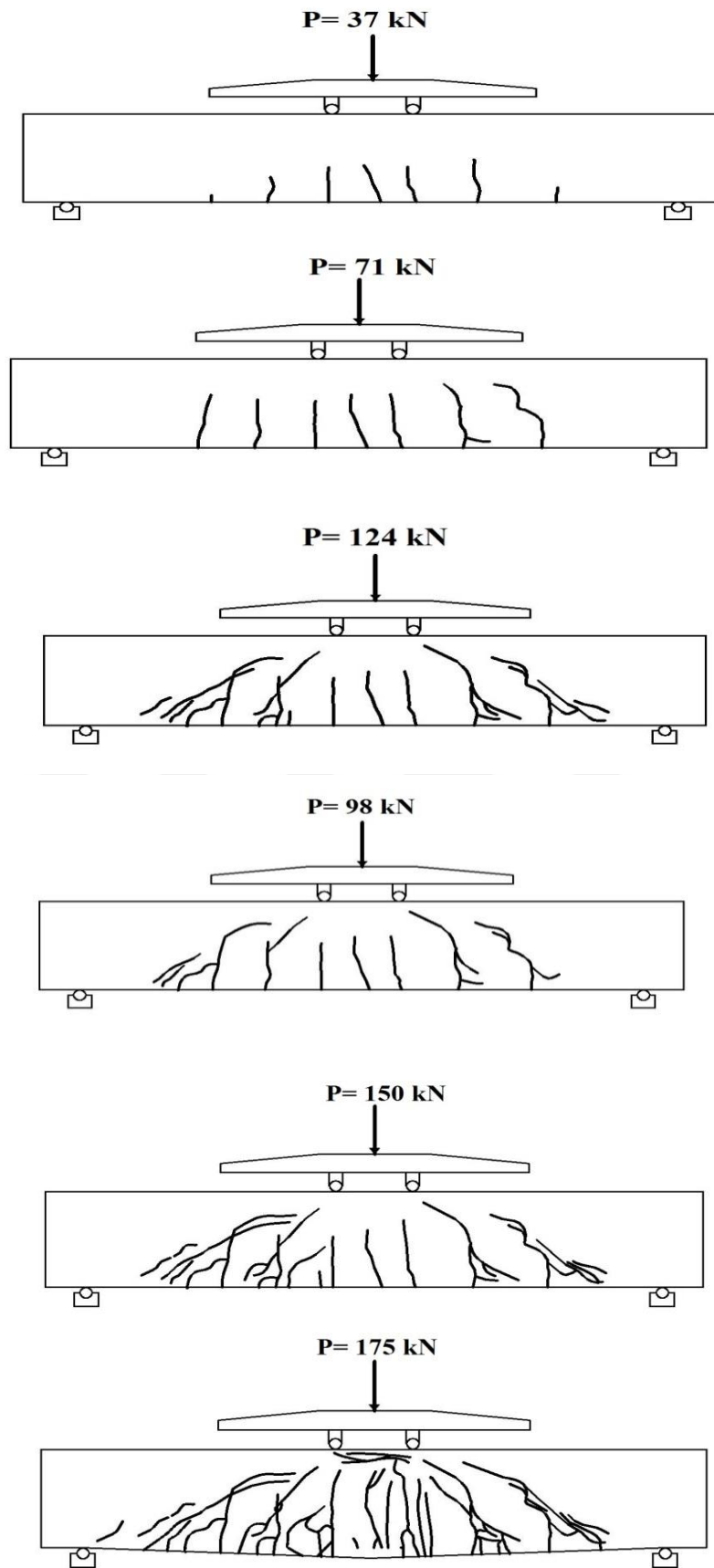


**Figure 4.43** Crack propagation of the beam B12

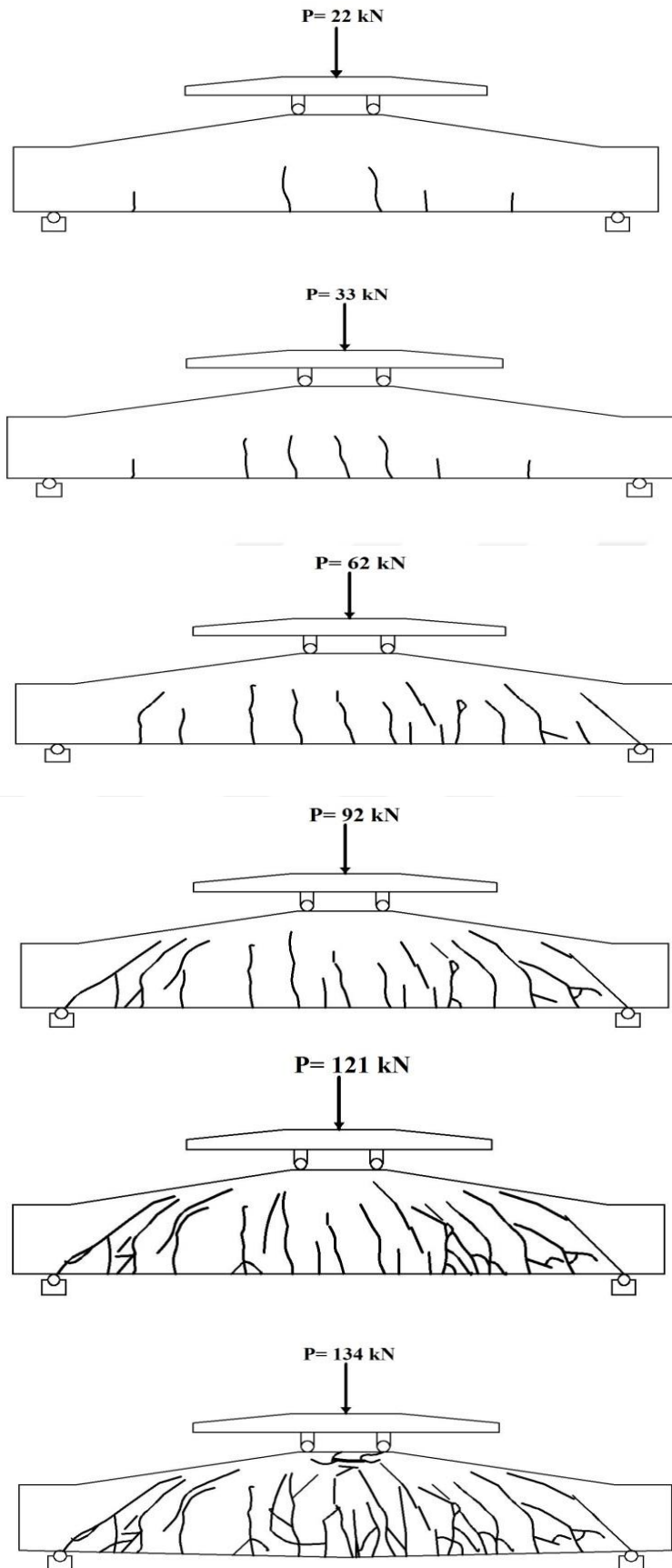


**Figure 4.44** Crack propagation of the beam B3

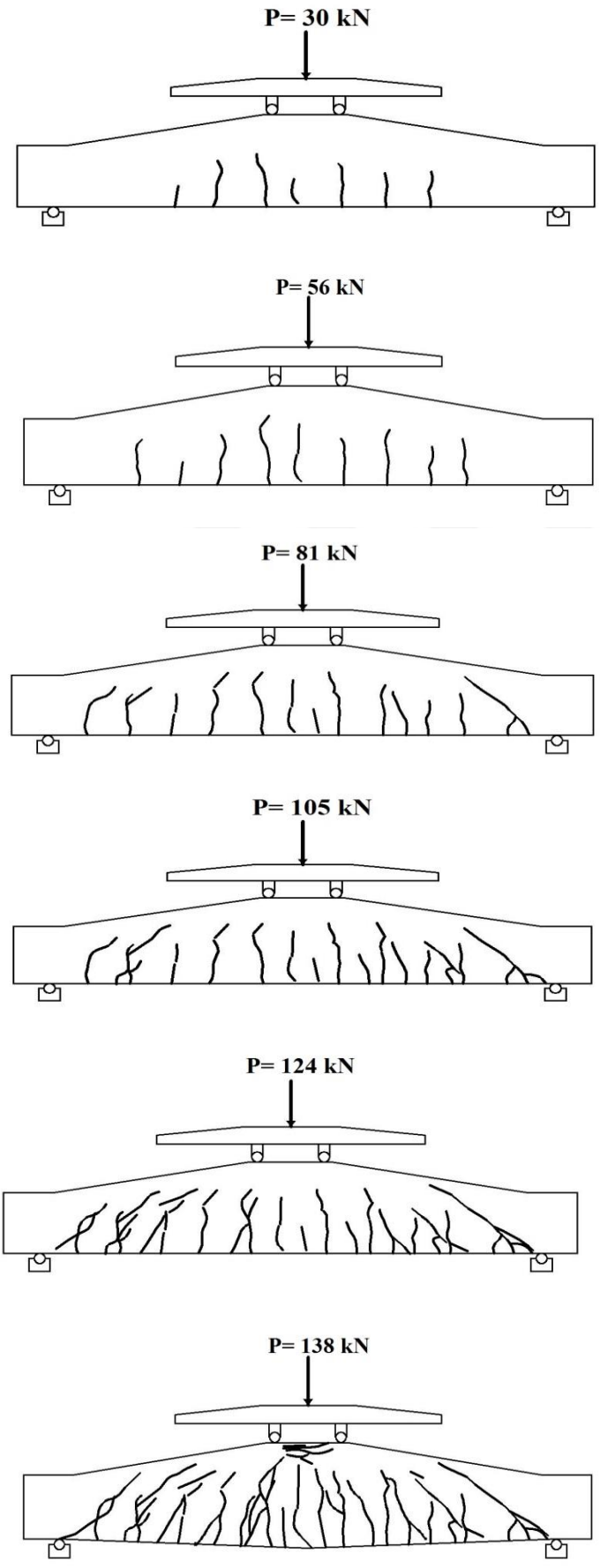


**Figure 4.45** Crack propagation of the beam B5

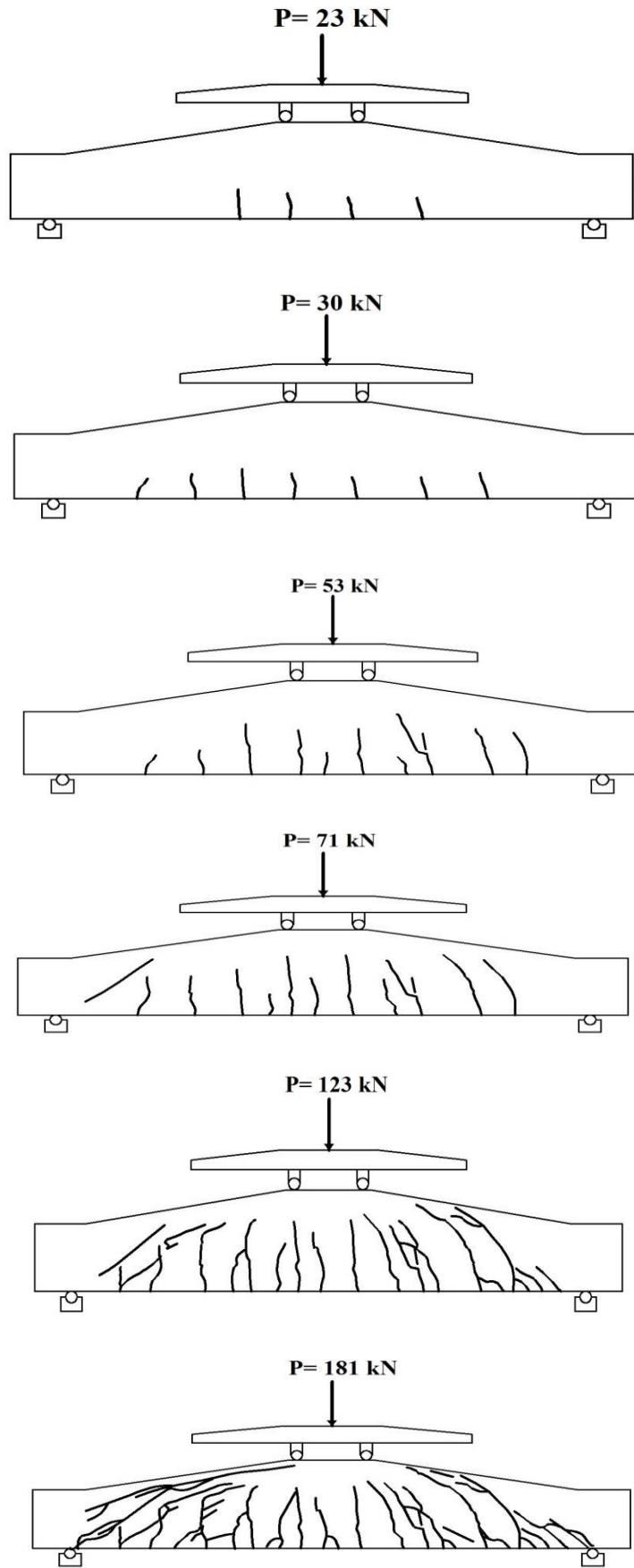


**Figure 4.46** Crack propagation of the beam B7

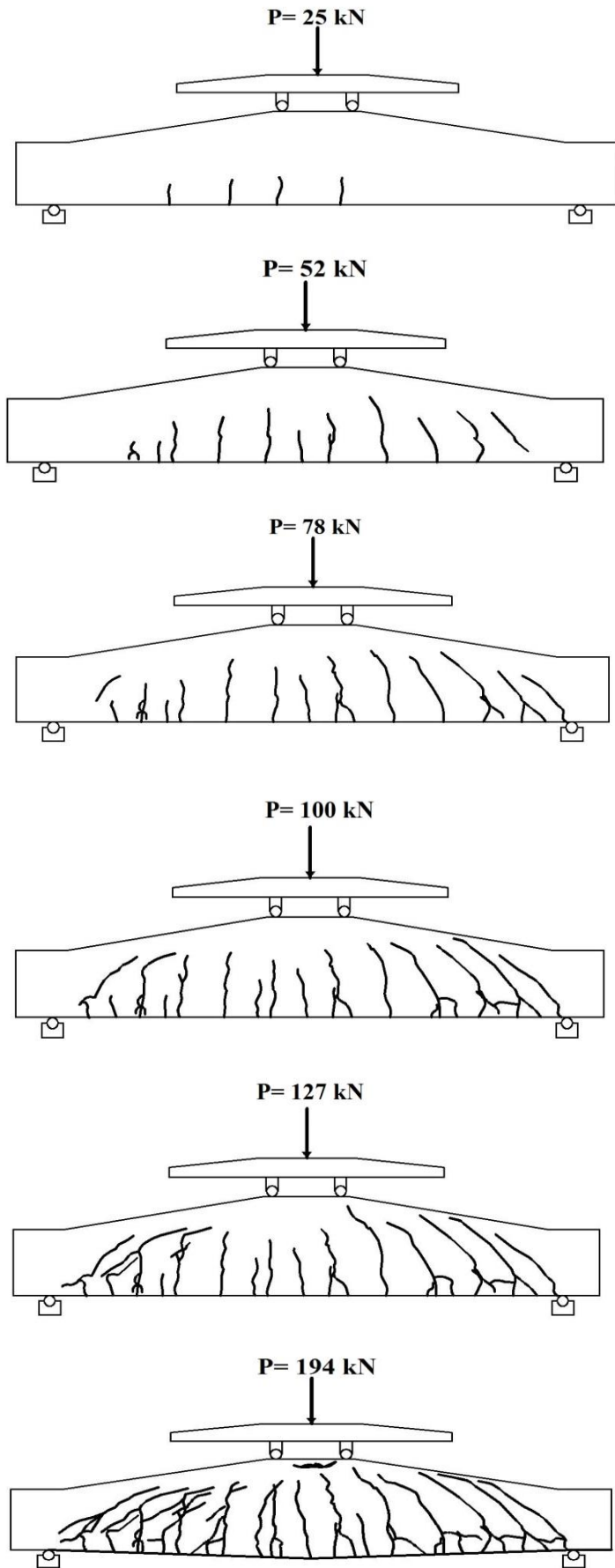


**Figure 4.47** Crack propagation of the beam B9

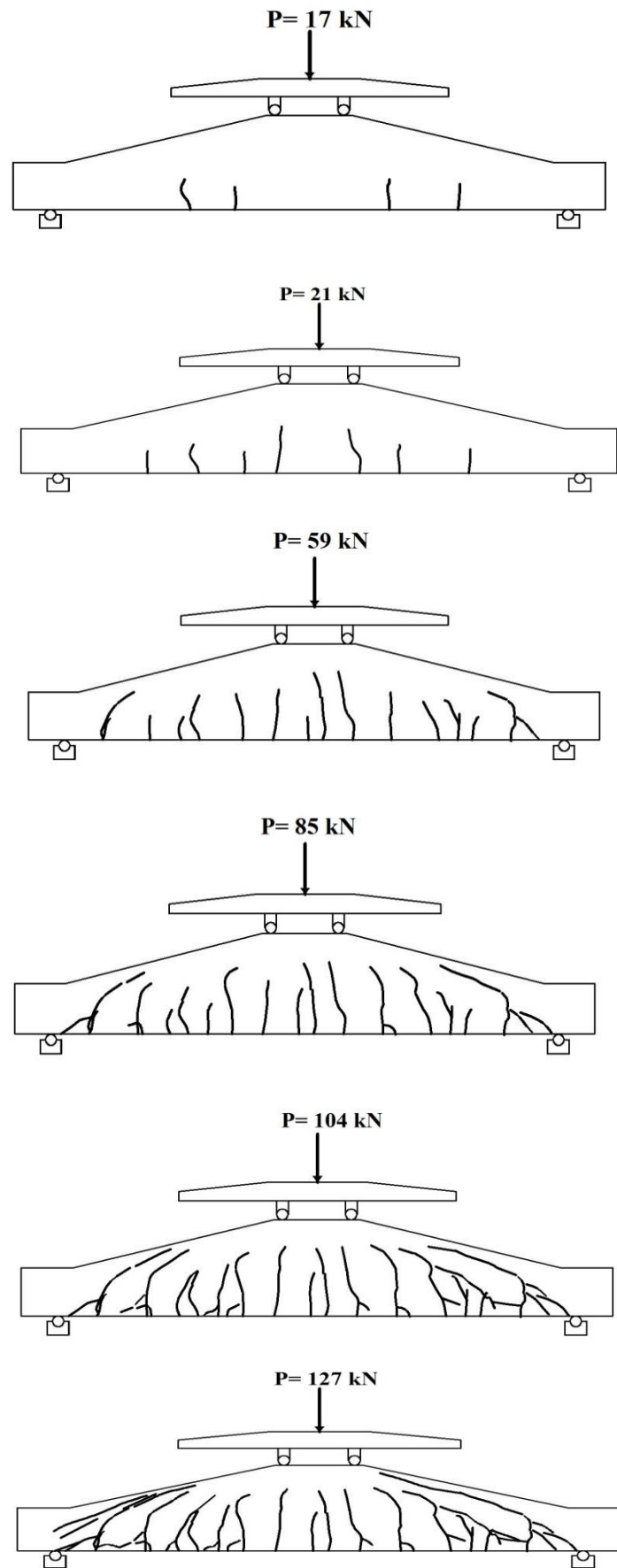


**Figure 4.48** Crack propagation of the beam B4

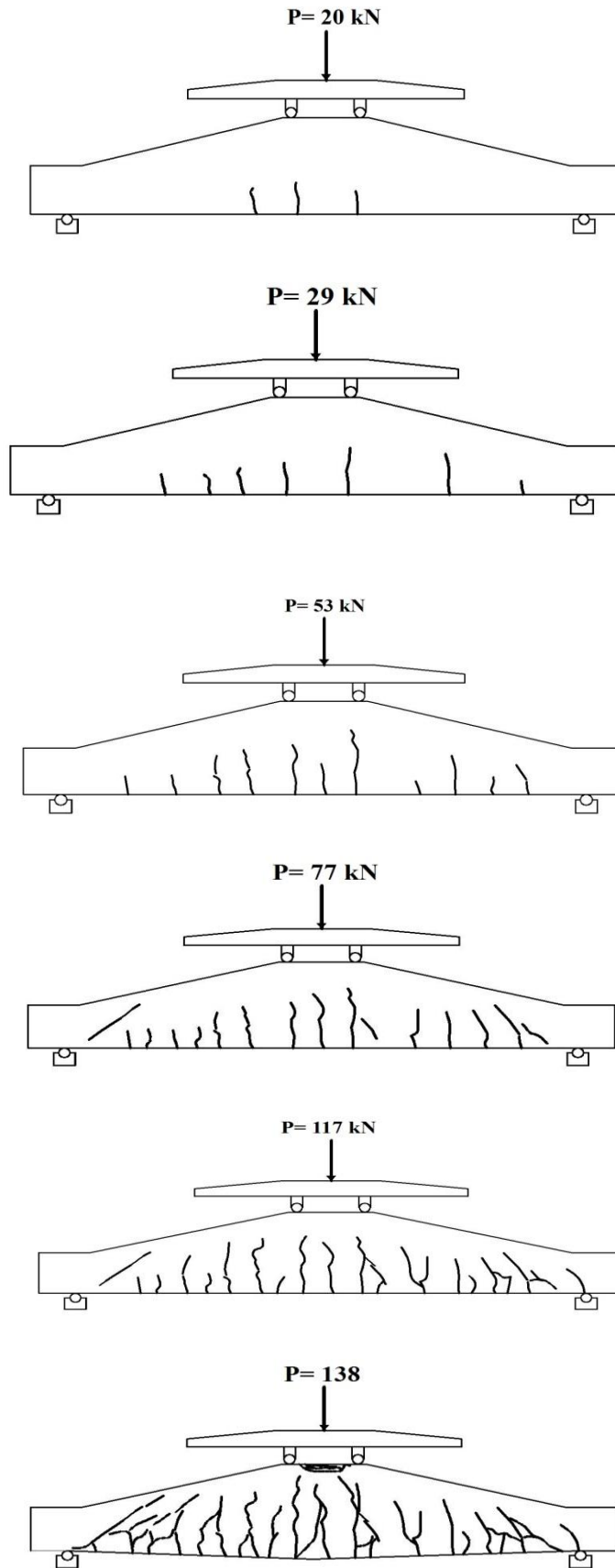


**Figure 4.49** Crack propagation of the beam B6

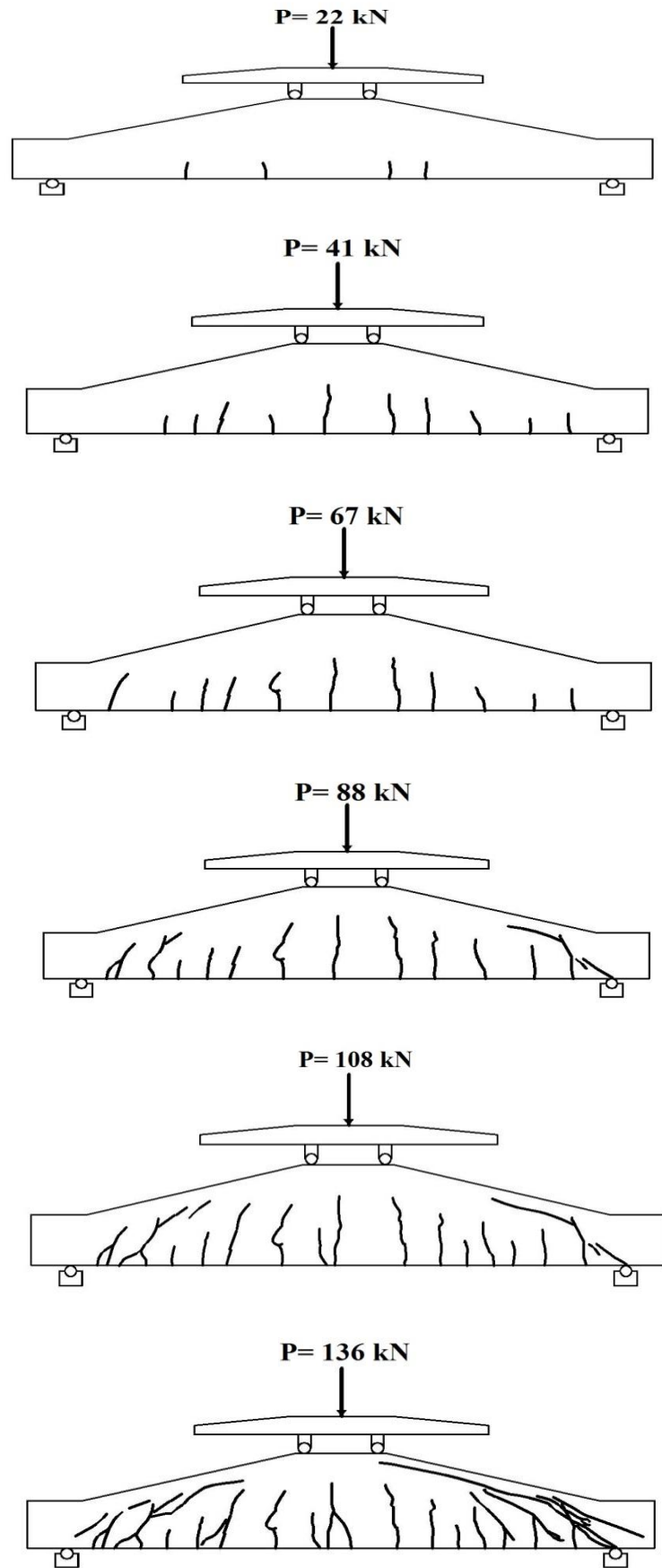


**Figure 4.50** Crack propagation of the beam B8

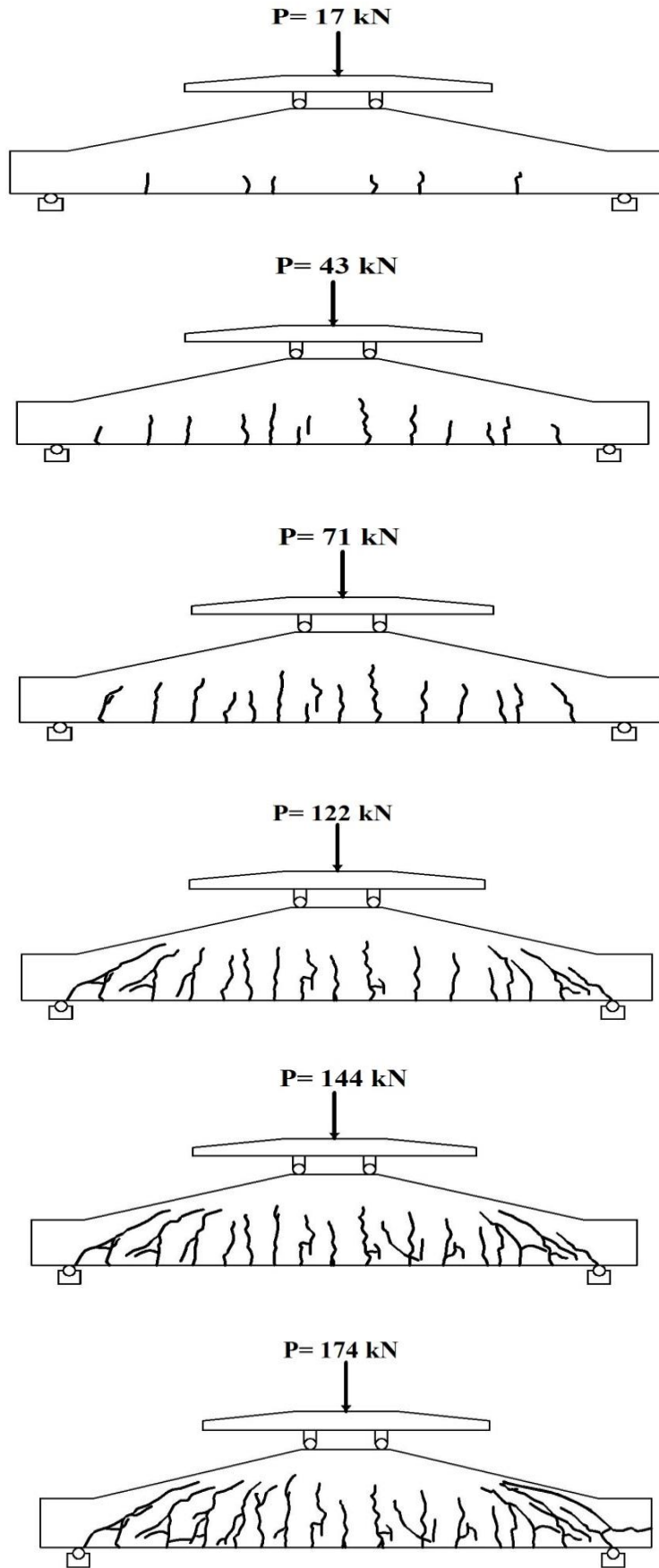


**Figure 4.51** Crack propagation of the beam B10

## CHAPTER FIVE

### CONCLUSIONS

#### 5.1 Overview

This research included the study of the shape of the failure and mechanical behavior of the haunched beams with steel fiber and was compared to the prismatic beams because the studies on the haunched beams were few and the studies did not cover the behaviors and designs of this kind of beams. The study included 12 beams that were classified into three groups (A, B, C) depending on the inclination angle of these beams (0, 10, and 15) degrees sequentially. All beams were designed with steel stirrups; two main reinforcement ratios were adopted. Each ratio was distributed to half the number of beams (6), As well as the steel fiber There were two ratios and also distributed each proportion on half the number of beams and the amount of 6 beams, and after conducting tests and the extraction of results were studied the effect of different parameters such as:

- Angle of inclination
- Steel reinforcement ratio
- Steel fiber ratio

The importance of the study of such beams type is that the section is considered economically and its architectural importance to enable the extension of drainage pipes or ducting of air conditioning in buildings. Moreover, to the study effect of the steel fiber because it is important in the modern construction method and to show the effect of mechanical behavior on concrete.

**5.2** The four prismatic beams have been adopted and encoded (A). These beams have been prepared to compare their results with haunched beam as these beams are standard and the results are as follows:

- When increasing the ratio of the main steel reinforcement from (0.02 - 0.310), the maximum load value of failure increased by 30%.

- When adding a steel fiber ratio 0.5%, the failure load value was significantly less effective than the increase in the ratio of the steel reinforcement.
- It has been noted that all these beams have been the form of failure in the type of flexure and this means that this type of beams and with the presence of steel stirrups are high resistant to the shearing force.

**5.3** For the four haunched beams with the symbol (B), the following results can be withdrawn:

- When increasing the ratio of the main steel reinforcement from (0.02 - 0.310), the maximum load value of failure increased by 40% compared to them with the same parameters and (10%) higher than the prism beams with the same parameters. This means that this type of haunched beams has reached a load failure higher than the corresponding prismatic beams with same parameters of the proportion of steel fiber and also the percentage of steel reinforcement, which gives a high ductility of concrete
- With respect to steel fiber, its rate of 0.5% did not significantly affect the value of the maximum load leading to failure, while its effect was very clear in increasing the shear strength resistance.

as in the case of the beam B 7, which was the form of failure when the Shear and the addition of a percentage of steel fiber change the form of failure to flexure and as in the beam B9.

- Three beams out of four were the shape of the failure in which the flexure except one was the form of failure in which shear.

**5.4** For the four haunched beams with the symbol (C), the following results can be withdrawn:

- When increasing the ratio of steel reinforcement from (0.02 - 0.310), the maximum load value increased by only 26% in the beam containing steel fiber compared to them while there was no increase in the load failure value compared to the prism, while not containing the steel fiber, the value of the maximum load causing failure increased by only 7%.

- The addition of 0.5% steel fiber ratio led to a noticeable increase in maximum load with the increase of the main steel reinforcement ratio. It also resulted in an increase in the resistance of the shear. This was evident in the haunched beam B6, which was the form of failure in flexure compared to the haunched B4, which was the form of failure in which shear.
- The results of this type of haunched beam at an angle of inclination 15 degree have been resistant to the weak shear strength and it was clear that three of four haunched beams are out of the shape of the shear failure.

### **5.5 Recommendations for Future Research**

Although, the experimental works shown their haunched beams behavior is different compared to prismatic section elements, the building design codes did not include a specific design formulation for these types of element for all that. Therefore, we recommend the following topics for future works:

- Study the mechanical behavior of RCHBs with stirrups for other types of percentage steel fiber that mean more than 0.5% ratio is used.
- Study the mechanical behavior of RCHBs for different types of loading, such as uniformly distributed load, cyclic loading and impact loading.
- Other types of fiber can be used instead of steel reinforcement stirrups, such as basalt fibers, glass fibers, to compare with this research and to study mechanical behavior and correlated economically.
- Investigate the behavior of other non-prismatic concrete members like columns, slabs and deck slabs.
- Include the design of these types of members by the international building design codes.
- Study influence of the uncertainty of the design parameters like material properties, geometry and loading on the mechanical behavior of the reinforced concrete members.
- Periodically, evaluate the existing design codes using the reliability analysis with the development of the materials and techniques in the construction industry.
- Study influence for more than one type of compressive strength of concrete.

## REFERENCES

ACI. American Concrete Institute. (2004). Building code requirements for structural concrete (ACI 318-05) and commentary (318R-05), Farmington Hills, Michigan.

ACI. American Concrete Institute. (2008). Building code requirements for structural concrete (ACI 318-08) and commentary (318R-08), Farmington Hills, Michigan.

ACI. American Concrete Institute. (1976). Recommended Practice for Evaluation of Strength Test Results of Concrete. ACI 214-77.

ACI. American Concrete Institute. (1998). Guide to Quality Control and Testing of High-Strength Concrete. 363.2R-98. American Concrete Institute Farmington Hills, MI 48331 U.S.A.

Albegmprli, H.M., Abdulkadir, Ç., Gülsan, M.E., Kurtoglu, A.E. (2015). Reliability analysis of reinforced concrete haunched beams shear capacity based on stochastic nonlinear FE analysis. *Computers & Concrete*, **15** , 259-277. doi:<http://dx.doi.org/10.12989/cac.2015.15.2.259>.

Albegmprli,H.M. (2017). Experimental Investigation and Stochastic FE Modeling of Reinforced Concrete Haunched Beams. Ph D thesis, Gaziantep University

Anderson, F. D. (1985). Statistical Controls for High Strength Concrete. High Strength Concrete, ACI SP-87. American Concrete Institute. Farmington Hills, Mich. 71 – 82.

Azizi, A.H, Hassan, H.F, Razzaq,M.A.(2016) Experimental Study on Shear Behavior of Reinforced Self-Compacted Concrete Tapered Beams. *Civil and Environmental Research*,**8**, 11-22.

Balaguru, P. and Dipsia, M. G. (1993).Properties of Fiber Reinforced High-Strength Semi lightweight Concrete. *ACI Materials Journal*, **90**, 399-405.

Bartlett, F.M., Macgregor, J. G. (1996). Statistical analysis of the compressive strength of concrete in structures. *Materials Journal*, **93**, 158-168.

Bayasi, M. Z. and Soroushian, P. (1992). Effect of Steel Fiber Reinforcement on Fresh Mix Properties of Concrete. *ACI Materials Journal*, **89**, 369-374.

BS1881-116, “ Method for Determination of Compressive Strength of Concrete Cubes”, British Standards Institute, London, 1983.

Carlos Zanuy, Juan M. Gallego, and Luis Albajar. (2015). Fatigue Behavior of Reinforced Concrete Haunched Beams without Stirrups. *ACI Structural Journal*, **112**, 371-382.

Chenwei, H., Matsumoto, K. (2015). Shear Failure Mechanism of Reinforced Concrete Haunched Beams. *Journal of JSCE*, **3**, 230-245.

Chmielewski, T., Konopka, E. (1999). Statistical evaluations of field concrete strength. *Magazine of Concrete Research*, **51**, 45-52.

Cohen M. (2012). Structural Behaviour of Self Consolidating Steel Fiber Reinforced Concrete Beams. MSc. thesis, Ottawa, University of Ottawa.

Choi, B-S., Scanlon, A., Johnson, P.A. (2004). Monte Carlo simulation of immediate and time-dependent deflections of reinforced concrete beams and slabs. *Structural Journal*. **101**, 633-641.

Cook, J.E. (1989). 10,000 psi concrete. *Concrete International*, **11**, 67-75.

De Schutter, G. 2001. Guidelines for testing fresh self-compacting concrete. European Research Project, Testing SCC. Growth Contract No GRD2-2000-30024.

Debaiky, S.Y., Elniema E.I. (1982). Behavior and strength of reinforced concrete haunched beams in shear. *ACI Structural Journal*, **79**, 184-194.

DIN 1045-01. 2001. Tragwerke aus Beton, Stahlbeton und Spannbeton, Teil 1 Bemessung und Konstruktion. Beuth Verlag GmbH, Berlin.und Konstruktion. Beuth Verlag GmbH, Berlin.

Ellingwood, B. 1980. Development of a Probability Based Load Criterion for American National Standard A58: Building Code Requirements for Minimum Design Loads in Buildings and Other Structures. (13) US Department of Commerce, National Bureau of Standards.

Ellingwood, B.R., Ang, A. H-S. (1974). Risk-based evaluation of design criteria. *Journal of the Structural Division*, **100**, 1771-1788.

Ellingwood, B.R., Ang, A. H-S. 1972. A Probabilistic Study of Safety Criteria for Design. University of Illinois at Urbana-Champaign.

El-Niema, E.I. (1988). Investigation of concrete haunched T-beams under shear. *Journal of Structural Engineering*, **114**, 917-930.

Ferrand, D. 2005. Reliability analysis of a reinforced concrete deck slab supported on steel girders. Doctoral dissertation, University of Michigan.

Firat, F.K. 2007. Development of Load and Resistance Factors for Reinforced Concrete Structures in Turkey. PhD thesis. Middle East Technical University. Turkey.

Freudenthal, A.M. (1947). The safety of structures. *Transactions of the American Society of Civil Engineers*, **112**, 125-159.

Graig, R.J.; Parr, J.A.; Germain, E.; Mosquera, V.; and Kamilaris; S. (1986). Fiber Reinforced Beam in Torsion. *ACI Materials Journal*, **83**, 934-942.

Guan, X.L., Melchers, R.E. (1994). An efficient formulation for limit state function gradient calculation. *Computers & Structures*, **53**, 929-935.

Gulsan, M.E., Cevik, A., Kurtoglu, A.E. (2015). Stochastic finite element based reliability analysis of steel fiber reinforced concrete (SFRC) corbels. *Computers and Concrete*, **15**, 279-304.

Hans, Archundia-Aranda, Tena-Colunga A., Grande-Vega, A. (2013). Behavior of reinforced concrete haunched beams subjected to cyclic shear loading. *Engineering Structures*, **49**, 27-42.

Hasofer, A. M., Lind, N. C. (1974). Exact and invariant second-moment code format. *Journal of Engineering Mechanics Division*, **100**, 111-121.

Hordijk, D. A. 1991. Local approach to fatigue of concrete . Ph D thesis, Delft University of Technology, Delft.

Huntington, D. E., Lyrintzis C. S. (1998). Improvements to and limitations of Latin hypercube sampling. *Probabilistic Engineering Mechanics*, **13**, 245-253.

Hwan Oh, B. (1992). Flexural Analysis of Reinforced Concrete Beams Containing Steel Fibers. *Journal of Structural Engineering*, **118**, 2821-2837.

Iman, R. L., Conover, W-J. (1982). A distribution-free approach to inducing rank correlation among input variables. *Communications in Statistics-Simulation and Computation*, **11**, 311-334.

Kömürcü, A. M. 1995. A probabilistic assessment of load and resistance factors for reinforced concrete structures considering the design practice in Turkey. Master thesis. Middle East Technical University. Turkey.

Kömürcü, A. M., Yüçemen, M. S. 1996. Load and resistance factors for reinforced concrete beams considering the design practice in Turkey, Concrete Technology for Developing Countries. Fourth International Conference, Eastern Mediterranean University, GaziMagusa, North Cyprus.

Kupfer, H., Hilsdorf, H. K. and Rusch, H. (1969). Behavior of concrete under biaxial stresses. *ACI Journal Proceedings*, 656–666.

Kurtoglu, A. E., Çevik, A., Albegmpri, H. M., Gülsan, M. E., Bilgehan, M. (2016). Reliability-based modeling of punching shear capacity of FRP-reinforced two-way slabs. *Computers & Concrete*, **17**, 87–106. doi:10.12989/cac.2016.17.1.087.

Liu, P-L., Der Kiureghian, A. (1991). Optimization algorithms for structural reliability. *Structural Safety*, **9**, 161-177.

MacLeod, I. A., Houmsi, A. (1994). Shear strength of haunched beams without shear reinforcement. *ACI Structural Journal*, **91**, 79-89.

Matos, J. C., Valente, I., Cruz, P. J. S. (2010). Uncertainty evaluation of reinforced concrete structures behavior. *The Fifth International Conference on Bridge Aintenance, Safety and Management-IABMAS 2010*.

Menetrey, P., William, K. J. (1995). Triaxial failure criterion for concrete and its generalization. *ACI Structural Journal*, **92**, 311-318.

Mier, van, Jan, G. M. (1986). Multiaxial strain-softening of concrete. *Materials and structures*, **19**, 179-190.

Mirza, S. A., Hatzinikolas, M., MacGregor, J. G. (1979). Statistical descriptions of strength of concrete. *Journal of Structural Division*, **105**, ASCE 14628 Proceeding.

Mirza, S. A., MacGregor, J. G. (1979). *Journal of Structural Division*, **105**, ASCE 14590 Proceeding.

Mitchell, D. Abrishami, H.H. Mindess, S. (1996).The Effect of Steel Fibers and Epoxy-Coated Reinforcement on Tension Stiffening and Cracking of Reinforced Concrete. *ACI Materials Journal*, **93**, 61-68.

Nghiep, Vu Hong. 2011. Shear design of straight and haunched concrete beams without stirrups. PhD Thesis. Technische Universität Hamburg, German.

Nilson, A. H., Darwin, D., Dolan, C.W. 2010. Design of concrete structures. McGraw-Hill Higher Education.

Novák, D., Teplý, B., & Keršner, Z. (1998). The role of Latin Hypercube Sampling method in reliability engineering. *Proc. of ICOSSAR*, **97**, 403-409.

Nowak, A. S., Szerszen, M. M. (2003). Calibration of design code for buildings (ACI 318): Part 1—Statistical models for resistance. *Structural Journal*, **100**, 377-382.

Park, R., Paulay, T. 1975. Reinforced Concrete Structures. John Wiley & Sons.

Pryl, D., Cervenka, J. 2013 .ATENA program documentation, part 1 of 1, troubleshooting manual. Cerv Consult Ltd, Prague.

Romualdi, J.P., and Batson, G.B. (1963). Mechanics of Crack Arrest in Concrete. *ASCE*, **89**,147-168.

Soroushian, P. and Lee, C. (1990). Distribution and Orientation of Fibers in Steel Fiber Reinforced Concrete. *ACI Materials Journal*, **87**,433-439.

Standard, A. C. I., 1976. Recommended Practice for Evaluation of Strength Test Results of Concrete. (ACI 214-77). ACI Manttal of Concrete practice, Part I .

Stefanou, G. D. (1983). Shear resistance of reinforced concrete beams with non-prismatic sections. *Engineering Fracture Mechanic*. **18**, 643-666.

Tabsh, S. W. (1997). Safety of reinforced concrete members designed following ACI 318 building code. *Engineering structures*, **19**, 843-850.

Tena-Colunga, A., Hans I. Archundia-Aranda, and Óscar M. González-Cuevas. (2008). Behavior of reinforced concrete haunched beams subjected to static shear loading. *Engineering Structures*, **30**, 478-492.

Val, D., Bljoger, F., Yankelevsky, D. (1997). Reliability evaluation in nonlinear analysis of reinforced concrete structures. *Structural Safety*, **19**, 203-217.

Vořechovský, M., Novák, D. (2009). Correlation control in small-sample Monte Carlo type simulations I: A simulated annealing approach. *Probabilistic Engineering Mechani*, **24**, 452-462.

Vorechovský, M. 2004. Stochastic fracture mechanics and size effect. Brno University of Technology, Brno, Czech Republic, ISBN, pp.80-214

